Frequency distribution of telomere maintenance mechanisms in soft tissue sarcoma

Vom Fachbereich Biologie
der Technischen Universität Darmstadt

zur Erlangung des Grades
eines Doktors der Naturwissenschaften
(Dr. rer. nat.)

genehmigte Dissertation von

Petra Sander
Darmstadt

Darmstadt 2010
D 17

Referent:	Prof. Dr. Gerhard Thiel
Korreferent:	PD Dr. Ralf Joachim Rieker
Korreferent:	Prof. Dr. Markus Engstler
Tag der Einreichung:	10. Dezember 2009
Tag der Disputation:	26. Januar 2010

Der höchste Lohn für unsere Bemühungen ist nicht das, was wir dafür bekommen, sondern das, was wir dadurch werden (John Ruskin).

Der Beginn aller Wissenschaften ist das Erstaunen, dass die Dinge sind wie sie sind (Aristoteles).

Meiner Familie

Contents

List of Figures

List of Tables

List of abbreviations

ALT	Alternative lengthening of telomeres
APB	ALT-associated PML nuclear bodies (ALT-assoziierende PML Kernkörperchen)
DAPI	4,6-Diamidino-2-phenylindol
DDLS	Dedifferentiated Liposarcomas (Dedifferenzierte Liposarkome)
DNA	Deoxyribonucleic acid (Desoxyribonukleinsäure)
EDTA	Ethylendiamintetraacetat
FISH	Fluorescence *in situ* hybridization
GFP	Green fluorescent protein (grün fluoreszierende Protein)
HRP	Horseradish peroxidase
LMS	Leiomyosarcomas (Leiomyosarkome)
MFH	Malignant Fibrous Histiocytoma (Maligne fibröses Histiozytome)
MPNST	Malignant Peripheral Nerve Sheath Tumors (maligne periphere Nervenscheidentumore)
MRCL	Myxoid Round Cell Liposarcomas (Myxoid rundzellige Liposarkome)
NHEJ	non-homologous end joining (nichthomologe Endverknüpfung)
PBS	phosphate buffered saline (phosphatgepufferte Saline)
PD	Population doublings (Anzahl der durchlaufenen Zellteilungen)
PLLS	Pleomorphic Liposarcomas (Pleomorphe Liposarkome)
PVDF	Polyvinylidenfluorid
RNA	Ribonucleic acid (Ribonukleinsäure)
RT	room temperature (Raumtemperatur)
SDS	Sodiumdodecylsulfate (Natriumdodecylsulfat)

SS Synovial Sarcoma (Synovial Sarkome)

STS Soft Tissue Sarcomas (Weichteilsarkome)

SSC sodiumchloride, sodium citrate (Natriumchlorid, Natriumcitrat)

TMM Telomere maintenance mechanism (Telomer-erhaltende Mechanismen)

TRIS Tris-hydroxymethyl-aminomethan

Zusammenfassung

Molekulare Mechanismen, die zu Veränderungen von Chromosomen-Telomeren führen, spielen eine wesentliche Rolle bei der Entstehung chromosomaler Instabilität. Telomere verkürzen sich mit jeder Zellteilung, was beim Erreichen einer kritischen Länge zu replikativer Seneszenz oder Apoptose der Zelle führt. In Tumorzellen wird diese gegen unbegrenztes Wachstum gerichtete Kontrolle durch Telomer-erhaltende Mechanismen (engl.: Telomere Maintenance Mechanismen = TM-Mechanismen) aufgehoben. Zu den bekannten TM-Mechanismen zählen die Telomerase-Aktivierung (TA) und der alternative Längenerhalt von Telomeren (ALT = Alternative lengthening of telomeres).

Primäres Ziel dieser Arbeit war die Bestimmung der Häufigkeitsverteilung des TA- und des ALT-Mechanismus in einem umfassenden Kollektiv an Weichteilsarkomen welches in vorangegangenen Projekten, pathologisch, molekular-genetisch und klinisch eingehend unter anderem hinsichtlich ihrer chromosomalen Veränderungen untersucht wurde. Ein Schwerpunkt der hier beschriebenen Arbeit lag zunächst in der Etablierung der Methoden zur Detektion des ALT-Mechanismus. Die hierzu am häufigsten verwendeten Marker sind zum einen Kolokalisationen zwischen Telomeren und PML-Kernkörperchen (PML: Promyelozytische Leukämie), auch ALT-assoziierte PML-Kernkörperchen (APBs) genannt, und zum anderen die Heterogenität in der Größe der Telomere mit dem zusätzlichen Auftreten von extrem großen Telomeren-Signalen. Hierzu wurde zunächst ein Protokoll für eine kombinierte Telomere Fluoreszenz *in situ* Hybridisierung (Detektion: Telomere) mit anschließender Immunfluoreszenz (Detektion: PML-Kernkörperchen) etabliert. Für die in diesem Zusammenhang erstellten konfokalen Aufnahmen wurde ein Programm zur automatischen Auswertung der Marker des ALT-Mechanism entwickelt. Für die Bestimmung der Telomerase-Aktivität wurde das TRAP-Verfahren (Telomeric Repeat Amplification Protocol) verwendet. Diese Daten wurden anschließend vergleichend mit den Daten der chromosomalen Veränderungen in Bezug gesetzt.

Die Studie sollte die Häufigkeitsverteilung von TM-Mechanismen in Weichteilsarkomen ermitteln und klären, ob diese mit spezifischen chromosomalen Imbalancen assoziiert sind. Die wichtigsten Ergebnisse dieser Arbeit lauten:

1. Das Auftreten der Telomer-erhaltenden Mechanismen ist stark von den einzelnen Weichteilsarkom-Subtypen abhängig. Telomerase-Aktivität variiert von 100% in synovialen Sarkomen bis hin zu 46% in pleomorphen Liposarkomen. Das Auftreten der Marker die den ALT-Mechanismus charakterisieren, sind ebenso mit den verschiedenen Weichteilsarkom-Subtypen assoziiert. Während in synovialen Sarkomen keine sehr große Telomere-Signale detektiert werden konnten, liegt dieser Anteil bei pleomorphen Liposarkomen bei 92%. Die Korrelation beider Telomer-

erhaltenden Mechanismen hat ergeben, dass die Anzahl der Kolokalisationen zwischen Telomeren und PML-Kernkörperchen als auch die der sehr großen Telomer-Spots mit der Höhe Telomerase-Aktivität assoziiert ist.

2. Neben Tumorgewebe wurde in dieser Arbeit auch ein umfangreiches Kollektiv von gesundem Gewebe auf Indikatoren des ALT Mechanismus untersucht. Die Ergebnisse der automatischen Analyse zeigen im gesunden Gewebe ebenso wie im Tumorgewebe das Auftreten von Kolokalisationen zwischen Telomeren und PML-Kernkörperchen. Im Vergleich zu Tumorgewebe konnten jedoch in gesundem Gewebe keine übergroßen Telomer-Spots detektiert werden. Diese Analyse stellt APBs als quantitativen Marker für den ALT-Mechanismus in Frage. Das Auftreten von sehr großen Telomere-Signalen wurde nur in Tumorgewebe gefunden wurde.

3. Die vergleichende genomische Hybridisierung (CGH) stellt einen Ansatz dar, mit welchem ein robuster Nachweis von chromosomalen Imbalancen aufgezeigt werden kann. Die Korrelation der CGH-Daten mit den Telomere-erhaltenden Mechanismen gibt keinen Hinweis darauf, dass bei einem der Mechanismen präferenziell mehr chromosomale Imbalancen auftreten. Die Analyse hat jedoch ergeben, dass Weichteilsarkome mit Telomerase-Aktivität ein differenziertes zytogenetisches Profil gegenüber solchen Weichteilsarkomen mit Marker für den ALT-Mechanismus aufweisen.

4. Im Rahmen diese Arbeit wurde für die automatische Quantifizierung von Kolokalisationen aus konfokalen mikroskopischen Aufnahmen ein Computerprogramm entwickelt. Mittels dieses Programms können Indikatoren für den ALT Mechanismus wie ALT-assoziierte PML Kernkörperchen und überdurchschnittlich große Telomere detektiert werden. Die Detektion der verschiedenen Marker innerhalb des Zellkerns, wird über die Kernsegmentierung ermittelt. Mit Hilfe der vollautomatischen Auswertung war es möglich über 500 konfokale mikroskopische Bilderstapel zu analysieren und auszuwerten.

Die Charakterisierung von Tumoren spielt in der klinischen Diagnostik und in der Beurteilung von Therapie-Entscheidungen eine wichtige Rolle. Mit dem Auftreten der ALT-assoziierten PML-Kernkörperchen in gesundem Gewebe, muss in weiteren Studien geklärt werden, wie stark diese spezielle Kernstruktur direkt mit dem ALT-Mechanismus assoziiert ist. Die Charakterisierung von Telomere-erhaltenden Mechanismen und ihre Rolle in der Tumorgenese könnten die Basis für neue gezielte therapeutische Ansätze bilden.

Abstract

Molecular mechanisms, which cause changes of the ends of chromosomes, the telomeres, play an important role in the generation of genomic instability. In normal somatic cells, the length of the telomeres are shortened during cell division due to the inability of the cells to replicate their chromosome ends completely. Telomeres below a critical length are dysfunctional and undergo apoptosis or permanent growth arrest referred to as replicative senescence. One possibility to bypass telomere dysfunction and maintenance of stable telomere length is the activation of a telomere maintenance mechanism. The currently known telomere maintenance mechanisms in humans are telomerase activity (TA-activity) and the alternative lengthening of telomeres (ALT-Mechanism).

The preliminary goal of the thesis was to assess the frequency distribution of the activation of telomerase and of the ALT-mechanism in the major soft tissue sarcomas subtypes, which had been genetically well characterized in preceding studies. A first step of the thesis was the establishment of a method to assess the ALT-mechanism. One hallmark of ALT positive tumors/cells is the presence of ALT-associated promyelocytic leukemia (PML) bodies (APBs). APBs are characterized by promyelocytic leukemia (PML) bodies, which colocalize with telomeric DNA or telomere-specific binding proteins. A further marker of ALT is their highly heterogeneous telomere length with some exceptionally long telomeres. In order to assess ALT in human soft tissue sarcoma subtypes by combined telomere fluorescence *in situ* hybridization and PML immunofluorescence, confocal laser scanning microscope was used. 3D images were acquired, which visualize telomere spots in the first channel, PML bodies in the second channel and DAPI stained nuclei in the third channel. The central task of image analysis was to automatically detect and classify APBs within the cell nucleus as well as to detect and quantify very large telomeres. Telomerase activity was evaluated by the TRAP assay (telomeric repeat amplification protocol). Afterwards, these data were correlated with the number of chromosomal imbalances detected by comparative genomic hybridization (CGH).

This study contributed to the understanding of the frequency distribution of telomere maintenance mechanisms in soft tissue sarcoma subgroups and whether these mechanisms are associated with specific chromosomal imbalances. The most important results based on this thesis are:

1. The study demonstrates that the occurrence of the telomere maintenance mechanism is characteristic for the subtype of soft tissue sarcoma. The presence of telomerase activity ranges from 100% in synovial sarcoma to 46% in pleomorphic liposarcomas. The frequency of the marker for the ALT mechanism depends on

the subtype of soft tissue sarcoma. While the telomeres detected in synovial sarcomas were equal in length, 92% of all cases of pleomorphic liposarcomas showed exceptionally long telomere signals. Furthermore, the correlation of both telomere maintenance mechanisms has shown that in tumors with high telomerase activity, the markers for the ALT-mechanism are significantly reduced.

2. In order to investigated an abundant number of healthy tissue with regard to markers for the ALT mechanism automatic quantification were performed. Healthy tissue, as well as our investigated tumor samples, show the appearance of ALT-associated PML bodies, whereas no telomeres with heterogeneous size and exceptionally long telomeres could be detected in healthy tissue. Therefore an important questions remains: how tightly are APBs linked to the ALT mechanism?

3. Comparative genomic hybridization (CGH) allows for a genome-wide screen for chromosomal imbalances in tumor samples. The correlation of the CGH data and the telomere maintenance mechanisms revealed that tumors with telomerase activity show a different cytogenetic profile compared to those tumors with markers for ALT. In respect to the frequency of chromosomal imbalances, such as gains and losses, there were no differences between both telomere maintenance mechanisms.

4. A new approach for an automated quantification of telomere and PML spots as well as colocalization in multi-channel 3D microscopy images to assess the ALT mechanism were developed. To discriminate between spots inside and outside the cell nucleus, DAPI staining was used for the nuclear segmentation. With our program more than 500 confocal images were successfully analyzed.

The characterization of tumors is highly relevant for tumor diagnostics and treatment planning. Due to the appearances of APBs in healthy tissue, one important question remains. How tightly are these structures linked to the ALT-mechanism? Further investigation is needed to clarify if in healthy tissue APBs are induced by the ALT mechanism or other nuclear processes besides ALT. Therefore, the characterization and understanding of telomere maintenance mechanism in tumorigenesis could have important implications in the development new treatments for these malignancies.

1 General Introduction

1.1 Cancer: General aspects

Cancer is one of the most common causes of death in Germany and the Western world after cardio-vascular diseases. In Germany, in 2006, approximately 22% and 28% of all deaths of women and men, respectively, were cancer-related. More recently, Jemal et al. (2008, 2005) estimated that cancer will be the most frequent cause of death in the near future.

In 2000, Hanahan and Weinberg (2000) summarized six universal hallmarks of cancer (Table 1.1), which are crucial steps in the transformation process from normal to malignant cells. In each malignant transformation not all six hallmarks have to be fulfilled and the mechanistic pathway may vary from cell to cell. Nevertheless, most tumor cells have acquired more or less of these properties. These capabilities described in malignant cells are gained during transformation and induced by genomic and/or epigenetic mutation. This does not mean that every hallmark needs to be caused by an individual mutation. Mutator genes with several control functions can lead to gains of several functions at once. These changes can be point mutation, microsatellite instability or loss of heterozygosity, and affect genes that control DNA replication, cell cycle checkpoints and DNA repair (Klein et al. 2007). In general, cancer cells acquire their functional capabilities by mutations that affect two classes of genes: oncogenes and tumor suppressor genes. Cancer-promoting oncogenes are activated by gain-of-function and are mostly involved in pathways that change the properties of the transformed cells including proliferation,

Table 1.1: The six hallmarks of cancer (Hanahan and Weinberg 2000)

Hallmarks of cancer	**Cellular effects**
Evasion of apoptosis	Allows cell growth despite of genetic mutations and internatal or external anti-growth signal(s)
Self-sufficient in growth signals	Unchecked growth
Insensitivity to anti-growth signals	Unchecked growth
Sustained angiogenesis	Allows tumor to growth beyond limitations of passive nutrition
Limitless replicative potential	Immortality of cancer cells
Tissue invasion	Metastasis

apoptosis prevention, loss of tissue boundaries and invasion. A predominant example for a proto-oncogene is *RAS*, which is important for the molecular switch between apoptosis and survival of normal cells. *RAS* mutation promotes survival of tumor cells and is constitutively active and therefore insensitive to cellular negative control mechanisms (Klein et al. 2007).

Tumor suppressor genes, on the other hand, are inactivated in tumors by loss-of-function mutation and normally protect cells from cancer. The normal function of tumor suppressor genes are regulation of DNA replication, DNA repair, cell cycle control, cellular orientation within a tissue, adhesion within tissues or promotion of apoptosis. The most famous example of a tumor suppressor gene is *TP53*, which is affected in almost all cancers (Wang and Harris 1996; Weinberg 2007). Nevertheless, the formation of a tumor remains a complex process that usually proceeds over decades.

Nonetheless, nearly every tissue of an organism can be affected by cancer. Frequently affected tissues in both genders are gut, lung, stomach and bladder. For women, the tissue mostly effected by cancer is breast tissue and for men prostate tissue. The majority of human tumors arise from epithelial tissues, whereas a small group is derived from non-epithelial tissues sharing a common origin in the mesoderm of the embryo. The latter, the sarcomas, are focus of this study.

1.2 Soft tissue sarcomas: An overview

Sarcomas are a heterogeneous group of rare tumors that arise predominantly from the embryonic mesoderm and share a putative mesenchymal cell origin (Table 1.2). The different types of sarcomas include bone sarcomas, Ewing‘s sarcomas, peripheral primitive neuroectodermal tumors and soft tissue sarcomas, the latter being the most frequent. Soft tissue sarcomas can involve connective tissue structures as well as viscera and integument. There are approximately 9 000 new cases diagnosed as soft tissue sarcomas per year in the United States, which constitutes less than 1% of adult solid malignancy. There are nearly 3 660 deaths by soft tissue sarcomas per year (Jemal et al. 2004).

Soft tissue sarcomas may occur anywhere in the body, but they are often located at the extremities (59%), the trunk (19%), the retroperitoneum (15%), or the head and neck (9%) (DeVita et al. 2001). Currently, the soft tissue sarcoma classification includes more than 50 different histologic subtypes. The most frequent types are malignant fibrous histiocytomas (28%), leiomyosarcomas (12%), liposarcomas (15%), synovial sarcomas (10%), and malignant peripheral nerve sheath tumors (6%) (Coindre et al. 2001) (see also section 1.3). The most common soft tissue sarcomas of childhood are the rhabdomyosarcomas.

Table 1.2: Typification of soft tissue sarcomas (Fletcher et al. 2002)

Histologic subtypes	Tumor (e.g.)
SOFT TISSUE TUMORS	
Fibroblastic/Myofibroblastic tumors	Fibrosarcoma
	Fibrous histiocytoma
Adipocytic tumors	Liposarcomas
	Lipomatosis
Smooth muscle tumors	Leiomyosarcoma
	Angioleiomyoma
Skeletal muscle tumors	Rhabdomyosarcoma
	Embryonal rhabdomyosarcoma
Vascular tumors	Angiosarcoma of soft tissue
	Epithelioid haemangioendothelioma
Pericytic tumors	Myopericytoma
	Glomus tumors
So-called fibrohistiocytic tumors	Giant cell tumors of tendon sheath
	Deep benign fibrous histiocytoma
Chondro-osseous tumors	Soft tissue chondroma
	Extraskeletal osteosarcoma
Tumors of uncertain differentiation	Synovial sarcomas
	Clear cell sarcomas of soft tissue
BONE TUMORS	
Cartilage tumors	Osteochondroma
Osteogenic tumors	Osteoid osteoma
Fibrogenic tumors	Desmoplastic fibroma of bone
Fiborhistiocytic tumors	Malignant fibrous histiocytoma of bone
Ewing sarcomas/ Primitive neuroectodermal tumors	Ewing tumor/ PNET
Haematopoietic tumors	Plasma cell myeloma
Giant cell tumors	Giant cell tumors
Notochordal tumors	Chordoma
Vascular tumors	Angiosarcoma
Myogenic, lipogenic, neural, and epithelial tumors	Schwannoma
Tumors of undefined neoplastic nature	Simple bone cyst
Congenital and inherited syndromes	Werner syndrome

1.2.1 Epidemiology and genetics

Soft tissue sarcomas have no clearly defined etiology even though several associated or predisposing factors have been identified. In general, soft tissue sarcomas occur de novo and do not seem to result from malignant changes or the dedifferentiation of benign tumors. Despite the high variety of histological subtypes, soft tissue sarcomas have many clinical and pathologic features in common. For instance, most soft tissue sarcomas show a similar clinical behavior as defined by the staging system, which is determined by the anatomic location (depth), grade, and size of the tumor. Soft tissue sarcomas disseminate predominantly hematogenous. Lymph node metastasis are less than 5% except for a few histologic subtypes of soft tissue sarcomas, such as synovial sarcomas and rhabdomyosarcomas (Fong et al. 1993).

The development of soft tissue sarcomas as a result of radiation therapy are shown in several studies. The risk for a soft tissue sarcoma is increased eightfold to 50-fold in patients treated with radiation therapy of breast, cervix, ovary or lymphatic system cancers. The most common histologic subtypes of radiation-induced tumors are extraskeletal osteogenetic, malignant fibrous histiocytomas and angiosarcomas/lymphangiosarcomas (Brady et al. 1992; Zahm and Fraumeni 1997). Another known risk factor for the development of lymphangiosarcomas is lymphedema (Muller et al. 1987). Further risk factors include exposure to certain chemicals like phenoxyherbicides and chlorphenols (Hardell and Sandström 1979; Smith et al. 1984).

Similar to other cancers, genetic factors play a decisive role in the initiation and progress of sarcomas. It is supposed that genetic mutations in pluripotent mesenchymal stem cells give rise to malignant transformation. Furthermore, specific inherited genetic alteration are associated with an increasing risk of the bone and soft tissue sarcomas. These include, for example, neurofibromatosis typ1 (von Recklinghausen disease), retinoblastoma, Li-Fraumeni syndrome, Gardner syndrome and Werner syndrome.

The onco-genes that have been implicated in malignant formation and progression are *MDM2, MYCN, ERBB2* and members of the *RAS*-family. In several subtypes of soft tissue sarcomas, amplification of these genes correlates with an adverse patient outcome (Levine 1999). Cytogenetic analysis of these tumors identified chromosomal translocations that code for onco-proteins associated with specific histological subtypes. Well characterized gene rearrangements are found, for example, in Ewing‘s sarcomas (*EWS-FLI-1* fusion), myxoid liposarcomas (*TLS-CHOP* fusion) and synovial sarcomas (*SSX-SYT* fusion) (Vorburger and Hunt 2002). Further typical gene rearrangements that are found in sarcomas are listed in Table 1.3.

Tumor suppressor genes play an important role in cell growth inhibition and in the suppression of growth. These genes can be inactivated by two events: hereditary or sporadic. Two such genes that are relevant in soft tissue tumors are the retinoblastoma gene *RB1* and the tumor suppressor gene *TP53*. Deletions or mutations in the *RB1* gene can induce the development of retinoblastomas, soft tissue sarcomas and sarcomas of the bone. Mutation in the tumor suppressor gene *TP53* is the most frequent mutation

Table 1.3: Specific translocation in soft tissue sarcomas (Helman and Meltzer 2003)

Tumor type	Chromosomal translocation	Involved genes
Ewing-Sarkom/PNET	t (11;22) (q24; q12)	EWSR1-FLI1
	t (21;22) (q22; q12)	EWSR1-ERG
	t (7;22) (p22; q12)	EWSR1-ETV1
Desmoplastic small round-cell tumor	t (11;22) (p13; q12)	EWSR1-WT1
Clear cell sarcomas of soft tissue	t (11;22) (q13; q12)	EWS-ATF1
Myxoides chondrosarcoma	t (9;22) (q31; q12)	EWS-TEC
Alveolar rhabdomyosaroma	t (2;13) (q35; q14)	PAX3-FOXO1A
	t (1;13) (p36; q14)	PAX7-FOXO1A
Myxoid liposarcomas	t (12;16) (q13; p11)	FUS-DDIT3
	t (12;22) (q13; q12)	EWSR1-DDIT3
Synovial sarcomas	t (X;18) (p11; q11)	SYT-SSX
Dermatofibrosarcoma protuberans	t (17;22) (q22; q13)	COL1A1-PDGFB

in human solid tumors and is also noted in 30% to 40% of soft tissue tumors. Some rare cases of soft tissue sarcomas (i.e. with Li-Fraumenti syndrome) arise due to germline mutations in the gene *TP53* (Latres et al. 1994; Hieken and Das Gupta 1996).

1.2.2 Grading and staging of soft tissue sarcomas

Developing robust und reproducible criteria for grading and staging systems is critical in patient management. Staging and grading enable the physician to plan therapies, the comparison of experiences among centers and different treatments over time.

The grading system, based on the histological parameters predicts the malignancy of these tumors. The criteria defining the grade are the degree of differentiation, necrosis as well as the number of mitoses. A score is attributed to each of the three parameters independently. The grade is obtained by adding the three attributed scores (Table 1.4).

Staging is based on clinical and histological parameters and provides information concerning the extent of the tumor, with more information concerning prognosis and therapies.

For staging, the classification of soft tissue sarcomas by the TNM-system is needed and incorporates tumor size and depth (T), regional lymph node involvement (N) and distant metastasis (M) (Table 1.5). The TNM-classification comprises a 2, 3 and 4-tiered grading system (Table 1.6) (Fletcher et al. 2002).

The staging system was developed by the international Union against Cancer (UICC) and the American Joint Committee on Cancer (AJCC). It is clinically useful and acts is associated with different prognosis.

Table 1.4: Histopathologic grading of soft tissue sarcomas. Modified from Coindre et al. (1986)

Score	Description
Tumor differentiation	
Score 1	sarcomas closely resembling normal adult mesenchymal tissue
Score 2	sarcomas for which histological typing is certain
Score 3	embryonal and undifferentiated sarcomas, sarcomas of doubtful type
Mitotic count	
Score 1	0 - 9 mitoses per 10 high power field*
Score 2	10 - 19 mitoses per 10 high power field*
Score 3	20 or more mitoses per high power field*
Tumor necrosis	
Score 0	no necrosis
Score 1	less than 50 % tumor necrosis
Score 2	50 % or more tumor necrosis
Histological grade	
Grade 1	Score 2-3
Grade 2	Score 4-5
Grade 3	Score 6-8

*One field measures 0,1734 mm^2

Table 1.5: TNM-classification of soft tissue sarcomas. Modified from Fletcher et al. (2002)

Stage	description	local extent
T		**Primary tumor**
	TX	Primary tumor cannot be assessed
	T0	No evidence of primary tumor
	T1	Tumor maximal 5 cm in greatest dimension
		a) Superficial tumor
		b) Deep tumor
	T2	Tumor bigger than 5 cm in greatest dimension
		a) Superficial tumor
		b) Deep tumor
N		**Regional lymph nodes**
	NX	Regional lymph nodes cannot be assessed
	N0	No regional lymph node metastasis
	N1	Regional lymph node metastasis
M		**Distant metastasis**
	MX	Distant metastasis cannot be assessed
	M0	No distant metastasis
	M1	Distant metastasis
G		**Histologic grade (G)**
	GX	Grade cannot be assessed
	G1	Well-differentiated
	G2	moderately differentiated
	G3 - 4	poorly differentiated / undifferentiated

Table 1.6: Translation table for three and four to two grade system. Modified from Fletcher et al. (2002)

TNM two grade system	Three grade system	Four grade system
Low grade	Grade 1	Grade 1
		Grade 2
High grade	Grade 2	Grade 3
	Grade 3	Grade 4

The staging system described by UICC 2002 including four major stages is listed in Table 1.7 and is defined as follows:

- **Stage IA**: low grade, small, superficial or deep, no sign of any spread
- **Stage IB**: low grade, large, superficial or deep, no sign of any spread
- **Stage IIA**: high grade, small, superficial or deep, no sign of any spread
- **Stage IIB**: high grade, large, superficial, no sign of any spread
- **Stage III**: high grade, large, deep, no sign of any spread
- **Stage IV**: any grade, any T, regional lymph node metastasis, no distant metastasis or any grade, any T, any N, distant metastasis

Authentic predictive factors are essential for the classification of patients with cancer into useful staging categories. Due to the new insights into the molecular biology of cancer, new specific markers (e.g. c-Kit in gastrointestinal stromal tumors or estrogen receptor in breast cancer; Lahat et al. (2009)) for characterization have been found. The development of new techniques such as tissue microarray analyzes, have resulted in powerful tools for analyzing a large number of tumor entities to detect expression levels of relevant genes and their related proteins. Evaluation of hundreds of molecular markers in the same tumor specimens can be integrated in describing tumor progression, treatment response and survival.

1.2.3 Therapy

When the histological diagnosis and grade is established, a multidisciplinary team of surgeons, radiologist and medical oncologists should plan the most effective therapy for the patient.

Table 1.7: Staging of soft tissue sarcomas (Fletcher et al. 2002)

Stage IA	T1a	N0, NX	M0	low grade
	T1b	N0, NX	M0	low grade
Stage IB	T2a	N0, NX	M0	low grade
	T2b	N0, NX	M0	low grade
Stage IIA	T1a	N0, NX	M0	high grade
	T1b	N0, NX	M0	high grade
Stage IIB	T2a	N0, NX	M0	high grade
Stage III	T2b	N0, NX	M0	high grade
Stage IV	any T	N1	M0	any G
	any T	Jedes N	M1	any G

1.2.3.1 Surgery

Surgery remains the primary treatment of sarcomas. Nevertheless the physician must balance the goal of minimizing local and distant recurrence with the aim of maintaining function and quality of life. In general, the extent of the excision is based upon the size of the tumor, its anatomic location relating to normal structures and the degree of function that would be lost after surgery. For subcutaneous or intramuscular high grade sarcomas less than 5 cm or low grade tumors of any size, surgery alone should be sufficient if wide resection margins can be achieved. In case of extramuscular involvement or if the tumor is too close to the resection margins, adjuvant radiotherapy can be added to reduce local recurrence (Fletcher et al. 2002).

1.2.3.2 Adjuvant and neo-adjuvant therapy

For high grade sarcomas, there are certain treatment strategies with the aim of achieving good local control and also reducing the risk of development of subsequent metastasis. The outcome of systemic chemotherapy depends on the entity of the sarcomas. For certain soft tissue tumors, adjuvant chemotherapy is reasonable even if the primary tumor is resected, because of the risk of developing subsequent metastasis. In general, the histological type and location of soft tissue sarcomas are important predictors of sensitivity to chemotherapy. The most frequently used drugs in soft tissue sarcomas are doxorubicin and ifosfamide (Fletcher et al. 2002).

For the treatment of large high grade extremity sarcomas several multimodal protocols of chemotherapy, radiation and surgery have been investigated. In general there are three approaches (Fletcher et al. 2002):

1. neoadjuvant chemotherapy > surgery > adjuvant chemotherapy + post operative radiotherapy

2. neoadjuvant chemotherapy interdigitated with preoperative radiotherapy > surgery > adjuvant chemotherapy

3. neoadjucant chemotherapy > preoperative radiotherapy > surgery > adjuvant chemotherapy

Because of the large size, the tendency to invade nearby organs and the difficulty in achieving a complete surgical resection of retroperitoneal and visceral sarcomas, a complex strategy is demanded. For this, a new modality has been designed termed intraoperative radiotherapy (IORT). This approach allows the sterilization of microscopic diseases *in situ* with high single doses of radiation while minimizing the dose to adjacent normal tissues. For these reasons, patients with recurrent and locally advanced malignancies, IORT is appropriate, in addition to resection (Tran et al. 2008). Nevertheless, local control remains a significant problem that leads to unresectable local disease and death in many cases.

1.3 Analyzed soft tissue sarcomas

1.3.1 Liposarcomas

Adipose tumors incorporate the most common group of mesenchymal tumors, because of the high prevalence of benign lipomas and benign angiolipomas. Liposarcomas represent the largest group of soft tissue sarcomas with three main subtypes:

- well differentiated/dedifferentiated
- myxoid
- pleomorphic

Histological subtypes of liposarcomas are different entities with different morphology, genetics and natural histology. The distinctive karyotypic aberrations can assist in diagnosis (Fletcher et al. 2002).

1.3.1.1 Dedifferentiated Liposarcomas

Dedifferentiation, the loss of form or function, occurs in approximately 10% of well differentiated liposarcomas of any subtype. The risk of dedifferentiation seems to be higher in deep located lesions and is significantly less in the limbs. The probability of dedifferentiation represents more a time dependent than a site-dependent phenomenon. There is no sex predilection. Dedifferentiated liposarcomas arise most frequently *de novo* while 10% occur as recurrence (Weiss 2001).

The retroperitoneum is the most frequent location of dedifferentiated liposarcomas, followed by the soft tissue sarcomas of the extremities (ratio of 3:1). Rare sites of locations include the spermatic cord, the head and neck and subcutaneous tissue.

Dedifferentiated liposarcomas most often have ring or giant marker chromosomes even if the number of karyotyped cases is too little to establish significant differences to well differentiated liposarcomas (Fletcher et al. 1996; Meis-Kindblom et al. 2001; Mertens et al. 1998). Molecular cytogenetics and genetic studies with comparative genomic hybridization (CGH) and fluorescence *in situ* hybridization (FISH) have identified an amplification of the 12q13-21 region associated with co-amplification of other regions. Southern blot analyzes revealed *MDM2* amplification in 5/5 retroperitoneal cases, but no amplification in 4/4 non-retroperitoneal dedifferentiated liposarcomas cases. In addition the non-retroperitoneal cases without amplification on the *MDM2* locus are found to have *TP53* mutations (Pilotti et al. 1997; Schneider-Stock et al. 1998; Dei Tos et al. 1997) .

Dedifferentiated liposarcoma is characterized by relapse in at least 40% of cases. The incidence of distant metastases ranges from 15-20% with an overall mortality between 28 and 30% at five years follow-up (Henricks et al. 1997; McCormick et al. 1994; Weiss and Rao 1992). The anatomic location of dedifferentiated liposarcomas is the most important prognostic factor and retroperitoneal lesions have the worst outcome. The size of dedifferentiated regions does not seem to influence the clinical outcome. Even with high grade morphology, dedifferentiated liposarcomas are less aggressive in their clinical behavior than other types of high grade tumors such as pleomorphic sarcomas. The cause of this difference is not yet known, but it is to be assumed that the absence of complex karyotypic aberrations as well as integrity of the *TP53* gene in most cases may explain the discrepancy between morphology and clinical outcome (McCormick et al. 1994; Weiss and Rao 1992; Cordon-Cardo et al. 1994).

1.3.1.2 Myxoid Liposarcomas

Myxoid liposarcomas (MLS) represent approximately 10% of all adult soft tissue sarcomas and they account for more than one third of liposarcomas. The most common location of myxoid liposarcomas is the deep soft tissue of the extremities and, in more than two-thirds of the cases, MLS occurs within the musculature of the thigh. MLS arise less frequent in the retroperitoneum or in subcutaneous tissue.

In more than 90% of cases the karyotypic hallmark of myxoid and round cell liposarcomas is the t(12;16)(q13;p11) translocation, wich leads to the fusion of the *DDIT3* (a.k.a.*CHOP*) and *FUS* (a.k.a. *TLS*) genes and generates the hybrid protein FUS/DDIT3 (Table 1.3). A rare variant chromosomal translocation in MLS is t(12;22)(q13;q12). In these cases, *DDIT3* fuses with *EWS* (Sreekantaiah et al. 1992; Turc-Carel et al. 1986). The occurrence of the *FUS/DDIT3* fusion in MLS entity is highly sensitive and specific and is absent in other cases, which show features of MLS (Antonescu et al. 2000a). High histologic grade and *TP53* overexpression are predictors of unfavorable outcome. In comparison with some other translocation-associated sarcomas, the presence of fusion

transcripts in MLS does not seem to influence the impact on histologic grade or clinical outcome (Antonescu et al. 2001; Smith et al. 1996).

1.3.1.3 Pleomorphic Liposarcomas

The rarest subtype of liposarcomas are pleomorphic liposarcomas, accounting for about 5% of all liposarcomas and 20% of pleomorphic sarcomas. The majority of this tumor entity arises in older patients (>50 years). There is no sex predilection (Azumi et al. 1987; Fletcher 1992).

The occurrence of pleomorphic liposarcomas is most common in the extremities whereas the trunk and the retroperitoneum are infrequently affected. Although most cases arise in deep soft tissue, rare sites of involvement include regions such as the mediastinum, the paratesticular region and dermis (Klimstra et al. 1995; Cai et al. 2001; Dei Tos et al. 1998; Downes et al. 2001).

The karyotypic data from 11 investigated pleomorphic liposarcomas have shown a high number of chromosomal imbalances, complex structural rearrangements, including numerous indefinable marker chromosomes and polyploidy (Sreekantaiah et al. 1992; Mertens et al. 1998). The intratumoral heterogeneity has made the identification of specific rearrangements challenging.

Unlike well differentiated liposarcomas, amplification of the 12q14-15 region did not appear consistently in all pleomorphic liposarcomas (Fritz et al. 2002). Analyzes by comparative genomic hybridization (CGH) identified a number of chromosomal gains and losses (Szymanska et al. 1996). The amplification of the *MDM2* gene was detected in about one third of the cases and could be associated with the occurrence of ring chromosomes. In 4/9 of cases studied, *TP53* alterations or loss of heterozygosity were observed, whereas all 4 cases were negative for *MDM2* amplification (Schneider-Stock et al. 1998; Nilbert et al. 1994).

For pleomorphic liposarcomas, tumor depth and size, the amount of mitoses and necrosis are associated with clinical prognosis (Downes et al. 2001; Miettinen and Enzinger 1999).

1.3.2 Leiomyosarcomas

Leiomyosarcoma of the soft-tissue usually occurs in middle-aged or older persons even though it may develop in young adults and in children (de Saint Aubain Somerhausen and Fletcher 1999; Swanson et al. 1991). Leiomyosarcoma arise most frequently in the retroperitoneum and are the predominant sarcomas arising from larger blood vessels. In general, tumor location is associated with sex incidence. A clear majority of patients with retroperitoneal and inferior vena cava leiomyosarcoma are women, but there is no sex predilection of leiomyosarcoma in other soft tissue sites (Hisaoka et al. 2008; Berlin et al. 1984; Kevorkian and Cento 1973). The most common location of soft tissue leiomyosarcoma is the retroperitoneum followed by leiomyosarcoma arising in large

blood vessels such as the inferior vena cava or the large veins of the lower extremity, and sometimes in arteries. A third group constitutes leiomyosarcomas involving non-retroperitoneal soft tissue. This subtype is found for example in the lower extremity, intramuscular or subcutaneous regions (Dahl and Angervall 1974; Farshid et al. 2002; Hashimoto et al. 1986).

Karyotypes from around 100 leiomyosarcomas have shown complex rearrangements and no consistent aberrations (Wang et al. 2001). Chromosomal losses include the regions 3p21-23, 8p21-pter, 13q12-13 and 13q32-qter, whereas the chromosomal regions 1q21-31 show gains. In addition, comparative genomic hybridization (CGH) has identified numerical changes, including gains of chromosomes 1, 15, 17, 19, 20, 22 and losses of chromosomes 1q, 2, 4q, 9p, 10, 11q, 13q and 16. No significant differences among the different subtypes are found, but tumor size-related differences are observed, such as gains of 16p and 17p for smaller tumors and gain of 6p and 8q for larger tumors (Mandahl et al. 2000; Wang et al. 2001; El-Rifai et al. 1998). Further molecular genetic analyzes show abnormalities of the *RB1* gene as well as proteins involved in the Rb-cyclinD pathway (Stratton et al. 1990). Involvement of the two genes *TP53* and *MDM2* appears less frequently than in other sarcomas types (Dei Tos et al. 1996).

Soft tissue leiomyosarcomas are marked by local recurrence and distant metastasis whereas local lymph node metastasis is rare. The most important prognostic factors are localization and size of the tumor. The majority of cases of leiomyosarcomas of the retroperitoneum are lethal due to the large size and the difficulty or impossibility in resecting the tumor completely. Even when leiomyosarcomas are completely resected, there is still a poor prognosis due to local recurrence and metastasis of soft tissue leiomyosarcoma, which become obvious within the fist few years and, in some cases, up to 10 years after diagnosis (Fletcher et al. 2002).

1.3.3 Synovial Sarcomas

Synovial sarcomas accounts for 5 to 10% of soft tissue sarcomas (Kransdorf 1995). They arise mainly in young adults and more common in males even though rare cases are reported in the elderly (Fletcher et al. 2002). Despite of its nomenclature, synovial sarcomas is unrelated to synovia and less than 5% originate within a joint or bursa, whereas more than 80% arise in deep soft tissue of extremities. About 5% occur in the head and neck region, however it seems that any site can be affected (Argani et al. 2000; Fisher 1998; Flieder and Moran 1998). There are no specific predisposing factors, but synovial sarcomas has a chromosomal translocation that is probably relevant in pathogenesis.

The cytogenetic hallmark of synovial sarcomas is the t(X;18)(p11;q11) translocation, found in about 90% of the 150 cases investigated (Mitelman and Mertens 2009). The genes affected by the t(X;18) translocation are isolated and include the *SS18* (=*synovial sarcoma translocation, chromosome 18*) on chromosome 18 and the genes *SSX1, SSX2* and *SSX4* on chromosome X (Clark et al. 1994; de Leeuw et al. 1995). Several stud-

ies have shown that the t(X;18) translocation arises exclusively in synovial sarcomas whereas two-thirds show an *SS18/SSX1* fusion, one-third an *SS18/SSX2* fusion and three separate cases an *SS18/SSX4* fusion of at least 350 investigated synovial sarcomas (Sandberg and Bridge 2002; dos Santos et al. 1997, 2001).

The probability of recurrence of synovial sarcomas is approximately 50%, usually within 2 years but sometimes up to 30 years after diagnosis (Weiss 2001). About 40% of the tumors show metastasis, commonly to lung, and bone and in some cases, with regional lymph node involvement. Postoperative radiotherapy and local excision can control local recurrence. The following features are predictors for a good patient outcome in synovial sarcomas (Lewis et al. 2000; Friedberg et al. 1999; Spillane et al. 2000):

- occurrence in childhood patient
- tumors less than 5 cm in diameter
- tumors with less than 10 mitosis /hpf (Table 1.4)
- tumors with no necrosis (Table 1.4)
- tumor is eradicated locally

Synovial sarcomas with the *SS18/SSX2* translocation have a better prognosis (Antonescu et al. 2000b; Nilsson et al. 1999). The overall 5 year survival rate is between 36-76% and the 10 year survival rate is between 20-63% (Weiss 2001).

1.3.4 Maligne Peripheral Nerve Sheath Tumors (MPNST)

MPNST account for nearly 5% of malignant tumors of soft tissue (Lewis and Brennan 1996). Almost one half to two thirds arise from neurofibromatosis (Ducatman et al. 1986), often of the plexiform type and in association with neurofibromatosis type 1 (NF1). Less frequently, MPNST arise *de novo* from peripheral nerves (Scheithauer and Woodruff J.M. 1999). Only a few cases occur in conventional schwannomas (Woodruff et al. 1994), ganglioneuroblastomas/ ganglioneuromas (Ricci et al. 1984) or phaeochromocytomas (Sakaguchi et al. 1996).

Adults in the third to the sixth decades of life are most frequently affected by MPNST. Patients with NF1-associated MPNST are approximately 28-36 years old, whereas patients with sporadic MPNST are about 40-44 years (Ducatman et al. 1986). NF1-associated MPNST are more frequent in males, while non-NF1-associated cases are more frequent in females. Large and medium-size nerves are more often involved than small nerves. Most frequently affected sites include the buttock and thigh, brachial plexus and upper arm and the paraspinal region, where the sciatic nerve is most commonly involved (Best 1987). MPNST occur less frequently, for example intraparachymal or in the cranial nerve (Sharma et al. 1998).

Genetic analyses in sporadic and NF1-associated MPNST have shown complex karyotypic abnormalities that are both numerical and structural. These findings include near-triploid or hypodiploid chromosome numbers, chromosomal losses, loss of genetic material related to structural aberrations and recombinations (Sharma et al. 1998). Analyses of 10 MPNST have shown that structural abnormalities of chromosome 17 involving the *NF1* and the *TP53* loci were frequent. Gains of chromosomes 2 and 14 and losses of chromosomes 13, 17 and 18 are noted, but no cytogenetic differences between sporadic and NF1-associated cases are established (Jhanwar et al. 1994; Kobayashi et al. 2006).

In NF1-associated MPNST cases, inactivation of both *NF1* alleles are detected, involving this gene in MPNST development (Legius et al. 1993). Sporadic MPNST also show alterations at the *NF1* locus, which are thought to be involved in early stages of nerve sheath tumorigenesis such as in neurofibroma-genesis rather than in malignant progression to MPNST. The latter one seems to be associated with alterations of genes controlling cell cycle regulation such as the gene *TP53*, which is mutated and altered in MPNST (Legius et al. 1994). In addition, homozygous deletion of the gene *CDKN2A*, which encodes the $p16^{INK4a}$ and $p14^{ARF}$ cell cycle inhibitory molecules, is found in the progression of neurofibromatosis to MPNST but not in neuro-fibromas. This deletion also inactivates the adjacent *CDKN2B* gene that encodes the p15 molecule (Perrone et al. 2003; Nielsen et al. 1999). Furthermore, these events seem to inactivate the p53 and pRb regulatory pathways in almost 75% of MPNST cases (Perrone et al. 2003).

MPNST are extremely aggressive tumors with a poor prognosis, except for those with perineural cell differentiation. The mortality is about 60% Ducatman et al. (1986), and even higher in patients with paraspinal lesions (80%) (Kourea et al. 1998) and those with divergent angiosarcomas (100%) (Scheithauer and Woodruff J.M. 1999). The 5- and 10-years survival rates are between 34% and 23% (Ducatman et al. 1986).

1.3.5 Malignant Fibrous Histiocytoma (MFH)

Although the precise origin of MFH has been discussed for decades, the term of MFH gives the impression that the origin of the tumor cells is fibroblastic and histiocytic. With the improvement of diagnostic techniques such as immunohistochemistry, cell culture and electron microscopy, a number of studies have tried to clarify the histogenesis of MFH. These studies suggest that MFH is a sarcomas of either fibroblast or primitive mesenchymal origin. While the nomenclature of MFH is still discussed, the WHO maintained the term MFH in its 2002 classification of soft tissue tumors. Currently five subtypes of MFH are distinguished which are listed in Table 1.8, including the old and the current nomenclature (Al-Agha and Igbokwe 2008).

1.3.5.1 Undifferentiated High-grade Pleomorphic Sarcomas (WHO 2002)

Undifferentiated high-grade pleomorphic sarcomas arise most frequently in the extremities, especially the lower limb, and less commonly in the trunk. The second most

Table 1.8: Old and current nomenclature of MFHs (Al-Agha and Igbokwe 2008)

old Nomenclature	current Nomenclature of MFH (WHO 2002)	Tumor-Category
storiform-pleomorphic MFH	undifferentiated high-grade pleomorphic sarcomas	Fibrohistiocytic
Myxoid MFH	Myxofibrosarcoma	Myofibroblastic
Giant cell MFH	undifferentiated pleomorphic sarcomas with giant cells	Fibrohistiocytic
Inflammatory MFH	undifferentiated pleomorphic sarcomas with prominent inflammation	Fibrohistiocytic
Angiomatoid MFH	Angiomatoid fibrous histiocytoma	Tumors of uncertain differentiation

common cases occur in deep (subfascial) tissue, whereas less than 10% are primarily subcutaneous. Undifferentiated high-grade pleomorphic sarcomas are aggressive tumors with an 5-year survival rate of 50-60% (about genetics see chapter 1.3.5.4) (Fletcher et al. 2002).

1.3.5.2 Undifferentiated Pleomorphic Sarcomas with Giant Cells (WHO 2002)

Tumors in this general category arise predominantly in deep soft tissue of the limbs or trunk. The most common organs in which giant cell-rich tumors occur include pancreas, thyroid, breast and kidney. In consideration of prognostic factors, undifferentiated high-grade sarcomas with osteoclastic giant cells have a similar prognosis to other pleomorphic sarcomas (about genetics see section 1.3.5.4) (Fletcher et al. 2002).

1.3.5.3 Undifferentiated Pleomorphic Sarcomas with Prominent Inflammation

The most frequent location of undifferentiated pleomorphic sarcomas with prominent inflammation is the retroperitoneum, but intra-abdominal and deep soft tissue location have also been observed. Two-third of the patients with persistence or recurrence died due to their diseases, whereas one-fourth of patients developed distant metastasis. Similar to other retroperitoneal sarcomas, these patients have a poor prognosis which is related to the extent of the tumor and the difficulty of complete resection at the time of diagnosis (about genetics see section 1.3.5.4) (Fletcher et al. 2002).

1.3.5.4 Genetics in MFH

On the basis of the shifting diagnostic criteria between the past and the present, the genetic aspects of malignant fibrous histiocytomas are challenging to evaluate. In consideration of these shortcomings, cytogenetic aberration are observed in more than 50

cases of MFH subtypes such as storiform or pleomorphic (Mitelman and Mertens 2009). Currently just a few cases of giant cell and inflammatory MFH are investigated. However, genetic analyses have shown complex karyotypes with extensive intratumoral heterogeneity and chromosome numbers in the triploid or tetraploid range (Mandahl et al. 1985; Molenaar et al. 1989; Orndal et al. 1994; Simons et al. 2000). Although no specific structural or numerical aberrations are observed, telomeric associations and ring chromosomes are frequent. Due to the occurrence of numerous marker chromosomes in almost all cases, the proper determination of genomic imbalances is difficult to assess from these cytogenetic data (Fletcher et al. 2002).

Genomic imbalances include frequent losses of the chromosomal region 2p24-pter and 2q32-qter, and losses on 11, 13 and 16 (Larramendy et al. 1997; Mairal et al. 1999; Parente et al. 1999; Simons et al. 2000) whereas gains are found on 7p15-pter, 7q32 and 1p31.

Several proto-oncogenes such as *SAS, MDM2, CDK4* or *CHOP* are related to the chromosome region 12q13-15 and are suggested to be involved in the development of MFH-like pleomorphic sarcomas. The candidate gene *MASL1* is found on the chromosomal region 8p23.1 (Berner et al. 1997; Reid et al. 1996; Sakabe et al. 1999).

No clear relationships are found between clinical outcome and alterations (such as mutation and/or deletion) of *TP53, RB1* and *CDKN2* although they are suggested to play a crucial role in pleomorphic sarcomas development (Reid et al. 1996; Simons et al. 2000).

1.3.5.5 Myxofibrosarcoma

Myxofibrosarcoma is one of the most frequent sarcomas that commonly occurs in older patients with a slight male predilection. The most common affected sites are the limbs including the limb girdles. These tumors occur less frequently in the trunk, in the head and neck, and on the hands and feet. They are seen only rarely in the retroperitoneum and abdominal cavity. Interestingly, about two-third of myxofibrosarcoma arise in dermal/subcutaneous tissue with a proportion occurring in the underlaying fascial and skeletal muscle (Mentzel et al. 1996; Merck et al. 1983; Weiss and Enzinger 1977).

In about 25 cases diagnosed as myxoid MFH or myxofibrosarcoma cytogenetic aberrations such as complex karyotypes with high intratumoral heterogeneity and triploid or tetraploid chromosomes are detected. Ring chromosomes were found in five investigated cases. In addition, comparative genomic hybridization (CGH) was identified genomic imbalances, including loss of 6p and gains of 9q and 12q (Mandahl et al. 1985; Molenaar et al. 1989; Orndal et al. 1994; Simons et al. 2000; Meloni-Ehrig et al. 1999).

The occurrence of metastasis and tumor associated mortality in deeply located and high grade lesions is much higher, whereas the depth and grade of malignancy do not have the high rate of local recurrence. In addition, tumor associated mortality is notably increased in cases with local recurrence in less than 12 months (Mentzel et al. 1996; Merck et al. 1983; Weiss and Enzinger 1977). There is a slight association between histological tumor grade and proliferating activity, as well as the percentage of aneuploid cells and

tumor vascularity, but nevertheless, no strong relation with the clinical outcome (Mentzel et al. 1996, 2001).

1.3.5.6 Angiomatoid Fibrous Histiocytoma (AFH)

Angiomatoid fibrous histiocytoma (AFH) account for about 5% of tumors described as malignant fibrous histiocytoma and approximately 0.3% of all soft tissue sarcomas. AFH occur most commonly in children and young adults but other age groups may also be affected (Argenyi et al. 1988; Fanburg-Smith and Miettinen 1999). There is no clear gender predilection (Costa and Weiss 1990; Enzinger 1979).

AFH arise most commonly in the extremities, followed by the trunk and head and neck (Fanburg-Smith and Miettinen 1999).

Only one case of angiomatoid MFH was so far analyzed showing chromosomal aberration. These observed rearrangements include chromosome 2, 12, 16 und 17 as well as del(11)(q24). Furthermore, translocation on chromosome band 16p11 and 12q13 with the FUS/ATF1 protein are found (Waters et al. 2000).

Less than 1% metastasis and almost 2-11% recurrence were described in AFH (Costa and Weiss 1990; Fanburg-Smith and Miettinen 1999). These tumors are generally non-lethal and have a low mortality due to the late distant metastasis (Costa and Weiss 1990; Enzinger 1979). Furthermore, AFH show no clinical morphological or genetic factors that predict metastasis (Costa and Weiss 1990; Fanburg-Smith and Miettinen 1999).

1.4 Telomere-maintenance mechanisms in soft tissue sarcomas

Telomere shortening in consequence of cell division, due to the incomplete synthesis of linear DNA during replication, plays an important role in both the suppression and pathogenesis of cancer. Therefore, the activation of a telomere maintenance mechanism (TMM) is essential for cellular immortalization and thus for long-term tumor growth. Most human cancers, especially those of epithelial origin, use the activation of telomerase as their telomere maintenance mechanism, whereas others use an alternative lengthening of telomeres (ALT) mechanism. The latter one in particular includes subtypes of soft tissue sarcomas (Henson et al. 2002) and occurs most commonly in tumors with complex karyotypes, astrocytic brain tumors and osteosarcomas. The prognostic significance in either ALT or telomerase positive tumors varies according to the type of tumor. Therefore, the characterization and understanding of the telomere maintenance mechanism in tumorigenesis could have important implications for the diagnosis, treatment and the development of new strategies for therapy.

Table 1.9: Telomere sequences and lengths in different organisms (modified by Moon and Jarstfer (2007))

Group (Organism)	Telomere length dsDNA	Telomere sequences (5' to 3' toward the end)
Vertebrate (Human)	5-15 kb	TTAGGG
Vertebrate (Mouse)	about 30-120 kb	TTAGGG
Filamentous fungi (Didymium)	100-400 bp	TTAGGG
Ciliate (Tetrahymena)	250-400 bp	TTAGGG
Ciliate (Euplotes)	exactly 28 bp	TTTTGGGG
Higher plant (Arabidopsis thaliana)	2,5-5 kb	TTAGGG(T/C)
Green algae (Chlamydomonas)	300-350 bp	TTTAGGG
Insect (Bombyx mori)	6-8 kb	TTAGG

1.4.1 Telomeres: A brief insight

Modern interest in telomeres has its roots in experiments carried out by Hermann J. Müller and Barbara McClintock in the 1930s. Both investigators, working separately and with different organisms, realized that chromosome ends are special structures that provide stability. The term "telomere", coined by Müller, originate from the Greek for "end" (telos) and "part" (meros). Hermann J. Müller observed that X-ray irradiation leads to structural chromosomal changes and that the natural chromosome ends were never affected in these rearrangements (Müller 1938). In addition, McClintock discovered that without these end caps, chromosomes stick one to another, undergo structural changes and misbehave in some other ways (McClintock 1941). In 1978, the precise assembling of the telomeres was determined by discovering that telomeres in *Tetrahymena thermophila* are composed of an extremely short and simple sequence of Thymines (T) and Guanines (G) -TTGGGG- repeated 20-70 times (Blackburn and Gall 1978).

1.4.1.1 The telomere sequence

Telomeres are repetitive DNA sequences located at the termini of linear chromosomes of all mammalian cells, likely of almost all eukaryotes and in a few prokaryotic organism. The telomere length varies between species from about 300-600 bp in yeast (Shampay et al. 1984) and up to many kilobases in human (Table 1.9). The mammalian chromosomes are composed of linear tandem TTAGGG repeats which in humans are naturally 10-15 kb long (Blasco 2005). However, regardless of arrangements and the number of telomeric repeats, all telomeres share some characteristics: one strand of the repeated telomeric DNA sequence is marked by clusters of guanine (G) residues, the so called G-rich strand and a complementary cytosine (C), C-rich strand. The G-rich strand is always found at the 3'end of each chromosomal DNA (Klobutcher et al. 1981). The ex-

Table 1.10: Telomere proteins

Telomere Proteins	abbreviation
Telomeric-repeat-binding factor 1	TRF1
Telomeric-repeat-binding factor2	TRF2
TRF1-interacting nuclear factor2	TIN2
TRF2-interacting RAP1	RAP1
Putative telomere-end-binding protein	POT1
Binding protein of POT1	TPP1

ception proves the role: Instead of the typical telomeric repeats the species *Drosophila melanogaster*, for example, has retrotransposons and the mosquito *Anopheles gambiae*, as well as the onion *Allium cepa*, show complex-sequence tandem repeats (McEachern et al. 2000).

1.4.1.2 Telomeric proteins and higher order telomere structure

A number of specific proteins were identified that directly, or via other proteins, interact with telomeric DNA. Six of them (Figure 1.1 and Table 1.10) exclusively are dedicated to specifically bind to telomeres throughout the cell cycle, and they do not accumulate or function elsewhere in the nucleus. These are the telomere repeat factor 1 and 2 complexes (TRF1 und TRF2) and the protection of telomeres 1 protein (POT1), which all bind directly to the double-stranded telomeric repeats. Further proteins of the six, such as TRF1-interacting nuclear protein 2 (TIN2), do not directly bind to DNA but nevertheless are components of the regulatory complexes. The TRF1 complex consists of both TIN2 and POT1 and is involved in telomere-length homeostasis, whereas the TRF2 complex protects the telomere integrity by remodeling telomeres into telomere-loops. TRF1, TRF2, POT1 and TIN2, in association with TPP1 and RAP1, have been detected as a telomeric core, referred to as the shelterin complex with its function to distinguish their natural chromosome ends from DNA breaks, repress DNA repair reaction, and regulate telomere-based telomere maintenance. The shelterin complex and its proteins specially localize to telomeres, and do not function elsewhere in the nucleus (de Lange 2005; Calcagnile and Gisselsson 2007).

Telomeres and their associated proteins form a higher order structure. Currently two models are discussed:

- T-loop model (Figure 1.1)
- G-quadruplex structure (Figure 1.2)

As mentioned before (1.4.1.1), human telomeres end in a 150-200 nucleotide G-rich single-stranded overhang. The G-rich overhang is capable of folding back and annealing

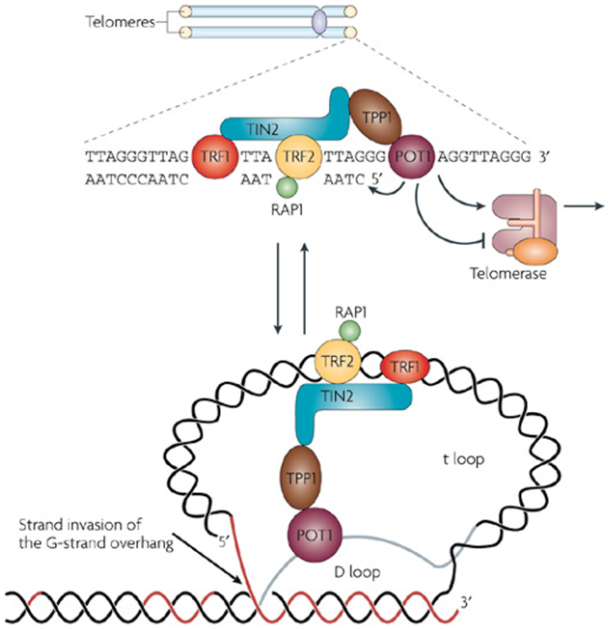

Figure 1.1: Telomere structure and telomere-associated proteins. **a)** TTAGGG repetitive sequence of mammalian chromosomes that end in a 3'single-stranded overhang. Telomeric DNA is composed of six-proteins (shelterin complex) which are TRF1, TRF2, TIN2, TPP1, RAP1 and POT1. **b)** Formation of duplex loops; double stranded DNA is folded in the so called T-loop, while a single-stranded overhang undergoes limited strand invasion to form the D-loop. (taken from Deng et al. (2008))

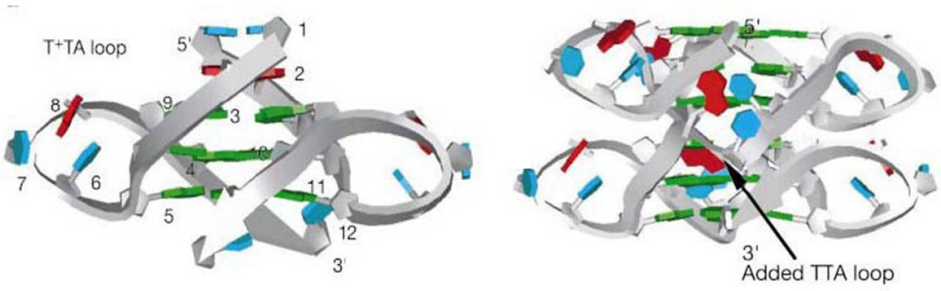

Figure 1.2: Models of G-quadruplex structure. **left)** quadruplex with the phosphate sugar backbone ribbon (gray) showing 5'-3'directionality **right)** G-quadruplex repeats could be stacked 3'to 5' whereas the upper stack has been rotated relative to the lower quadruplex, with a TTA loop medelled between the two to link them (taken from Parkinson et al. (2002))

with the double-stranded region of the TTAGGG repeats to form a telomeric loop (Figure 1.1), termed T-loop (Calcagnile and Gisselsson 2007; Blasco 2005). As a result, a part of the strand along the length of the overhang-invasion is displaced and forms a single strand DNA region which is known as D-loop (Shin et al. 2006). T-loops are composed of only telomeric sequences and therefore the loop size is proportional to the telomere length of human and mouse cells. The T-loop structure has been assumed as a mechanism for chromosomal end-protection. These telomere "capping" structures defend the telomeres from being degraded, fused with one another or recognized as double-stranded breaks through checkpoints and therefore initiate senescence or apoptosis (Blasco 2005; Calcagnile and Gisselsson 2007).

Crystal analysis of telomeres resulted in an alternative model, the G-quadruplex structure (Figure 1.2). The G-rich ends of human telomeres can fold into four-stranded G-quadruplex structures and can be inter- and intramolecular. The intermolecular quadruplexes are formed by two or four separate strands, which associate, whereas the intramolecular quadruplex is formed by either two or four repeats such as the four repeats in human telomeric DNA (d[AGGG(TTAGGG)$_3$]) (Smith and Feigon 1992; Parkinson et al. 2002).

Telomeric ends of chromosomes are essential in protecting the cell from recombination and degradation. Disruption of telomere maintenance potentially inhibits tumor growth, which can be utilized for developing therapeutic strategies. Furthermore, it was shown that a quadruplex structure could negatively influence the telomeric complex which causes dysfunctional telomeres. (Parkinson et al. 2002; Yanez et al. 2005). Therefore, the stabilization of telomeric ends as G-quadruplex structures seems to be an approach in developing new therapeutic strategies. These strategies could destabilize telomere maintenance in tumor cells. (reviewed in Raymond et al. (2000); Boukamp and Mirancea (2007)).

1.4.1.3 Telomere length regulation

Telomere length regulation and telomere-length-dependent interaction play a significant role in genomic integrity and were studied extensively in the past. It is known that critical short telomeres play an important role in genomic instability and therefore in the pathology of human disease.

But how do critically short telomeres arise? It was believed that all cultured cells were potentially immortal, as it is the case for several cancer cell lines such as HeLa. In 1961 it was observed by Hayflick and Moorhead that normal human diploid fibroblast have a limited replication capacity (HAYFLICK and MOORHEAD 1961). Human fibroblast taken from different embryonic donors underwent a finite number of population doublings (PDs) between 40 and 60, the so called Hayflick limit (Hayflick 2000). The so called "Mitotic clock", responsible for the Hayflick limit, was unknown until it was shown that *in vitro* telomere length decreases with each population doubling (Harley et al. 1990).

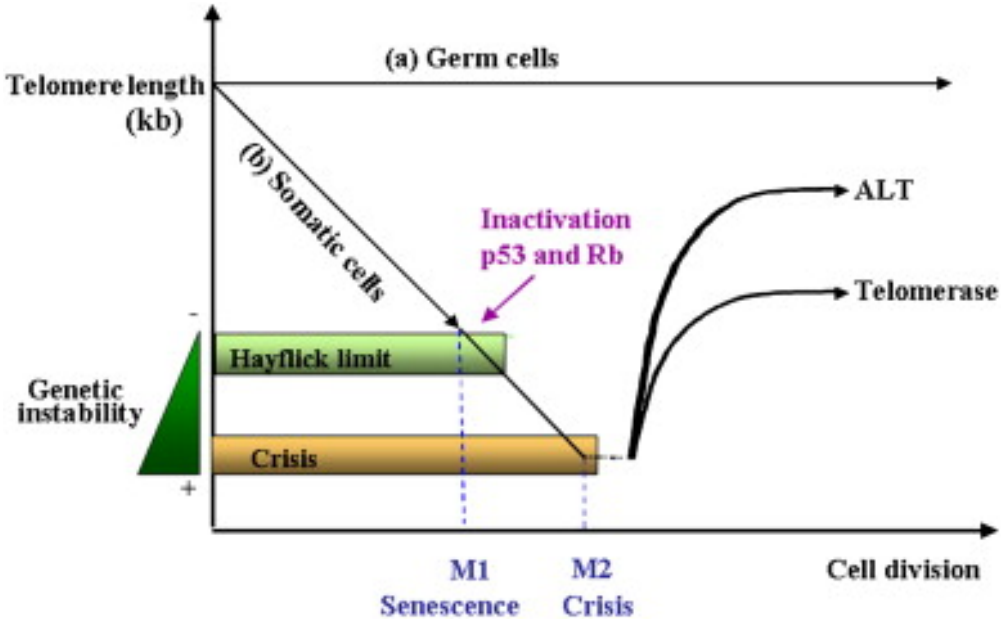

Figure 1.3: Hypothesis of telomere length and its assumed effect Telomere shorten due to the end-replication problem until they reach the first block, known as senescence. Cells undergo senescence by loss of both p53 and Rb tumor suppressor pathway and continue to divide until they reach the second block, referred to as crises. Rare cells emerge crises by the activation of a telomere maintenance mechanism such as telomerase activity or the ALT mechanism. (taken from Nittis et al. (2008))

1.4.1.4 Telomere shortening

At the time of their switch to linear genomes, eukaryotes must have designed a mechanism to reorganize their chromosome ends, exhibiting two major problems. The first one is the known end-replication problem. It was proposed independently by Olovnikov (1971, 1973) and Watson (1972) that DNA polymerase is not able to fully replicate the linear ends of DNA with each replication cycle. The DNA-replication machineries use short primers to initiate DNA synthesis. Elimination of the terminal primers at the end of the lagging-strand leads to a small gap that cannot be filled. This gap results in the loss of terminal sequences. The second problem is that cells must distinguish between their natural chromosome ends and sites of DNA damage in order to avoid checkpoint activation and inappropriate DNA-repair (de Lange 2004).

Telomere lengths shorten in normal somatic cells after each cell division due to the inability of the cell to replicate their chromosomes ends completely (Harley et al. 1990). Furthermore, telomeres below a certain size threshold cause irreversible growth arrest referred to as replicative senescence. In this state, cells stop dividing but are still viable. One possibility for cells to bypass senescence is the inactivation of the p53 and Rb tumor suppressor pathway, resulting in cellular proliferation and further telomere shortening (Figure 1.3). These cells then reach a second block, which is called crisis and is characterized by telomere dysfunction and cell death. The bypass of crisis and the maintenance

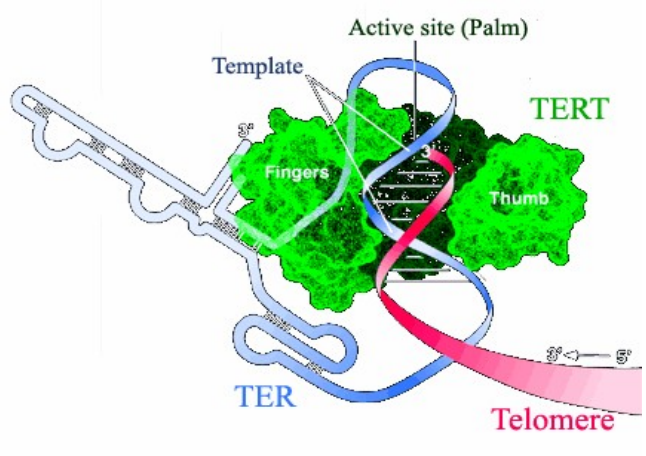

Figure 1.4: Telomerase as ribonucleoprotein complex; telomerase act as reverse transcriptase and contains an RNA template (TER, blue) and the catalytic protein component (TERT, green) which adds telomeric repeat sequences to the telomere DNA strand (red) (Telo).

of stable telomere length may be achieved by the activation of telomere maintenance mechanisms such as the activation of telomerase and/or the alternative lengthening of telomeres (ALT) (Wei and Sedivy 1999; Shay and Roninson 2004).

1.4.2 Telomerase activity as telomere length maintenance

Telomerase, a large multisubunit ribonucleoprotein complex, is responsible for synthesising telomeric repeats and thus for telomere length maintenance. Telomerase is a reverse transcriptase and uses this mechanism to copy an RNA template into DNA. This reverse transcriptase contains its own template RNA (TR) that, together with a protein component (hTERT), constitutes a core enzyme. Telomeric DNA is synthesized by copying an RNA template sequence *de novo* in the 5' to 3' direction within the RNA moiety of telomerase (Figure 1.4). The over-extension of telomeres is regulated by a multi-component "telomere homeostasis" system. Interaction among the telomere-associated proteins is important for this function (Blackburn 1992, 2005)

High levels of telomerase activity are found in cells of the germ line. In these cells it is essential to maintain stable telomere length for limitless replication. In somatic cells, on

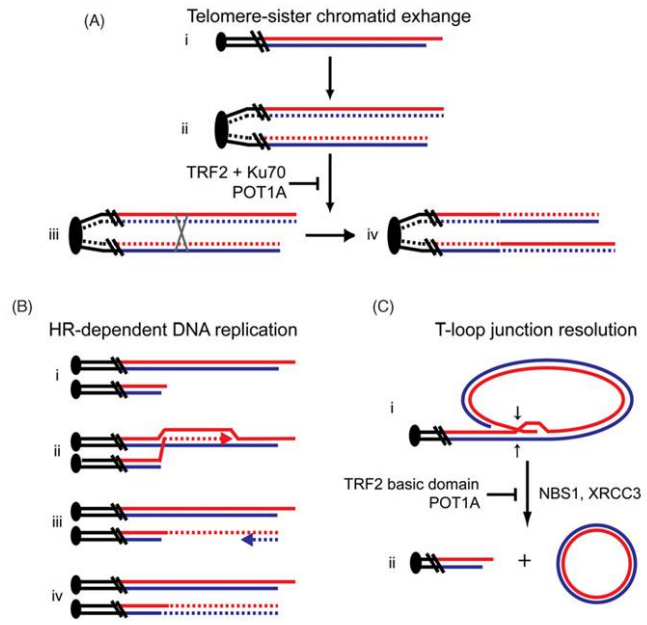

Figure 1.5: Forms of recombination in ALT (A) Showing telomere-sister chromatid exchanges:(i) TTAGGG sequence in red, CCCTAA in blue;(ii) second step, semi-conservative DNA replication, dotted lines showing new synthesized DNA;(iii) homologous recombination, (iv) post replicative telomere exchanges; **(B)** (i to iv) telomere elongation after strand invasion of a 3'overhang into an adjoining telomere; followed by elongation of the immigrated strand by DNA polymerase (red dotted line) thus the C-rich strand can also be filled; **(C)** t-loop junction resolution: (i and ii) misarrangement of the t-loop structure results in free t-circles and segregated telomeres(taken from Cesare and Reddel (2008))

the other hand, telomerase activity was not initially detected, except in lymphopoietic tissue and regenerative epithelia. Furthermore, telomerase activity was found in all epithelia along the gastrointestinal tract and the epidermis (Bachor et al. 1999; Taylor et al. 1996). Telomerase activity seems to play an essential role in the lifetime of regenerative capacity and in normal epithelia.

1.4.3 The alternative lengthening of telomeres (ALT)

The occurrence of alternative lengthening of telomeres (ALT) was first observed in some cell lines, which maintained telomere length over many hundred population doublings (PDs) in the absence of telomerase (Bryan et al. 1995). This telomerase-independent mechanism involves extension of telomeric DNA by a recombination-mediated replication mechanism (Figure 1.5). Fortunately, ALT is generally associated with some phenotypic characteristics. One indication of ALT are telomeres that are highly heterogeneous in length, with some commonly found very long telomeres. Analysis by telomere fluorescence *in situ* hybridization (FISH) on metaphase spreads shows that in ALT cells,

telomeres are ranging from less than 2kb to longer than 50kb in length, whereas some lack any observable telomere signals (Bryan et al. 1995; Henson et al. 2002). Further studies in ALT cell lines showed that the dynamics of telomere lengths in these cells are highly complex. Both rapid elongation and rapid deletion events are present in ALT cells (Murnane et al. 1994). Further it seems that the deletion events generate extra chromosomal telomeric DNA which can be linear (Tokutake et al. 1998; Ogino et al. 1998), or circular (also known as t-circles Figure 1.5). Particulary, these t-circles seem to be abundant in ALT cells, therefore becoming another characteristic of the ALT mechanism (Cesare and Griffith 2004; Fasching et al. 2007).

A further phenotypic marker of the ALT mechanism are promyelocytic leukemia nuclear bodies (PML), that contain telomeric DNA or proteins, which are termed ALT-associated PML bodies (APBs) (Yeager et al. 1999). ALT-associated PML bodies are characterized by telomeric DNA, which colocalizes with the shelterin protein complex or with DNA repair, recombination or replication factors (Yeager et al. 1999; Henson et al. 2002). Further investigations showed that APBs primarily accumulate linear extrachromosomal telomeric DNA, which presumes that an additional function of APBs is to keep linear DNA away from being recognized as DNA double strand breaks (DSBs) (Fasching et al. 2007). All these listed phenotypic hallmarks of ALT are just markers, as it is not yet known in which way and how tightly they are linked to the ALT mechanism. For example, some types of glioblastoma multiforme tumors and some cases of soft tissue sarcomas show neither detectable telomerase activity nor any usual hallmarks of ALT.

1.4.4 Telomere maintenance in soft tissue sarcoma

Telomere maintenance by telomerase, a large ribonucleoprotein complex that connects hexanucleotide repeats to the telomeres, are most common in tumors of epithelial origin. The recombination based ALT maintenance mechanism seems to be more frequently activated in tumors of mesenchymal origin, such as soft tissue sarcomas (see below).

In the last years, much work was done to characterize the telomere maintenance mechanism in resected lesions. First analyses on this topic was focused on the detection of telomerase. Later on, the identification of ALT led to increased investigation of both telomerase activity and the ALT mechanism in tumors and cell lines including tumor-derived cell lines. In recent studies based on the detection of both telomere maintenance mechanisms in osteosarcomas, a considerable number was found to be ALT positive, at a frequency of 35 % and 47 % (Henson et al. 2005; Ulaner et al. 2003). Further studies in glioblastoma multiforme revealed about 19 % of cases using the ALT mechanism, which is higher than typically seen in carcinomas (about 5-10 %) (Hakin-Smith et al. 2003). Other studies of soft tissue sarcoma subtypes, such as liposarcomas, exhibit the ALT mechanism at a frequency of 33 %, 24 % and 24 %, observed from 3 independent studies (Costa et al. 2006; Johnson et al. 2005; Henson et al. 2005). In two of these studies (Costa et al. 2006; Johnson et al. 2005) about 50 % of the investigated liposarcomas showed no indication of either telomerase or ALT, although telomere maintenance is believed to be

necessary in tumorigenesis. he activation of a telomere maintenance mechanism remains a likely contributor to tumor progression as it is important for infinite cell proliferation, which characterizes most malignancies (Counter et al. 1998).

1.4.4.1 Telomere maintenance: tumor progression and chromosomal instability in sarcomas

On one hand, recent studies, based on the identification of the interrelationship among telomere maintenance mechanism activation and tumor grade in soft tissue sarcomas, have shown in liposarcomas that 70 % of grade I tumors give no evidence of ALT or telomerase activation. On the other hand, liposarcomas of grade II and III have shown typical hallmarks of ALT, telomerase or both mechanisms (Costa et al. 2006). The results of these studies showed a positive correlation between activated telomere maintenance mechanism and tumor grade in liposarcomas.

The characterization of both telomere maintenance mechanisms regarding their level of chromosomal instability revealed marked differences. Crucial work was done by Scheel et al. (2001) using both telomere and multiplex fluorescence *in-situ* hybridization (FISH) in osteosarcoma-derived cell lines that utilized either ALT or telomerase for their telomere maintenance. Using telomere FISH analysis, ALT positive cells showed telomere length heterogeneity, dicentric chromosomes and misbehavior in telomere configuration. Furthermore, analysis of ALT-positive cells by multiplex FISH revealed an increased number of translocations, deletions and complex rearrangements in comparison with the telomerase positive cell lines. In a recent study of osteosarcomas by Ulaner et al. (2004), the authors detected the ALT mechanism in 38 of 60 cases. In contrast, in Ewing's sarcomas 21 of 30 cases were telomerase positive. The authors have concluded a possible association between activated telomere maintenance mechanisms and specific chromosomal translocations. Indeed all of the 30 investigated Ewing's sarcomas were positive for chromosomal translocation whereas the frequency of ALT seems to occur more often in sarcomas with complex karyotypes. These results are consistent with the findings that ALT occurs less frequently in translocation associated sarcomas such as Ewing's sarcomas or synovial sarcomas (Montgomery et al. 2004).

1.4.4.2 Telomere maintenance in sarcomas: association with patient outcome

As shown before, both mechanisms of telomere maintenance are not equivalent, especially in their efficiency of functional telomere maintenance. Such differences might have implication on tumor progression and patient outcome. An interesting study was done by Hakin-Smith et al. (2003), who examined the effect of telomere maintenance on tumor behavior in glioblastoma multiforme. This study showed that the median survival of patients with ALT-positive tumors was about 540 days, while those of non-ALT tumors was 247 days (median). In addition, tumors of the non-ALT group did not show significant changes in the survival rate, if telomerase was expressed. Therefore, in glioblastoma

multiforme the ALT mechanism might be used as a positive indicator of prognosis. A related study published by Ulaner et al. (2003) demonstrated the relationship between telomere maintenance and patient outcome in osteosarcoma. The authors found that patients without detectable telomere maintenance mechanism have an increased survival rate (90 % five-year survival). In contrast, tumors positive for ALT, telomerase or both mechanisms showed a higher mortality (60 % 5-year survival). In summary, studies both from Hakin-Smith et al. (2003) and Ulaner et al. (2003) showed that the association among the activated telomere maintenance mechanism and patient survival varies depending on the specific type of malignancy. Since the TMM can vary significantly in soft tissue sarcomas with different implications on patient outcome, further studies for the characterization of the TMM are crucial for developing new strategies for anti-tumor therapies.

1.4.5 Promyelocytic leukemia nuclear bodies (PML NBs) and its role in soft tissue sarcomas

The nucleus of mammalian cells is a complex organelle, suborganized into multiple nuclear domains and includes a heterogenous family of nuclear bodies such as promyelocytic leukemia nuclear bodies (PML NBs). The PML nuclear bodies are distinct structures particulary with regard to the number of different proteins containing different functions in the nucleus. PML bodies are shown to be involved in a number of different biological regulations of the cell such as apoptosis, senescence and DNA damage response (Figure 1.8). Furthermore, cells that undergo ALT have shown a type of PML nuclear bodies, which colocalize with telomeric DNA, telomere-associated proteins or proteins involved in DNA-repair or recombination and are referred to as ALT-associated PML bodies (Yeager et al. 1999) (see also chapter 1.4.3). PML nuclear bodies are also plays a role in telomere length regulation in ALT tumors and therefore in soft tissue sarcomas which use the alternative lengthening of telomere maintenance. In addition, a recent study of Matsuo et al. (2008) proposed that the presence of PML bodies indicate a poor prognosis for patients with soft tissue sarcomas such as liposarcomas and malignant fibrous histiocytomas.

1.4.5.1 Structure and function of PML NBs: a brief insight

PML nuclear bodies were first identified in acute promyelocytic leukemia where the human *PML* gene is fused with the retinoic acid receptor alpha*(RARA)* gene by the t(15;17) chromosomal translocation (de Thé et al. 1990, 1991). The promyelocytic leukemia protein PML localizes as punctated structures within the nucleus. A typical number of PML signals in the human nucleus are 1 to 30 bodies per nucleus with a diameter ranging between 0.2 to 1.0 µm (Bernardi and Pandolfi 2007). Number and size of PML NBs are dependent on different factors such as cell cycle phase, cell type and differentiation stage (Dellaire and Bazett-Jones 2004). PML NBs are dynamic structures that move

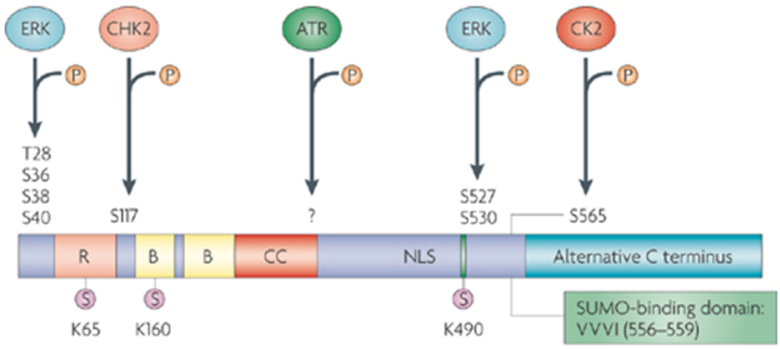

Figure 1.6: Illustration of post-translational modifications of PML. Demonstration of the protein promyelocytic leukemia (PML) with its functional sites; Several kinases such as extracellular-regulated kinase (ERK), checkpoint kinase-2 (CHK2), ataxia telangiectasia mutated (ATM)- and RAD3-related (ATR) and casein kinase-2 (CK2) are known to phosphorylate PML at the three sumoylation sites (S) or the SUMO-binding domain of PML. All post-translational modifications occur in the conserved region of the protein and, therefore, are common in all PML isoforms. (taken form Bernardi and Pandolfi (2007))

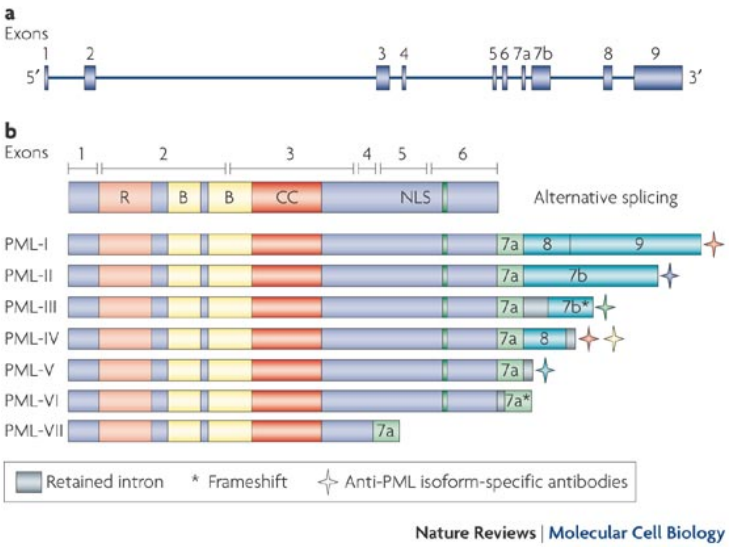

Figure 1.7: The *PML* gene and its protein isoforms The gene *PML* contains approximately 53.000 bases and nine exons. All isoforms contain exon 1 to 3 and the seven subgroups are generated by alternative splicing of exon 7 to 9 at the C-terminal end. Further splicing variants between exon 4,5 and 6 has been reported to result in cytoplasmic PML proteins, as exon 6 contains the nuclear location signal (NLS) (taken from Bernardi and Pandolfi (2007))

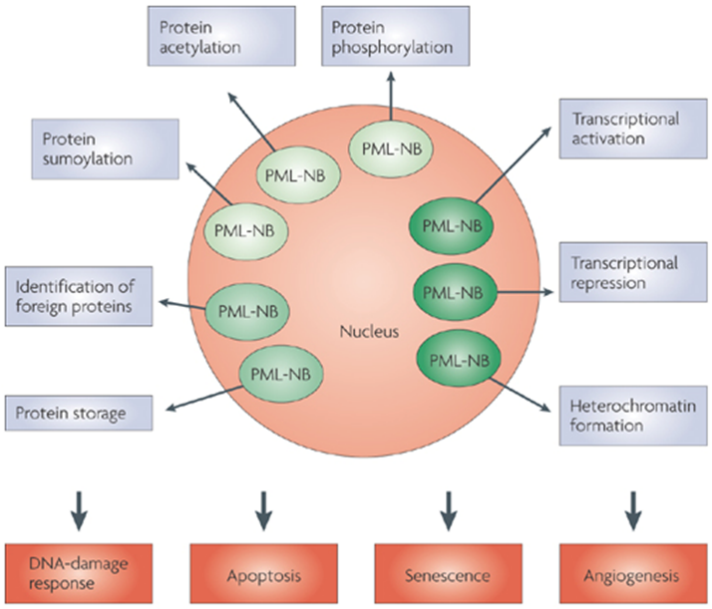

Figure 1.8: Promyelocytic leukemia nuclear bodies and its many functions PML NBs are structures that are involved in several cellular functions such as DNA-damage response, apoptosis, cellular senescence and angiogenesis. Further functions which are regulated by PML NBs are: identification and storage of proteins; post-translational modifications of proteins and regulation of nuclear activities such as transcriptional regulation and chromatin organization. However, it is not yet known whether PML NBs regulate such different function or whether there is functional heterogeneity. The functional heterogeneity of PML might be dependent on position in the nucleolus relating to chromatin or special compartments, or may depend on the biochemical arrangement (taken from Bernardi and Pandolfi (2007)).

within the nucleus and are tightly bound to the nuclear matrix. Studies by electron microscopy have shown that PML NBs are composed of a ring-like protein structure without detectable nucleic acids in the center of the ring. At the periphery of the ring PML NBs are in contact with chromatin fibres. The interaction with chromatin fibres is suggested as a mechanism for stabilization of PML NBs position in the nucleus. Furthermore, localization to other nuclear structures seems also not to be random (Borden 2002; Grande et al. 1996). The work of Görisch et al. (2004) have impressively shown that nuclear bodies such as PML and Cajal bodies diffuse within an chromatin corral whereas these chromatin corrlas move within the nucleus.

PML and its constitutive component Sp100 seem to be highly modified by SUMO (= small ubiquitin-related modifier) (Seeler and Dejean 2003). The protein PML contains three SUMO modification sites and one SUMO interaction motif as demonstrated in Figure 1.6. Not only PML NB but also a number of PML NB components are sumoylated or bind to SUMO, demonstrating the important role of SUMO in PML NB formation. Furthermore, the protein PML includes a N-terminal RING finger, two *B*-boxes and a leucine-rich-coiled-coiled domain, which are encoded by exon 1 to 3 of the *PML* gene and

belong to the RBCC family (Fagioli et al. (1998); Jensen et al. (2001)). The gene *PML* is located on chromosome 15q22 and contains nine exons, whereas alternative splicing of the C-terminal exons leads to generation of the PML isoforms I-VII, which are shown in Figure 1.7 (Jensen et al. 2001). Most isoforms are predominantly located in the nucleus due to the nuclear localization signal (NLS) added by exon 6. (Condemine et al. 2006).

However, it has been suggested that different PML isoforms bind to specific interaction partners and thus perform specialized function. Individual expression of single PML isoforms in the cell, where several isoforms are expressed in combination, contributes to a special PML NB structure. The cellular function of PML NBs has focused on the identification of proteins that bind to these structures. As a result, many proteins were found to localize to PML NBs partially or temporally with the consequence that PML has been implicated in several biological functions as shown in Figure 1.8. The distinct nature of the proteins that accumulate in PML NBs has made it difficult to define the function of PML and its related structures. Currently, just a few models try to explain the biological function of PML (Dellaire and Bazett-Jones 2004; Borden 2002; Zhong et al. 2000b). A first model proposes that PML NBs act as nuclear storage for the aggregation of proteins involved in both pathological or normal situations. In a second model, PML NBs operate as a catalytic surface for proteins, where they accumulate and are modified after translation. Another proposed function of PML is an active platform for specific functions of the nucleus such as transcription or chromatin regulation. Further studies on PML NBs in the future will be crucial to confirm or to regenerate these models. Although recent studies suggested that PML nuclear bodies may be heterogenous in composition, mobility and function, open questions remain such as: How can a single protein carry out so many functions and what is the evolutionary advantage? (Bernardi and Pandolfi 2007).

1.5 Aim of the project

Human tumors maintain an indefinite replicative potential through the activation of telomere maintenance mechanisms. Telomerase activity is the most common mechanism used to maintain telomeres. A number of tumors was shown to maintain telomeres by a recombination-based mechanism that has been termed alternative lengthening of telomeres (ALT). In particular, ALT tumors mainly include specific subtypes of soft tissue sarcomas associated with complex karyotypes.

Aim of the thesis was:

- evaluation of the frequency distribution between ALT-positive and telomerase positive tumors in different subgroups of soft tissue sarcomas
- correlation of the telomere maintenance mechanisms with number of imbalances (CGH) with the intention to determine, whether the activation of a telomere maintenance mechanism associates with specific genetic alterations

- development of an spot analyses program for automatic quantification of colocalizations in multi-channel 3D microscopy images, to quantify a large number of tumors by ALT-associated PML bodies and telomere size distribution
- investigations of PML nuclear bodies in order to study whether one of the PML isoforms preferentially bind to telomeres in ALT positive cell lines

Since the telomere maintenance mechanism (TMM) can vary significantly in soft tissue sarcomas, the characterization of these malignancies and their TMM is crucial for developing new strategies for anti-tumor therapies.

2 Publications - in preparation and submitted - based on this thesis

The work of the manuscript "Frequency distribution of TMM in soft tissue sarcomas" (in preparation) was performed by the author Petra Sander and include: writing of the whole manuscript; preparing of the Figures 2.1, 2.2, 2.3, 2.4, 2.5, 2.8, 2.9, 2.10, 2.11, 2.12 and Table 2.1; establishment of the combined telomere fluorescent *in situ* hybridization and PML immunofluorescence; staining procedures of all investigated samples; took all confocal images of tumor samples and non-tumor samples and prepared them for analyses (see chapter 2.2); had the idea for the automatic quantification of the ALT-mechanism; brought all data sets together (including TRAP analyses, CGH data, detection of ALT markers), interpreted them and prepared the data for further correlation analyses.

The work of the manuscript (chapter 2.2) "3D Geometry-Based Quantification of Colocalizations in Three-Channel 3D Microscopy Images in Soft Tissue Tumors" has been done in cooperation with Stefan Wörz (Dept. Bioinformatics and Functional Genomics, Biomedical Computer Vision Group, University of Heidelberg, BIOQUANT, IPMB, and DKFZ Heidelberg). The author of this thesis (Petra Sander) was involved in this work by: initiating the contact to Stefan Wörz; had the idea for automatically analysis of markers for the ALT-mechanism of confocal images (stacks); wrote the biological part of introduction in the manuscript; took and provided all confocal images which were used to develop the software; did the verification of the single spot analyses and DAPI-segmentation and defined the parameter settings for image analyses by this programm; set the threshold for very large telomeres; suggested the different types of colocalizations and has been involved in many discussion that addressed the development of the automatic quantification of the confocal images, such as the quantification of very large telomere spots. This manuscript is accepted for the SPEI conference (February 13-18, 2010 in San Diego, California USA). A shorter version of this manuscript is also accepted for the Workshop "Bildverarbeitung für die Medizin (BVM 2010, Aachen, Germany) and a longer version is submitted for a Special Issue on Multivariate Microscopy Image Analysis in IEEE Transactions on Medical Imaging. Unpublished data which included the verification of the program in chapter 2.2.6 was written by author of this thesis (Petra Sander) and Figures were provided by Stefan Wörz.

2.1 Frequency distribution of TMM in soft tissue sarcomas *(in preparation)*

Petra Sander[1], Stefan Wörz[2], Martin Pfannmöller[3], Axel Benner[4], Ralf Joachim Rieker[5,6] Karsten Richter[1], Stefan Joos[1], Petra Boukamp[7], Peter Lichter[1], Gunhild Mechterheimer[6]

[1]*Dep. Molecular Genetics, German Cancer Research Center (DKFZ), Heidelberg;* [2]*Dept. Bioinformatics and Functional Genomics, Biomedical Computer Vision Group, University of Heidelberg, BIOQUANT, IPMB, and DKFZ Heidelberg;* [3]*Cell Networks, Heidelberg University;* [4]*Dept. of Biostatistics, German Cancer Research Center, Heidelberg;* [5]*Dept. of Pathology, Innsbruck Medical University, Austria;* [6]*Dept. of Pathology, University Hospital, Heidelberg;* [7]*Dept. Genetics of Skin Carcinogenesis, German Cancer Research Center (DKFZ),Heidelberg;*

2.1.1 Abstract

The activation of a telomere maintenance mechanism (TMM) is considered essential for cellular immortalization, and thus for long-term tumor growth. Most human cancers, especially those of epithelial origin, use the activation of telomerase as their telomere maintenance mechanism; others tumors displayed an alternative lengthening of telomeres (ALT) mechanism. The latter particularly includes subtypes of soft tissue sarcomas. Here, we assessed the frequency distribution of telomere maintenance within different subgroups of soft tissue sarcomas. In order to assay the ALT-mechanism, we quantified markers of ALT, namely the occurrence of ALT-associated PML bodies (APBs) and telomere length distribution. TRAP assay was performed in order to determine telomerase activity. In our findings, a high level of telomerase correlates inversely with both the occurrence of large telomeres and APBs. Comparative genomic hybridization (CGH) analyses revealed in telomerase and ALT-positiv tumors specific genetic alterations ($p < 0.05$). The level of genomic instability occurred similarly in both ALT-positive soft tissue tumors and telomerase positive tumors. Nevertheless, tumors with an incidence for ALT compared with tumors possessing telomerase activity showed reciprocal alterations at the same chromosome bands. This study suggests several genomic regions involved in the regulation of telomere maintenance mechanisms and might lead to new markers or targets for anti-cancer strategies.

2.1.2 Introduction

The transformation from normal to malignant cells is a multistep process, and includes accumulations of genetic changes (Batista and Artandi 2009). Telomere dysfunction is likely to be involved in genomic instability by inducing chromosomal rearrangements which can provide the genetic basis for tumor progression (Batista and Artandi 2009;

Blasco 2005).

Human telomeres are the ends of the chromosomes and are composed of the repetitive non-coding sequence TTAGGG, which, are 10-15kb long and end in a 150-200 nucleotide G-rich single stranded overhang (Blasco 2005). This G-rich overhang is capable of folding back and annealing with the double-stranded region of the TTAGGG to form the telomeric loop, termed T-loop (Blasco 2005). Consequently, a part of the strand along the length of the overhang-invasion is displaced and forms a single strand DNA region, which is referred to as the D-loop (Denchi 2009; de Lange 2002). The T-loop formation and special proteins bound to telomeric DNA has a putative important function: to protect chromosome-ends from being degraded, fused with one another or being recognized as double-stranded breaks through cell cycle checkpoints, which would initiate senescence or apoptosis (Blasco 2005). Specific proteins have been found that interact with telomeric DNA either directly or via other proteins, and are essential for proper telomere function (de Lange 2005). Six of them exclusively localize to telomeres throughout the cell cycle to form, the so called shelterin complex, and they do not accumulate or function elsewhere in the nucleus. These are TRF1, TRF2 (Telomeric Repeat binding Factor1 and 2) TIN2 (TRF1- and TRF2- Interacting Nuclear Factor 2), POT1 (Protection of Telomeres 1), TPP1 and RAP (Repressor/Activator Protein1). Other proteins were observed to be involved in mammalian telomere protection, which interact with the chromosome ends transiently and non-exclusively. Examples include the Mre11 complex which is involved in homologous recombination of double stranded breaks, and XPF/ERCC1, which are involved in nucleotide-excision repair (Denchi 2009). Telomere length shortening occurs in normal somatic cells after each cell division due to the inability of the cells to replicate their chromosomes end completely, which is also known as the end-replication problem (Blasco 2005). Furthermore, telomeres below a certain size cause an irreversible growth arrest, referred to as replicative senescence. One possibility for cells to bypass senescence is the inactivation of the p53 and Rb tumor suppressor pathway, resulting in cellular proliferation upon further telomere shortening. These cells then reach a second proliferation block called crisis which is characterized by telomere dysfunction and cell death (Wei and Sedivy 1999; Shay and Roninson 2004). With respect to tumor biology, critically short telomeres lead to contradicting consequences. On the one hand, telomere dysfunction can trigger a DNA damage response resulting in apoptosis and senescence and act, therefore, as a tumor suppressor mechanism (Denchi 2009). On the other hand, dysfunctional telomeres are thought to be the initiator for end-to-end fusion, leading to the breakage-fusion-bridge (BFB) cycle, which is characterized by chromosomal breakages, resulting in chromosomal loss or amplification and finally the generation of numerical and structural chromosomal aberrations (Denchi 2009; Boukamp et al. 2005). These aberrations, in turn, can aid in tumor development.

Cancer cells bypass crisis by maintaining stable telomere length through the activation of a telomere maintenance mechanism, which permits limitless replicative potential. Most human cancers, especially those of epithelial origin, activate the canonical telomerase (a large ribonucleoprotein complex) pathway. However a small number of tu-

mors (10%), use the alternative lengthening of telomeres. The occurrence of alternative lengthening of telomeres (ALT) was first observed in some cell lines which maintained telomere length over hundreds of population doublings in the absence of telomerase activity (Bryan et al. 1995). This telomerase-independent mechanism involves extension of telomeric DNA by a recombination-mediated replication mechanism. ALT is generally associated with certain phenotypic characteristics, such as highly heterogeneous telomeres in length, ranging from less than 2kb to longer than 50kb in length, while some chromosomes lack any observable telomeres (Bryan et al. 1995). Another phenotypic marker for ALT is the association of promyelocytic leukemia nuclear bodies (PML) with telomeres, termed ALT-associated PML bodies (APBs) (Yeager et al. 1999). These APBs are characterized by telomeric DNA, which colocalizes with shelterin or DNA repair proteins, as well as with recombination or replication factors (Jiang et al. 2005, 2007). These hallmarks of the alternative lengthening of telomeres seem to be more frequently present in tumors of mesenchymal origin, such as soft tissue sarcomas.

Soft tissue sarcomas include a heterogeneous group of mesenchymal tumors and can be subdivided into two groups based upon their cytogenetic aberrations. The first group is characterized by simple, near-diploid karyotypes and specific translocations. Ewing's sarcomas, alveolar rhabdomyosarcoma, and synovial sarcomas belongs to this group. The second group displays complex karyotypes and includes, malignant peripheral nerve sheath tumors (MPNST), liposarcomas and malignant fibrous histiocytomas (MFH) (Larramendy et al. 1997; Helman and Meltzer 2003).

In this study the occurrence of ALT was assessed in subgroups of soft tissue sarcoma (STS) such as leiomyosarcomas (LMS), malignant peripheral nerve sheath tumors (MPNST), malignant fibrous histiocytoma (MFH), synovial sarcomas (SS), pleomorphic liposarcomas (PLLS), myxoid round cell liposarcoma (MRCLS) and dedifferentiated liposarcoma (DDLS).

2.1.3 Material and Methods

2.1.3.1 Tumor and tissue material

The investigated tumor samples were collected between 1991 and 2008 at the Institute of Pathology, University of Heidelberg, Germany. Non-tumor tissue samples were collected and provided 2008/2009 at the National Center for Tumor Diseases (NCT), Heidelberg. Skin sections from healthy donors and fibroblast cell lines were provided by Petra Boukamp (German Cancer Research Center). Tumor tissues from surgical specimens or biopsies were snap-frozen in liquid nitrogen within 30 min after surgical removal and stored at -196°C until use. Before further use, cryo-sections of 4-6 µm thickness were prepared and stained with hematoxylin and eosin. Only tissue samples that contained at least 80% of tumor cells were used for further experiments.

2.1.3.2 Telomere Repeat Amplification Protocol (TRAP)

Cell lysis of tumor- and non-tumor tissues and telomerase assay were performed using the TRAPeze kit (Q-Biogene, Heidelberg, Germany) according to the manufacturers recommendations.

2.1.3.3 Quantification of colocalization in three-channel 3D microscopy images

For automated image analysis a program called CellSegmentation was used, which was especially designed for this approach. (see chapter 2.2). In brief: To segment the DAPI-stained cell nuclei, we applied 3D median and Gaussian filters for noise reduction with subsequent Otsu thresholding for segmentation of nuclei and non-nuclei compartments. To detect structures such as telomere- and PML-"spots", coarse center positions of "spots" were determined by detection of intensity maxima. In the next step, each detected spot candidate is quantified by the 3D intensity profile with an underlying Gaussian function. To determine colocalizations between telomeres and endogenous PML, we utilized the geometry of the structures based on the fitting results, i.e. 3D position, 3D orientation and 3D shape. A colocalization was defined as an (partial) overlap of two or more structures from the different channels using the geometry of these structures. Due to the geometric representation of those structures with sub-voxel resolution we were able to differentiate between different types of colocalization (see chapter 2.2).

2.1.3.4 Comparative genomic hybridization (CGH)

DNA extraction of frozen tumor samples was performed as described previously (Joos et al. 1995, 1996). Tumor DNA was isolated from 20 µm tissue sections using proteinase K digestion (2 mg/ml in 50 mM Tris-HCL, 1 mM EDTA, 0.5% Tween 20) followed by ethanol precipitation. Control DNA was isolated from placenta tissue. Tumor DNA was labeled using 16-dUTP (Roche) and control DNA was labeled with Digoxigenin-11-dUTP (Roche Mannheim, Germany) using nick translation according to the manufacturers instructions. Approximately, 1 µg of biotin-labeled tumor DNA, 1 µg of digoxigenin-labeled control DNA and 50 µg Cot-1-DNA (Gibco/BRL, Geithersburg, MD, USA) were denaturated at 75°C for 6 min and pre-annealed at 37°C for 30 min. The DNA was then added to normal metaphase slides (Vysis, Downers Grove, IL, USA) which had been denatured in a heat block at 75°C for 7 min followed by 37°C for 20 min. Hybridization was performed in a humid chamber at 37°C for 48 hours. Afterwards, several post-hybridization washes and detection of hybridized DNA by fluorescein and rhodamine were performed. Image analysis was carried out by a epifluorescence microscopy (Zeiss, Wetzlar, Germany) with a charged couple device (CCD) camera, and the CytoVision software 3.52 package (Applied Imaging, Sunderland, UK) or the ISIS CGH software package (MetaSystems, Altlußheim, Germany). Gray level images of 10-15 metaphase spreads were recorded separately for each fluorochrome and the ratio of FITC: TRITC

fluorescence intensities along each individual chromosome were calculated and averaged. Chromosomal imbalances were detected by ratio profiles deviating from the balanced value of 1.0 with the values of 1.25 and 0.75 as diagnostic cutoff levels for over- and underrepresentation of chromosomal material, respectively had been thoroughly tested in numerous studies and provided a robust diagnostic criteria. To avoid false positive results in critical chromosomal regions, such as the pericentromeric subregions 1q11-q12, 9q11-q12 and 16q11.1-11.2, chromosome subregion 1p32 as well as chromosomes 19 and Y, these regions were excluded from the analysis.

2.1.3.5 Statistical Analysis

The correlation between telomerase expression level (TRAP), ALT markers and genetic stability at selected chromosome bands was tested using permutation testes for testing independence in two-way contingency tables (Hothorn et al. 2008). A permutation version of Jonckheere's trend test (Jonckheere 1954) was used to test for changes in the total number of aberrations (gains/losses) with respect to telomerase expression and ALT markers level. All analyses were exploratory. Therefore no p-value adjustment for multiple testing was done. A result was considered as statistical significant if the P value of the corresponding test statistic was smaller than 5% ($p < 0.05$). All statistical computations were performed using R (R Development Core Team 2008), version 2.7.2 and R packages coin, version 0.6-9 and clinfun, version 0.8.2.

2.1.3.6 Fluorescence microscopy

3D fluorescence signals were detected in Z-stacks of about 10 to 30 frames with 0.28 µm spacing by confocal laser scanning microscopy (TCS SP2 Leica Microsystems, Germany). The PML nuclear bodies were detected by immunolocalization of PML PG-M3 (mouse monoclonal, Linaris; dilution 1:200). The secondary antibody used as a reporter was tagged with FITC (Linaris, Germany; dilution 1:200). The telomeres were identified by a Cy3-labeled $(CCCTAA)_3$ peptide nucleic acid (PNA) probe (Dako, Dennmark). For combined telomere-FISH and PML immunofluorescence, cells were fixed on glass slides with 3.7% formaldehyde (freshly prepared, J.T.Baker) in PBS (phosphate-buffered saline). After fixation, the specimens were washed in PBS. The slides were then dehydrated by a series of ethanol washes (70%, 90%, 100%), each incubated for 2 min, and briefly air dried. Eight µl of Cy3-labeled PNA probe was added and then denatured for 3 min at 80°C. After hybridization for 2 h at room temperature, the slides were washed several times at room temperature with 70% formamide/ 10 mM Tris-HCL, pH 7.2 (25 min), PBS (30 sec), 0.1 SSC for 5 min at 65°C, and PBS containing 0.05% Tween-20 (2 x 5 min at room temperature). After telomere-FISH, the specimens were permeabilized by incubation with 0.02% Triton X-100 (Sigma) in PBS for 3 minutes at room temperature. Then, a protein block was applied by incubation with 4% goat serum in PBS for 10 minutes. Antibodies, diluted in PBS containing 1% goat serum, were incubated for 30 minutes at

37°C (first antibody), and at room temperature (second antibody). Each antibody incubation was followed by three washes with PBS. Finally, slides were covered with 1 drop of antifade solution (VectaSield, Linaris) containing 4,6-Diamidino-2phenylindole (DAPI). Images were processed using MacBiophotonics ImageJ and subsequently exported and saved as either jpg- or tiff-files.

2.1.4 Results

2.1.4.1 Frequency distribution of telomerase expression levels in subgroups of STS

Since the telomere maintenance mechanism can vary significantly in soft tissue sarcomas (STS), we evaluated the frequency distribution of telomerase activation and ALT-mechanism in different soft tissue sarcoma entities. To investigate the regulation of telomerase in soft tissue sarcoma subtypes in more detail, we determined the telomerase status by TRAP assay. As shown in Figure 2.1, telomerase activity in different tumor samples varies from none or moderate (0 or 1) to high levels (2). HaCaT immortalized keratinocytes were used as a control for cells with high telomerase activity. In Figure 2.2, it is shown that telomerase activity varies significantly, from 100% (TRAP1 + TRAP2) in synovial sarcomas to about 46% in pleomorphic liposarcomas. In addition, our findings indicate that the expression levels of telomerase differ with different subtypes of soft tissue sarcoma (Figure 2.2). Furthermore, all tumor samples with specific translocations such as MRCL (myxoid round cell liposarcomas) and SS (synovial sarcomas) show an up-regulated telomerase activity compared to tumors with non-specific translocations, like pleomorphic and dedifferentiated liposarcomas (Figure 2.2). These data suggest that soft tissue sarcomas with specific translocations are more prone to expressing telomerase than tumors with complex karyotypes.

2.1.4.2 Correlation of telomerase expression level and markers for ALT-like STS

In order to study whether or not, these tumors show evidence of both ALT and telomerase activity, we combined telomere fluorescence *in situ* hybridization and PML immunofluorescence to detect ALT-associated PML bodies and heterogeneous telomere length distribution within the same tumor samples (Figure 2.3). Using confocal laser scanning microscopy, images were acquired from three independent regions of each sample, and were analyzed using an image analysis program (see chapter 2.2) designed exclusively for this approach. The colocalization of PML with telomeres were allocated to one of three types; the colocalization type Col 1 (Col 1 equates to c1 compare chapter 2.2) is where a telomere signal is fully within a PML nuclear body. In Col 2 (Col 2 equates to c3 compare chapter 2.2), both spots overlap and the center of each spot is located within the other spot. Both colocalization types are each an indication for ALT-associated PML-bodies. The third type, Col 3 (Col 3 equates to c7 compare chapter

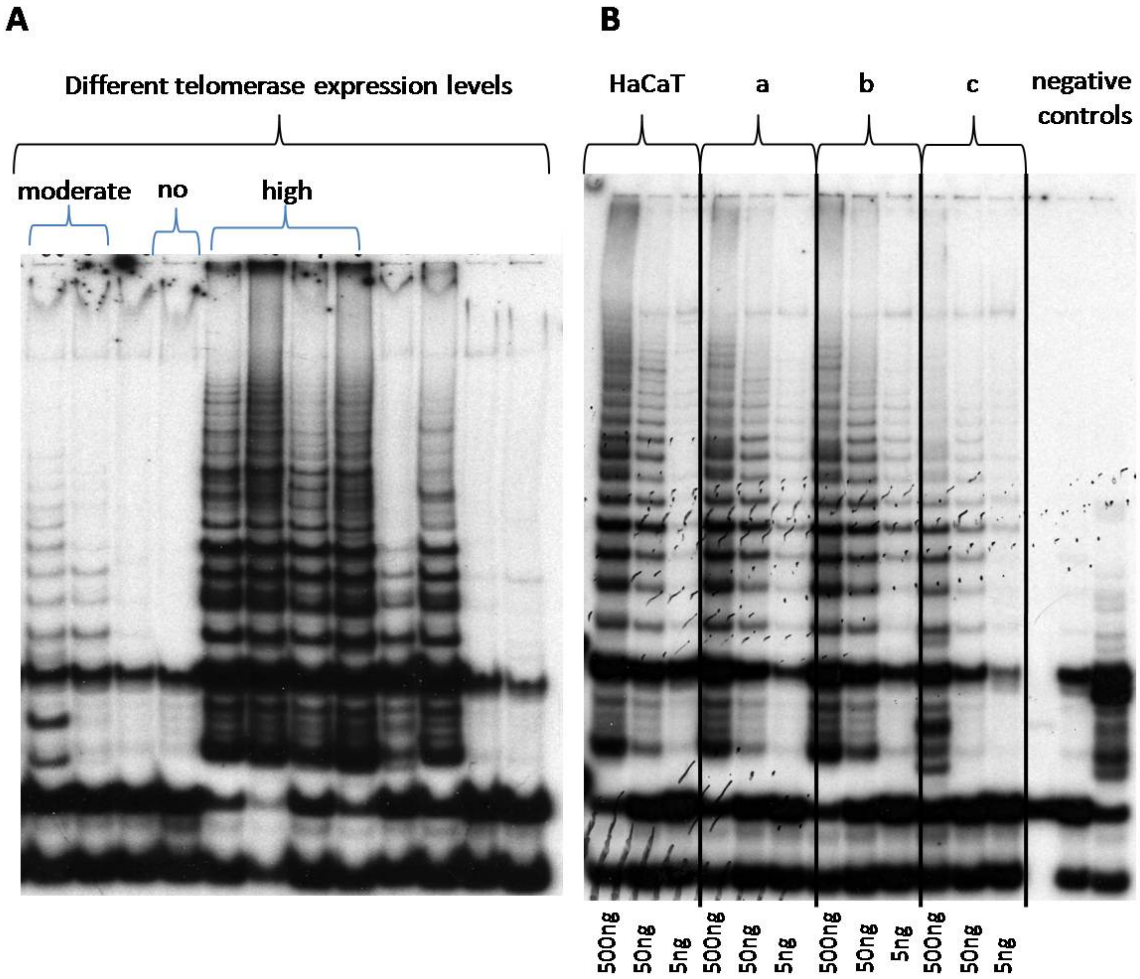

Figure 2.1: Different telomerase expression level in STS revealed by TRAP-assay. **(A)** Telomerase activity was determined by TRAPeze assay in subgroups of soft tissue sarcoma, most of which exhibit different telomerase expression levels (no, moderate and high), an example is shown in (A). Each column display a different tumor sample. HaCaT cells were used as positive control (data not shown in example A). **(B)** Fibroblasts, diluted buffer and HaCaT cells treated with RNase were used as negative control. In titration experiments, dilutions of 500ng, 50ng and 5ng of HaCaT extracts were compared with diluted extracts from all investigated soft tissue sarcomas (e.g. a, b and c). In order to study the regulation of telomerase in soft tissue sarcoma subtypes in more detail, we determined the telomerase status by TRAP assay. Telomerase activity varies from none/low to high levels (TRAP 0 = no telomerase activity, TRAP 1 = low/ moderate telomerase activity and TRAP 2 = high telomerase activity)

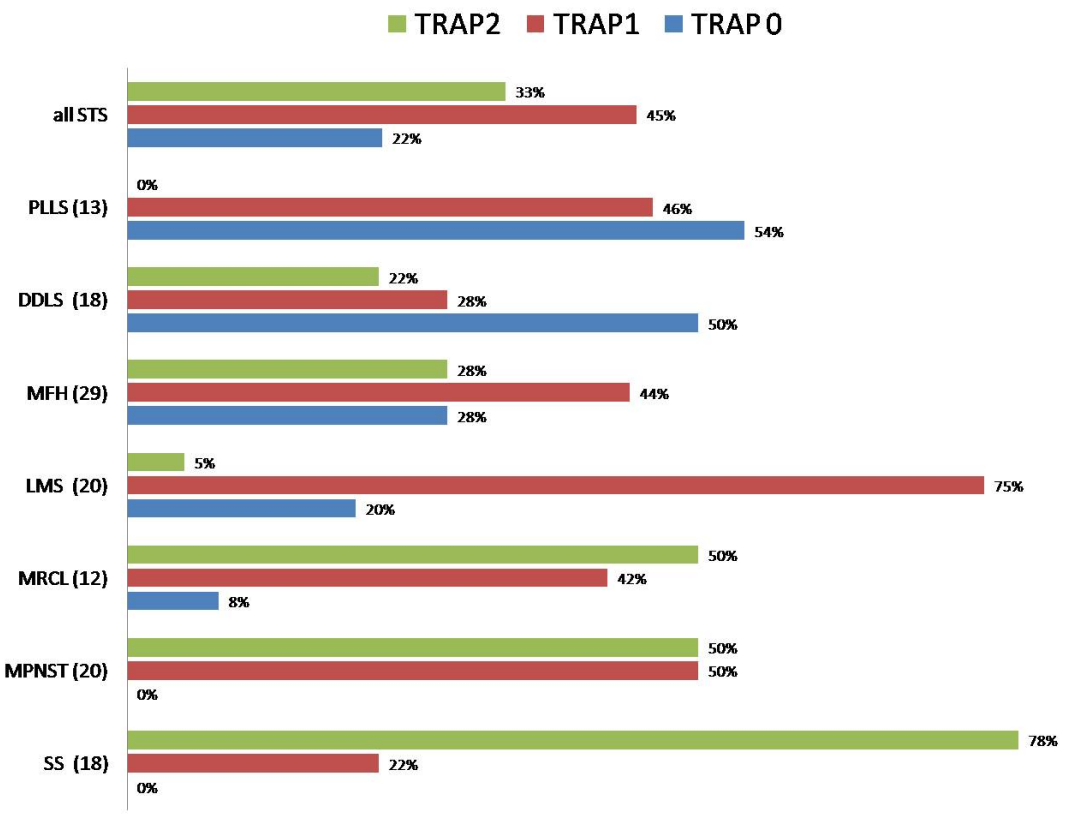

Figure 2.2: Different telomerase expression level in STS revealed by TRAP-assay. TRAP activity varies significantly, from 100% in synovial sarcoma to about 46% in pleomorphic liposarcomas. These data show that the expression levels are characteristic for different subtypes of soft tissue sarcoma. Zero telomerase expression level is shown in blue, moderate in red, and high in green. Total number of investigated samples are shown in parentheses. MCLS and SS belong to the group of translocation associated sarcomas, whereas the others exhibit a complex karyotype.

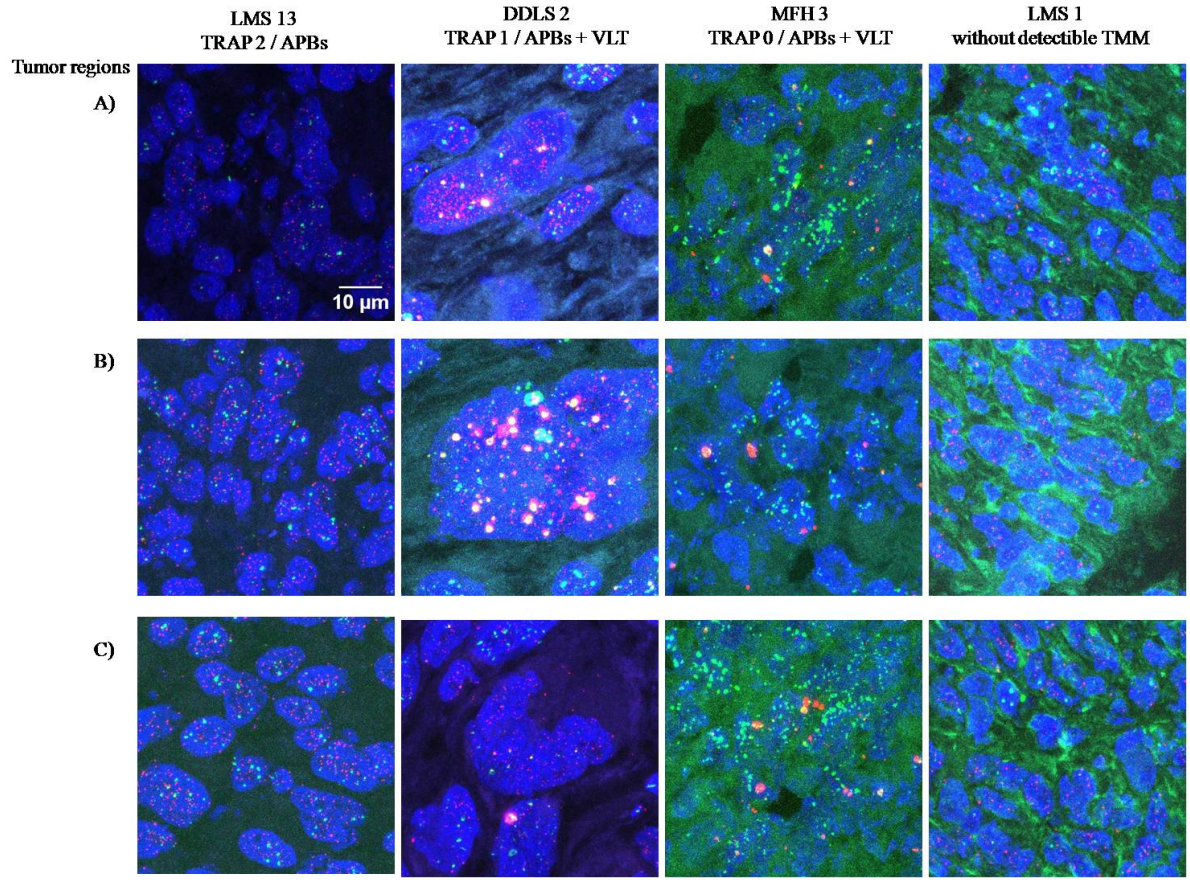

Figure 2.3: Images of soft tissue sarcomas exhibiting different TMM. ALT-associated PML bodies (APBs) and heterogeneous telomere spot size distribution with exceptionally long telomeres (VLT) were detected by combined telomere fluorescence *in situ* hybridization (red staining) and PML immunofluorescence (green staining) in frozen sections of different soft tissue sarcoma subgroups. Nuclei were counterstained with 4',6-diamidino-2-phenylindol. Using confocal laser scanning microscopy, 3D images were acquired from three independent regions of the tumor marked by A, B and C. Shown are examples of different cases; leiomyosarcomas (LMS13 and LMS1), dedifferentiated liposarcoma (DDLS2) and malignant fibrous histiocytoma (MFH3), which exhibited different variations of telomere maintenance mechanisms (TMM)

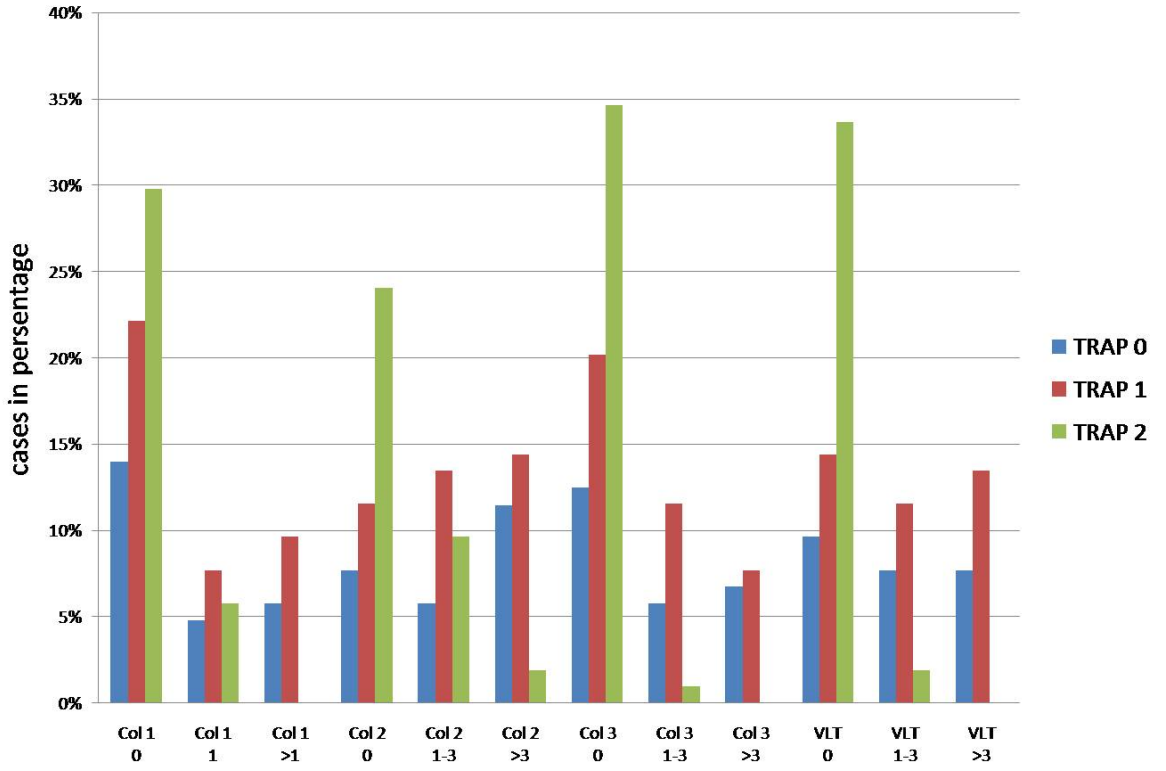

Figure 2.4: Correlation of telomerase expression level and markers for ALT Correlation of telomerase expression level with ALT-associated PML bodies (APBs) and very large telomeres (VLT) in all investigated soft tissue sarcoma subgroups. Telomerase activity was detected by TRAP and labeled either by 0, 1, 2. 0 denotes no, 1= low/moderate and 2 = high telomerase activity. Colocalizations (APBs) Col 1 are sub-grouped into 0, 1 and >1, which denotes none, one and more than one colocalization per sample respectively; Col 2, Col 3 and VLT (verly large telomeres) are each subdivided into 0, 1-3 and >3: denoting respectively none, 1 to 3 and more than 3 of Col 2, Col 3 colocalization or VLT spots per sample.

Figure 2.5: Correlation of telomerase expression level and markers for ALT. Correlation of telomerase expression level with ALT-associated PML bodies (APBs) and very large telomeres (VLT) relating to the investigated subgroups of soft tissue sarcomas (synovial sarcoma, malignant peripheral nerve sheath tumors, leiomyosarcomas, malignant fibrous histiocytomas, myxoid round cell liposarcomas, dedifferentiated liposarcomas and pleomorphic liposarcomas). Telomerase activity detected by TRAP and subdivided into 0, 1, 2. O being no, 1= moderate and 2 = high telomerase activity. Colocalizations (APBs) labeled by Col 1 with 0, 1 and >1 denotes none (0), one (1) and more than one (>1) colocalization per sample respectively; Col 2, Col 3 and VLT (verly large telomeres) are subdivided into 0, 1-3 and >3: to indicate none (0), 1 to 3 (1-3) and more than 3 (>3) colocalization of Col 2, Col 3 or VLT spot per sample

2.2), denotes the colocalization of a PML spot with telomere spots that are exceptionally long. Using the same program and images, we identified a heterogeneous telomere size (very large telomeres) by the quantification of telomere signal sizes. To compare the detected amount of Col 1, Col 2 and Col 3 and very large telomeres (VLT) within the nuclei of different tumor samples for statistical correlations, we performed segmentation of the nuclei based on DAPI-staining. The total amounts of analyzed Col 1, Col 2 and Col 3 co-localizations as well as very large telomeres were normalized to 10,000 µm^3 of the segmented DAPI-channel. Furthermore, for the Col 1 colocalization, we distinguished between none (0), one (1) and more than one (>1) colocalizations per tumor sample. For Col 2 and Col 3, we distinguished between no (0), 1-3 and more than 3 (> 3) colocalizations per investigated tumor sample. For very large telomere (VLT) spots, we distinguished between no (0), 1-3 and more than 3 (> 3) spot per sample. Further correlation of the telomere maintenance mechanisms include just tumors samples which are also analyzed by CGH. Therefore the number of tumor samples is lower (104 cases instead of 130 cases) when compared to those cases analysed by different expression level of telomerase, as demonstrated in Figure 2.2. As shown in Figure 2.4, a total of 104 soft tissue sarcomas were investigated for any correlation between telomerase expression levels and the abundance of APBs and very large telomeres (VLT). Statistical analysis revealed a significant correlation between telomerase expression levels and the abundance of markers for ALT (correlation of TRAP results and Col 1, $p = 0.01$, with Col 2, $p = 0.002$, with Col 3, $p < 0.0001$ and with VLT, $p < 0.0001$). As displayed in Figure 2.4, tumor samples with moderate telomerase expression levels showed an increased number of APBs and very large telomere spots compared to those tumors without telomerase activity. Furthermore, the number of ALT-markers again decreases significantly in samples with high telomerase expression level. These findings could not be confirmed for each subtype of soft tissue sarcoma, as the number of samples in each subgroup was too small to achieve a robust statistical result. Nevertheless, all investigated subgroups of soft tissue sarcomas showed a different signature with regard to their telomerase expression levels, number of APBs, and very large telomeres (Figure 2.5). In all different subgroups we observed that in tumors with high telomerase expression (TRAP2), the number of APBs and very large telomeres decreased. Furthermore, soft tissue sarcoma subtypes, such as synovial sarcoma and myxoid round cell liposarcomas, having specific translocations, had no heterogeneous distribution of telomere length (VLT) even when the tumors showed a moderate telomerase expression level (see MRCL in Figure 2.5). Our results revealed that high expression levels of telomerase might suppress the appearance of ALT-associated PML bodies but even more the distribution of heterogeneous telomere size. Besides high telomerase expression, our data showed that soft tissue tumors with specific translocations were associated with a decreased number of very large telomeres.

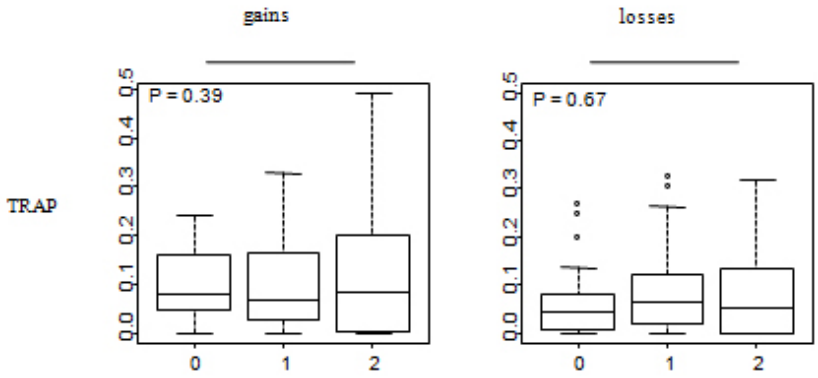

Figure 2.6: No correlation between genomic instability and telomerase expression The y axes represent the values of either gains or losses per investigated tumor sample (0.5 equates to 50%). The x axes labeled 0, 1, 2, denote 0= no, 1= low/moderate and 2 = high telomerase activity; p-values are shown within the box-plots.

2.1.4.3 Identification of genomic instability in tumors with telomerase expression and ALT-like tumors

To identify whether there is a correlation between telomere maintenance mechanisms (TMM) and genetic alterations, we performed CGH and analyzed the same fresh frozen tissue specimens of soft tissue sarcoma previously studied for the TMM distribution.

To evaluate the ALT-mechanism in respect to genetic alteration, APBs and telomere size distribution were used in the same way as before in studying TMM distribution. As shown in Figure 2.6, there are no significant differences regarding the number of imbalances, including gains and losses ($p = 0.39$ and 0.67, respectively), when compared to tumors showing elevated telomerase expression levels. Therefore, there is no evidence that those tumors with high telomerase expression levels exhibit fewer genomic imbalances compared to tumors without telomerase activity. I cannot be concluded that the maintenance of telomeres by telomerase prevents genomic instability.

Similar findings are observed for the ALT mechanism markers (Figure 2.7) such as Col 1 and Col 3 colocalization, as well as very large telomeres. These markers show no significant changes with regard to chromosomal gains and losses compared of those tumors without markers for ALT. However, there is an exception which comprises APBs, defined by Col 2 colocalization. This type of colocalizations show significantly ($p = 0.036$) more chromosomal gains with an increase in number of these colocalizations.

2.1.4.4 Telomerase and ALT-positive tumors reveal specific genetic alterations

CGH analysis is a robust method to characterize chromosomal imbalances. As shown in Table 2.1, analysis by CGH has shown that TMM correlates with specific genetic aberrations and these correlations are statistically significant ($p < 0.05$). The most frequent over-representations affecting chromosome bands ($p < 0.05$) in tumors with high

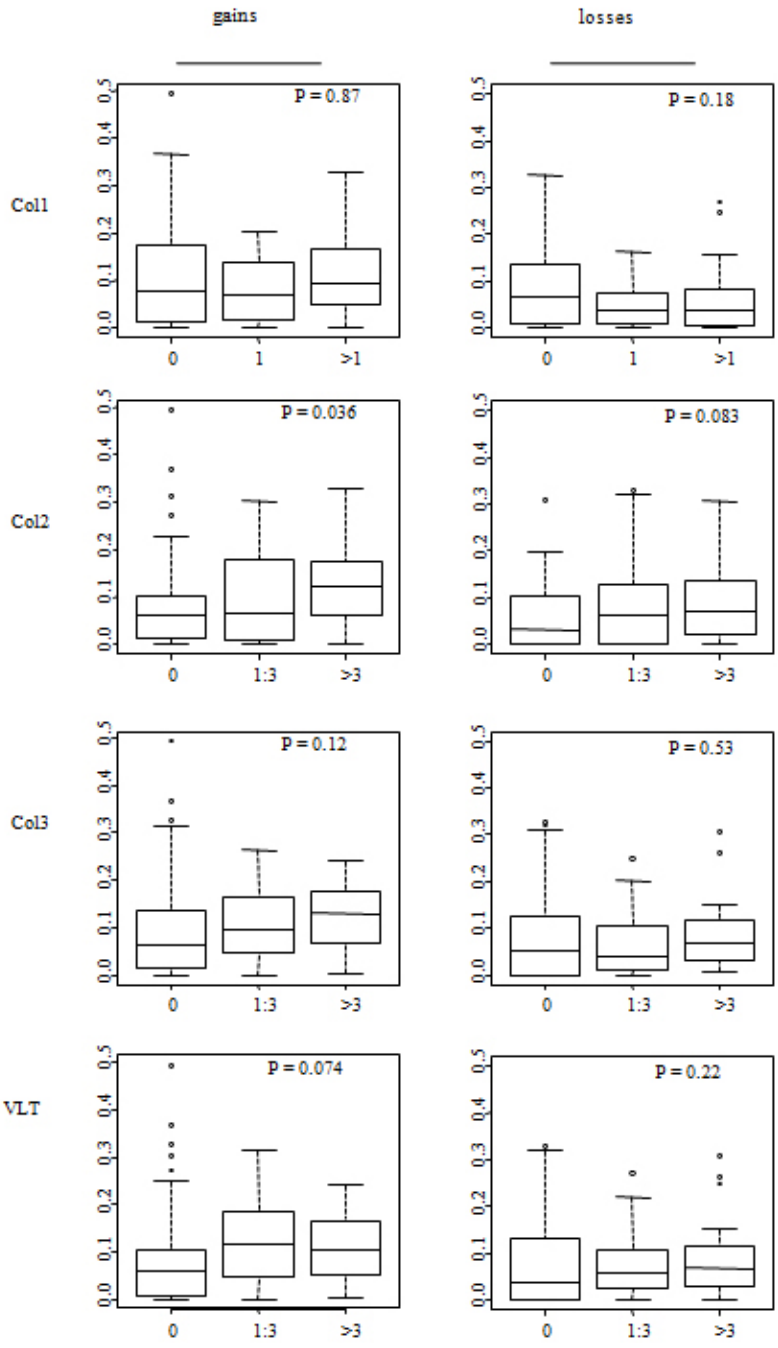

Figure 2.7: No correlation between genomic instability and ALT The y axes represent the values of either gains or losses per investigated tumor sample (0.5 equates to 50%). The x-axes for Col 1 labeled with 0, 1 and >1 denotes none (0), one (1) and more than one (>1) Col 1 colocalization per sample; Col 2, Col 3 and VLT (very large telomeres): subdivided into 0, 1:3 and > 3, indicate non (0), 1 to 3 (1:3) and more than 3 (>3) of Col 2, C 3 colocalization or VLT per sample; p -values are shown within the box-plots

Table 2.1: Chromosome bands with significant alteration in respect to TMM ($p<0.05$)

Markers for telomere maintenance mechanisms	**Chromosome bands with significant alteration ($P<0.05$)**
Telomerase expression	1p12; 1p13; 1p21; 1q32; 1q41; 2p23; 2p24; 2p25; 2q33; 2q34; 2q35; 4p15; 4p16; 5p15; 8q22; 8q23; 8q24; 11p12; 11p13; 11p14; 11p15; 11q11; 11q13; 11q14; 11q21 11q22; 17p13; 20q11; 20q12; 20q12; 20q13
Col 1 colocalizations (APBs)	1p12; 1p13; 1p21; 1p22; 1q32; 1q44; 2q32; 2q33 4p14; 4p14; 4q28; 6q26; 6q27; 8p12; 10q11; 11p11 11p12; 11p13; 11p14; 11p15; 13q12; 13q13; 18p11 20q11; 20q12; 20q13
Col 2 colocalizations (APBs)	1p12; 1p13; 1p21; 1p22; 1p31; 1q22; 1q32; 1q41; 1q42; 1q43; 1q44; 2p24; 2p25; 2q31; 2q32; 2q33; 2q34; 2q35; 2q36; 2q37; 3q26; 4p15; 4q35; 8p21; 8p22; 8p23 8q11; 8q23; 8q24; 10q25; 11q13; 12p11; 12p12; 12p13 12q11; 12q13; 12q15; 12q21; 16q22; 16q23; 17p11;17p12 17p13; 20p11; 20q11; 20q12; 20q13
Col 3 colocalizations	1p12; 1p13; 1p21; 1p22; 1p31; 1q22; 1q32; 1q41; 1q42; 1q43; 1q44; 2p24; 2p25; 2q24; 2q31; 2q32; 2q33; 2q34 2q35; 2q36; 2q37; 3q25; 3q26; 3q27; 3q28; 3q29; 4q12; 4q13; 4q21; 4q22; 4q23; 4q24; 4q25; 4q28; 4q31; 6q13;6q14; 6q22; 6q23; 6q24; 8q23; 11p15; 12q11; 12q12; 12q15; 12q21; 12q22; 13q34; 16q12; 16q22; 17p11; 17p12; 17p12; 17p22; 18q11; 20q11; 20q12; 20q13
very large telomeres (VLT)	1p12; 1p13; 1p21; 1p22; 1p31; 1q22; 1q32; 1q41; 1q42; 1q43; 1q44; 2q31; 2q32; 2q33; 2q34; 2q35; 2q36; 2q37; 3q25; 3q26; 3q27; 3q28; 3q29; 5p15; 5q12; 6q12;6q13;6q14; 6q22; 6q23; 6q24; 6q25; 6q26; 8p22; 8p23; 8q23; 9q21; 11p14; 11p15; 11q13; 11q14; 12q11; 12q12; 12q13; 12q14; 12q15; 12q21; 12q22; 16q12; 16q13; 16q22; 17p11; 17p12; 17p12; 20q11; 20q12; 20q13

telomerase activity (TRAP 2) were 8q22, 8q23 and 8q24 (36%, 39% and 36%), whereas losses were most frequently found on 11q14; 11q21-q22 (31%). As shown in Figure 2.8, several chromosome bands significantly altered ($p < 0.05$) in respect to the different telomerase expression levels. Our data revealed, that tumors with moderate telomerase levels were on several chromosome bands reciprocally altered compared to those tumors exhibiting a high telomerase expression level (Figure 2.8). For example, chromosome band 1p12 ($p = 0.022$) is more often deleted in tumors with high telomerase activity, whereas the same region is more often gained in tumors with a moderate expression of telomerase. These chromosomal regions which are reciprocally altered in tumors with moderate compared to those with high telomerase expression levels (Figure 2.8) are suggested to play a crucial role in the regulation of telomerase expression.

As shown in Figure 2.9 affected chromosome imbalances ($p < 0.05$) in tumors exhibiting ALT-mechanism markers, such as Col 1, Col 2, Col 3 and VLT are identically or similarly altered on several chromosome bands such as 1p12-p13, 1p21, 1q32, 1q44, 2q32-q33 and 20q12-q13 and 1p31, 1q22, 1q41-q43, 2q31, 2q34-q37, 3q26, 16q22, 17p11-p13 as examples for the markers Col 2, Col 3 and VLT (Figure 2.9). These findings indicate that these markers for ALT-mechanism have some properties in common and seem linked to one another.

As demonstrate in Figure 2.10 tumors detected as ALT positive by Col 1, Col 2, Col 3 and VLT, show on a few chromosome bands (e.g. 1p12, 1p13, 1p21) the same genetic alteration ($p < 0.05$) as tumors with moderate telomerase activity, but not with tumors with high telomerase activity. This indicates that ALT-positive tumors and tumors with moderate telomerase expression levels share some similar genetic alteration.

Furthermore, we observed that a few chromosome bands show the opposite correlation with respect to tumors with high telomerase expression levels and those exhibiting markers of ALT (Figure 2.10). Tumors identified as ALT positive by Col 1, Col 2, Col 3 and VLT showed gains on chromosomes e.g. 1p12-p13 and 1p21, whereas the same regions were more frequently deleted in tumors with high telomerase activity. Further opposite alterations observed on chromosome bands among tumors with high telomerase expression level and ALT-positive tumors are illustrated in Figure 2.10.

2.1.4.5 ALT markers in non-tumor samples

To see, whether the markers of ALT-positive tumors are exclusively expressed in tumor tissue, we investigated ALT-associated PML-bodies and the heterogeneous size distribution of telomeres (VLT) in non-tumor tissue and normal human fibroblasts cell lines. For this, we used tissue from skeletal muscle, peripheral nerve, adipose tissue (subcutaneous), articular capsule and skin tissue. As shown in Figure 2.11, there is a strong incidence of APBs in non-tumor tissue and normal fibroblast cells lines. Furthermore, Figure 2.12 shows that there is no indication that APBs are less or not expressed in non-tumor samples when compared with soft tissue tumors. With respect to telomere length distribution, neither the non-tumor tissue nor fibroblast cell lines showed any

Chr.bands		TRAP 0	TRAP 1	TRAP 2
1p12				
	-1	0	2	7
	0	81	81	86
	1	18	16	5
1p13				
	-1	0	4	10
	0	81	79	84
	1	18	16	5
1p21				
	-1	7	6	15
	0	66	76	78
	1	7	7	2
1q32				
	-1	22	6	2
	0	74	88	78
	1	3	4	18
1q41				
	-1	22	11	5
	0	74	83	81
	1	3	4	13
2p23				
	-1	0	9	2
	0	100	83	76
	1	0	6	21
2p24				
	-1	0	9	2
	0	96	86	76
	1	0	4	21
2p25				
	-1	3	9	0
	0	96	86	78
	1	0	4	21
2q33				
	-1	11	13	2
	0	88	81	86
	1	0	0	10
2q34				
	-1	11	16	2
	0	88	83	86
	1	0	0	10
2q35				
	-1	11	16	2
	0	88	81	86
	1	0	2	10
4p15				
	-1	0	4	7
	0	81	76	89
	1	18	18	2
4p16				
	-1	0	4	7
	0	81	76	89
	1	18	18	2
8q23				
	-1	11	13	2
	0	81	76	57
	1	7	9	39
11p12				
	-1	3	9	21
	0	81	79	76
	1	14	11	2
11q13				
	-1	0	6	15
	0	88	81	78
	1	11	11	5

Figure 2.8: Changes on specific chromosome bands correlates inversely with telomerase expression levels CGH analyses of all investigated STS revealed several significant ($p < 0.05$) alterations (compare also with 2.1) on different chromosomal bands; "Chr.bands"). Data is expressed as a frequency (percentage). -1 demonstrate losses, 0 no alterations and 1 gains (column). Different expression levels are shown in the first line. Lines labeled 0, 1 and 2 denote 0 as no, 1 as moderate and 2 as high telomerase activity. Red (losses) and green (gains) highlight chromosome bands with an higher frequency. Yellow indicates alteration with the same frequency.

Chr.bands	Col1			Col2			Col3			VLT		
	0	1	> 1	0	1-3	>3	0	1-3	>3	0	1-3	>3
1p12												
-1	5.71	0.00	0.00	6.67	3.33	0.00	5.71	0.00	0.00	6.67	0.00	0.00
0	85.71	78.95	75.00	88.89	83.33	73.33	87.14	68.42	81.25	88.33	68.18	82.61
1	8.57	21.05	25.00	4.44	13.33	26.67	7.14	31.58	18.75	5.00	31.82	17.39
1p13												
-1	8.57	0.00	0.00	8.89	6.67	0.00	8.57	0.00	0.00	10.0	0.0	0.0
0	82.86	78.95	75.00	86.67	80.00	73.33	84.29	68.42	81.25	85.0	68.2	82.6
1	8.57	21.05	25.00	4.44	13.33	26.67	7.14	31.58	18.75	5.0	31.8	17.4
1p21												
-1	14.29	0.00	6.25	15.56	10.00	3.33	14.29	5.26	0.00	16.67	0.00	4.35
0	74.29	78.95	62.50	77.78	76.67	63.33	75.71	63.16	75.00	78.33	59.09	73.91
1	11.43	21.05	31.25	6.67	13.33	33.33	10.00	31.58	25.00	5.00	40.91	21.74
1q22												
-1	0	0	0	0	0	0	0	0	0	0	0	0
0	82.2	70.0	53.3	82.2	70.0	53.3	75.7	79.0	37.5	80.0	63.6	52.2
1	17.8	30.0	46.7	17.8	30.0	46.7	24.3	21.1	62.5	20.0	36.4	47.8
1q32												
-1	8.57	5.26	18.75	2.22	10.00	20.00	4.29	10.53	31.25	3.33	9.09	26.09
0	75.71	94.74	81.25	82.22	80.00	76.67	81.43	89.47	62.50	81.67	86.36	69.57
1	15.71	0.00	0.00	7.00	3.00	1.00	14.29	0.00	6.25	15.00	4.55	4.35
1q41												
-1	0.0	16.7	26.7	7.14	15.79	31.25	6.67	13.64	26.09			
0	88.9	73.3	73.3	81.43	84.21	68.75	81.67	81.82	73.91			
1	11.1	10.0	0.0	11.43	0.00	0.00	11.67	4.55	0.00			
1q42												
-1	0.00	20.00	26.67	8.57	15.79	31.25	5.00	18.18	30.43			
0	88.89	73.33	73.33	81.43	84.21	68.75	85.00	77.27	69.57			
1	11.11	6.67	0.00	10.00	0.00	0.00	10.00	4.55	0.00			
1q43												
-1	0.00	16.67	26.67	7.14	15.79	31.25	3.33	18.18	30.43			
0	88.89	76.67	73.33	82.86	84.21	68.75	86.67	77.27	69.57			
1	11.11	6.67	0.00	10.00	0.00	0.00	6.00	1.00	0.00			
1q44												
-1	7.14	10.53	18.75	0.00	13.33	20.00	5.71	10.53	25.00	1.67	13.64	26.09
0	82.86	89.47	81.25	88.89	80.00	80.00	84.29	89.47	75.00	88.33	81.82	73.91
1	10.00	0.00	0.00	11.11	6.67	0.00	10.00	0.00	0.00	10.00	4.55	0.00
2q31												
-1	4.44	6.67	16.67	4.29	15.79	18.75	3.33	13.64	17.39			
0	91.11	90.00	83.33	91.43	84.21	81.25	93.33	81.82	82.61			
1	4.44	3.33	0.00	4.29	0.00	0.00	3.33	4.55	0.00			
2q32												
-1	8.57	10.53	25.00	6.67	6.67	23.33	7.14	15.79	25.00	3.33	22.73	21.74
0	85.71	89.47	75.00	86.67	90.00	76.67	87.14	84.21	75.00	91.67	72.73	78.26
1	5.71	0.00	0.00	6.67	3.33	0.00	5.71	0.00	0.00	5.00	4.55	0.00
2q33												
-1	8.57	15.79	25.00	6.67	10.00	23.33	7.14	21.05	25.00	3.33	27.27	21.74
0	85.71	84.21	75.00	86.67	86.67	76.67	87.14	78.95	75.00	91.67	68.18	78.26
1	5.71	0.00	0.00	6.67	3.33	0.00	5.71	0.00	0.00	5.00	4.55	0.00
2q34												
-1	4.44	10.00	23.33	5.71	21.05	25.00	1.67	31.82	17.39			
0	88.89	86.67	76.67	88.57	78.95	75.00	93.33	63.64	82.61			
1	6.67	3.33	0.00	5.71	0.00	0.00	5.00	4.55	0.00			
2q35												
-1	4.44	10.00	23.33	5.71	21.05	25.00	1.67	31.82	17.39			
0	88.89	86.67	73.33	88.57	73.68	75.00	93.33	63.64	78.26			
1	6.67	3.33	3.33	5.71	5.26	0.00	5.00	4.55	4.35			
2q36												
-1	4.44	10.00	23.33	5.71	21.05	25.00	1.67	31.82	17.39			
0	91.11	86.67	73.33	90.00	73.68	75.00	95.00	63.64	78.26			
1	4.44	3.33	3.33	4.29	5.26	0.00	3.33	4.55	4.35			
2q37												
-1	2.22	6.67	26.67	2.86	21.05	31.25	1.67	22.73	21.74			
0	93.33	90.00	70.00	92.86	73.68	68.75	95.00	72.73	73.91			
1	4.44	3.33	3.33	4.29	5.26	0.00	3.33	4.55	4.35			
11p15												
-1	20.00	0.00	6.25	18.57	5.26	6.25	18.33	13.64	4.35			
0	75.71	94.74	68.75	77.14	84.21	75.00	80.00	68.18	82.61			
1	4.29	5.26	25.00	4.29	10.53	18.75	1.67	18.18	13.04			
17p12												
-1	4.44	3.33	0.00	4.29	0.00	0.00	3.33	0.00	4.35			
0	82.22	80.00	50.00	80.00	68.42	43.75	85.00	63.64	47.83			
1	13.33	16.67	50.00	15.71	31.58	56.25	11.67	36.36	47.83			
17p13												
-1	4.44	6.67	0.00	4.29	5.26	0.00	3.33	0.00	8.70			
0	86.67	80.00	60.00	85.71	68.42	50.00	88.33	77.27	47.83			
1	8.89	13.33	40.00	10.00	26.32	50.00	8.33	22.73	43.48			
20q12												
-1	2.86	0.00	0.00	0.00	3.33	3.33	1.43	0.00	6.25	1.67	0.00	4.35
0	75.71	84.21	37.50	91.11	76.67	36.67	81.43	63.16	37.50	83.33	59.09	52.17
1	21.43	15.79	62.50	8.89	20.00	60.00	17.14	36.84	56.25	15.00	40.91	43.48
20q13												
-1	2.86	0.00	0.00	0.00	3.33	3.33	1.43	0.00	6.25	1.67	0.00	4.35
0	70.00	84.21	37.50	86.67	70.00	36.67	75.71	63.16	37.50	78.33	54.55	52.17
1	27.14	15.79	62.50	13.33	26.67	60.00	22.86	36.84	56.25	20.00	45.45	43.48

Figure 2.9: Same genomic alteration in STS in at least three (of the four) markers of ALT CGH analyses of all investigated STS revealed several significant ($p<0.05$) alteration (compare also with 2.1 on different chromosomal bands (Chr.bands). Data expressed as frequency (percentage). -1 demonstrate losses, 0 no alterations and 1 gains (collum). Markers for ALT are show in the first line: Col1 labeled with 0, 1 and >1 denotes none (0), one (1) and more than one (>1) colocalization per sample; Col2, Col3 and VLT (verly large telomeres): denotation by 0, 1-3 and > 3 indicate non (0), 1 to 3 (1-3) and more than 3 (>3) colocalization or VLT spot per sample. Red (losses) and green (gains) indicate chromosome bands with an higher frequency. Yellow demonstrate alteration with the same frequency.

Chr.bands	TRAP			Col1			Col2			Col3			VLT		
	TO	T1	T2	0	1	>1	0	1-3	>3	0	1-3	>3	0	1-3	>3
1p12				1p12			1p12			1p12			1p12		
-1	0	2	7	-1 5.71	0.00	0.00	-1 6.67	3.33	0.00	-1 5.71	0.00	0.00	-1 6.67	0.00	0.00
0	81	81	86	0 85.71	78.95	75.00	0 88.89	83.33	73.33	0 87.14	68.42	81.25	0 88.33	68.18	82.61
1	18	16	5	1 8.57	21.05	25.00	1 4.44	13.33	26.67	1 7.14	31.58	18.75	1 5.00	31.82	17.39
1p13				1p13			1p13			1p13			1p13		
-1	0	4	10	-1 8.57	0.00	0.00	-1 8.89	6.67	0.00	-1 8.57	0.00	0.00	-1 10.0	0.0	0.0
0	81	79	84	0 82.86	78.95	75.00	0 86.67	80.00	73.33	0 84.29	68.42	81.25	0 85.0	68.2	82.6
1	18	16	5	1 8.57	21.05	25.00	1 4.44	13.33	26.67	1 7.14	31.58	18.75	1 5.0	31.8	17.4
1p21				1p21			1p21			1p21			1p21		
-1	7	6	15	-1 14.29	0.00	6.25	-1 15.56	10.00	3.33	-1 14.29	5.26	0.00	-1 16.67	0.00	4.35
0	66	76	78	0 74.29	78.95	62.50	0 77.78	76.67	63.33	0 75.71	63.16	75.00	0 78.33	59.09	73.91
1	7	7	2	1 11.43	21.05	31.25	1 6.67	13.33	33.33	1 10.00	31.58	25.00	1 5.00	40.91	21.74
1q32				1q32			1q32			1q32			1q32		
-1	22	6	2	-1 8.57	5.26	18.75	-1 2.22	10.00	20.00	-1 4.29	10.53	31.25	-1 3.33	9.09	26.09
0	74	88	78	0 75.71	94.74	81.25	0 82.22	80.00	76.67	0 81.43	89.47	62.50	0 81.67	86.36	69.57
1	3	4	18	1 15.71	0.00	0.00	1 7.00	3.00	1.00	1 14.29	0.00	6.25	1 15.00	4.55	4.35
1q41							1q41			1q41			1q41		
-1	22	11	5				-1 0.0	16.7	26.7	-1 7.14	15.79	31.25	-1 6.67	13.64	26.09
0	74	83	81				0 88.9	73.3	73.3	0 81.43	84.21	68.75	0 81.67	81.82	73.91
1	3	4	13				1 11.1	10.0	0.0	1 11.43	0.00	0.00	1 11.67	4.55	0.00
2q33				2q33			2q33			2q33			2q33		
-1	11	18	2	-1 8.57	15.79	25.00	-1 6.67	10.00	23.33	-1 7.14	21.05	25.00	-1 3.33	27.27	21.74
0	88	81	86	0 85.71	84.21	75.00	0 86.67	86.67	76.67	0 87.14	78.95	75.00	0 91.67	68.18	78.26
1	0	0	10	1 5.71	0.00	0.00	1 6.67	3.33	0.00	1 5.71	0.00	0.00	1 5.00	4.55	0.00
2q34							2q34			2q34			2q34		
-1	11	16	2				-1 4.44	10.00	23.33	-1 5.71	21.05	25.00	-1 1.67	31.82	17.39
0	88	83	86				0 88.89	86.67	76.67	0 88.57	78.95	75.00	0 93.33	63.64	82.61
1	0	0	10				1 6.67	3.33	0.00	1 5.71	0.00	0.00	1 5.00	4.55	0.00
2q35							2q35			2q35			2q35		
-1	11	16	2				-1 4.44	10.00	23.33	-1 5.71	21.05	25.00	-1 1.67	31.82	17.39
0	88	81	86				0 88.89	86.67	73.33	0 88.57	73.68	75.00	0 93.33	63.64	78.26
1	0	2	10				1 6.67	3.33	3.33	1 5.71	5.26	0.00	1 5.00	4.55	4.35
8q23							8q23			8q23			8q23		
-1	11	13	2				-1 2.22	10.00	16.67	-1 5.71	5.26	25.00	-1 5.0	0.0	13.0
0	81	76	57				0 73.33	66.67	73.33	0 70.00	84.21	62.50	0 70.0	86.4	69.6
1	7	9	39				1 24.44	23.33	10.00	1 24.29	10.53	12.50	1 25.0	13.6	17.4
11p15				11p15						11p15			11p15		
-1	7	11	21	-1 20.00	0.00	6.25				-1 18.57	5.26	6.25	-1 18.33	13.64	4.35
0	77	79	78	0 75.71	94.74	68.75				0 77.14	84.21	75.00	0 80.00	68.18	82.61
1	14	9	0	1 4.29	5.26	25.00				1 4.29	10.53	18.75	1 1.67	18.18	13.04
17p13							17p13			17p13			17p13		
-1	0	7	2				-1 4.44	6.67	0.00	-1 4.29	5.26	0.00	-1 3.33	0.00	8.70
0	74	65	92				0 86.67	80.00	60.00	0 85.71	68.42	50.00	0 88.33	77.27	47.83
1	26	28	5				1 8.89	13.33	40.00	1 10.00	26.32	50.00	1 8.33	22.73	43.48
20q12				20q12			20q12			20q12			20q12		
-1	0	2	2	-1 2.86	0.00	0.00	-1 0.00	3.33	3.33	-1 1.43	0.00	6.25	-1 1.67	0.00	4.35
0	62	67	86	0 75.71	84.21	37.50	0 91.11	76.67	36.67	0 81.43	63.16	37.50	0 83.33	59.09	52.17
1	37	30	10	1 21.43	15.79	62.50	1 8.89	20.00	60.00	1 17.14	36.84	56.25	1 15.00	40.91	43.48
20q13				20q13			20q13			20q13			20q13		
-1	0	2	2	-1 2.86	0.00	0.00	-1 0.00	3.33	3.33	-1 1.43	0.00	6.25	-1 1.67	0.00	4.35
0	59	65	81	0 70.00	84.21	37.50	0 86.67	70.00	36.67	0 75.71	63.16	37.50	0 78.33	54.55	52.17
1	40	32	15	1 27.14	15.79	62.50	1 13.33	26.67	60.00	1 22.86	36.84	56.25	1 20.00	45.45	43.48

Figure 2.10: Different expression level of telomerase show invers alteration revealed to the same chromosome bands CGH analyses of all investigated STS revealed several significant ($p<0.05$) alteration (compare also with 2.1 on different chromosomal bands (Chr.bands). Data expressed as frequency (percentage). -1 demonstrate losses, 0 no alterations and 1 gains (collum). Different expression level are shown in the first line: lines labeled with 0, 1 and 2 denotes for 0 = no, 1 = moderate and 2 = high telomerase activity. Red (losses) and green (gains) indicate chromosome bands with an higher frequency. Yellow demonstrate alteration with the same frequency.

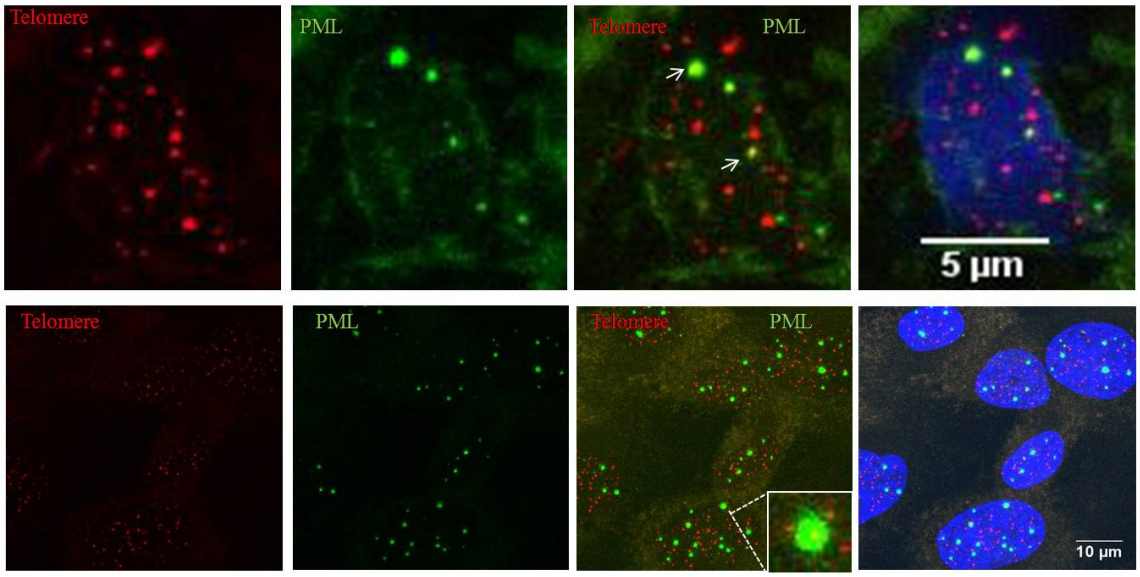

Figure 2.11: ALT-associated PML bodies in non-tumor samples. APBs and heterogeneous telomere spot size distribution were detected by combined telomere fluorescence in situ hybridization and PML immunofluorescence in frozen section of non-tumor samples and fibroblast cell lines. (A) Normal human skin-sections and (B) normal human fibroblasts showing the incidences of APBs. Arrows indicate APBs (telomere staining in red, PML staining in green) as well as enlarged picture (see cutout). No heterogeneous size distributions of telomeres were observed; neither in the samples of normal fibroblast cell lines nor in the non-tumor sections. Nuclei were counterstained with 4',6-diamidino-2-phenylindol (blue). Using confocal laser scanning microscopy, 3D images were acquired from at least three independent regions of the investigated specimens.

large telomere spots (Figure 2.12). This analyses shows that APBs as marker for ALT are independently found in both, non-tumor samples and tumors samples, whereas very large telomeres are exclusively detected in the investigated tumor specimens.

2.1.5 Discussion

Telomere length regulation, on the one hand, can provide a tumor suppressor function by limiting replicative potential, and on the other hand, allow tumor cells to proliferate indefinitely due to the activation of a telomere maintenance mechanism. Consequently, the establishment of a TMM has received greater attention as a target for new chemotherapeutic strategies. We focused our study on the frequency distribution of telomere maintenance mechanisms in different subtypes of soft tissue sarcomas. A better characterization of telomere maintenance mechanisms would facilitate a more tightly focused development and testing of telomerase as a therapeutic target and might initiate the development of a target-oriented therapy against tumors that exhibit ALT mechanism. It is suggested that mesenchymal tissue have a slower cell turnover and less telomere shortening than epithelia, which may lead to a stronger repression of telomerase activity.

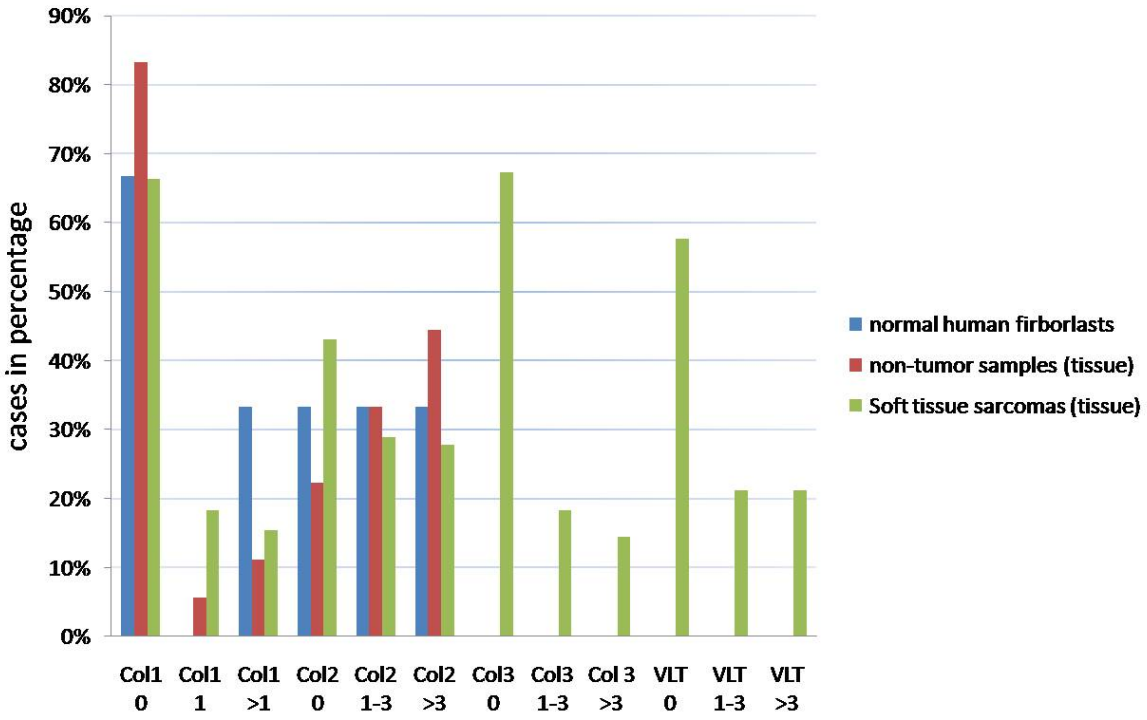

Figure 2.12: ALT-associated PML bodies in non-tumor samples and soft tissue tumors. Comparison of ALT markers in soft tissue sarcoma and non-tumor samples. There is a strong incidence of a similar level of APBs in non-tumor samples (red) and normal human fibroblasts (blue) compared to those tumors of the soft tissue (green). Nevertheless, no heterogeneous size distributions of telomeres were observed in non-tumor section or in normal human fibroblast cell lines. Colocalizations (APBs) labeled Col 1 with 0, 1 and >1 denotes none (0), one (1) and more than one (>1) colocalization per sample respectively; Col 2, Col 3 and VLT (very large telomeres) are subdivided into 0, 1-3 and >3: to indicate none (0), 1 to 3 (1-3) and more than 3 (>3) colocalizations of Col 2, Col 3 or VLT spot per sample.

The activation of ALT is more likely to occur in sarcomas than in carcinomas (Henson et al. 2002).

We analyzed the frequency of telomerase expression levels (low, moderate and high) in different subtypes of soft tissue sarcomas, such as leiomyosarcomas (LMS), malignant peripheral nerve sheath tumors (MPNST), malignant fibrous histiocytoma (MFH), synovial sarcomas (SS), pleomorphic liposarcomas (PLLS), myxoid round cell liposarcoma (MRCLS) and dedifferentiated liposarcoma (DDLS). Our data revealed that each subgroup of soft tissue sarcomas has a different signature in the expression level of telomerase. This could lead to a different efficient response to therapies that would target telomerase. Tumor samples with specific translocations such as MRCL (myxoid round cell liposarcomas) and SS (synovial sarcomas) show an up-regulated telomerase activity compared to those tumors with non-specific translocations, like pleomorphic and dedifferentiated liposarcoma. These data suggest that soft tissue sarcomas with a specific translocation, are more prone to expressing telomerase unlike tumors with more complex karyotypes.

In order to determine the prevalence of the ALT mechanism, we detected markers for ALT such as ALT-associated PML-bodies (APBs) and heterogeneous size distribution of telomere signals, with exceptionally long telomeres and correlated these data with the different expression levels of telomerase. Our study shows for the first time an inverse correlation between telomerase expression levels and markers for ALT. High telomerase expression level correlates with a decreased number of APBs and very large telomeres (VLT). We only occasionally detected a large amount of huge telomere spots in tumors with a high level of telomerase expression. Only two cases, one in MFH and the other in MPNST, displayed large telomere signals, despite having a high telomerase expression level. This could explain why carcinomas, which usually maintain telomere length by the reactivation of telomerase, show telomere, which are equal in length without exceptionally long telomeres. These data are also consistent with further studies that showed in vitro that ALT is suppressed upon fusion of ALT positive cell lines with telomerase-positive cell lines (Perrem et al. 1999).

In our study we observed, that APBs as well as VLT, are increased in tumors with moderate telomerase activity compared to those tumors without telomerase activity. The data indicate that both mechanisms can exist in the same tumor but preferentially, when tumors express a moderate telomerase expression level in alignment with other studies (Johnson and Broccoli 2007). We cannot conclude whether in these cases telomerase is slightly repressed by the induction of APBs and VLT, or whether, for some other reason, these tumors are up-regulating telomerase to a low level, allowing, in turn, an increased number of APBs and VLT. The mechanism of telomerase reactivation remains unknown, but epigenetic mechanism are suggested to be involved in the regulation of telomerase expression (Atkinson et al. 2005), and could partially explain why some tumors express high telomerase activity whereas others are more prone to the ALT pathway. While our data show that both mechanisms can be detected in the same tumor sample, it is not yet known whether both mechanisms function in the same cells, different cells, or in specific

regions of the same tumor.

Investigation of non-tumor samples and normal human fibroblasts showed the presence of APBs in similar form and quality, whereas, in contrast heterogenous size distribution and very large telomeres were exclusively detected in tumor samples. Based on the observation that ALT-associated PML bodies (APBs) contain telomeric DNA and proteins, which are involved in DNA repair and recombination, one can agree that APBs play an important role in the ALT mechanism (Yeager et al. 1999; Johnson et al. 2001). Studies by, Kumar et al. (2007) showed that PML NB and SATB1 regulate chromatin-loop architecture like t-loops (telomeric loops). The latter are accomplished by proteins such as Mre11, NBS1 and RAD50. Based on this finding, it is possible that not only recombination-based proteins are involved in t-loop conformation, but also in PML, which might then lead to the formation of APBs. Recent studies by Jiang et al. (2009) showed that APBs are also induced in growth-arrested senescent cells. From our data we cannot conclude whether the presence of APBs in non-tumor samples is also induced by the ALT-mechanism or by another mechanism besides of ALT. Further studies will need to be done to address this issue and clarify how tightly these nuclear structures are linked to ALT mechanism and whether APBs can still be used as markers for the detection of ALT-like tumors. Altogether, the data suggest that very large telomeres (VLT) signals have a stronger association with the ALT-mechanism than ALT-associated PML bodies.

A previous study by Johnson et al. (2007) revealed that ALT positive tumors have on average, a higher level of genomic instability than tumors without incidences of ALT or compared with tumors exhibiting telomerase activity. To investigate whether telomere maintenance mechanisms correlate with genomic instability, we performed comparative genomic hybridization (CGH). Our data revealed that the occurrence of a TMM did not influence the amount of genomic aberration i.e. copy number of chromosome bands. Except for Col 2 colocalization as a marker for ALT has shown significant more amplification with an increased number of these colocalizations. These findings are not entirely consistent with the work of Johnson et al. (2007) and Scheel et al. (2001). The group of Johnson et al. (2007) investigated by whole-genome profiling of liposarcomas and found in ALT positive tumors, a higher level of genomic instability. The latter group analyzed osteosarcoma-derived cell lines that utilized either ALT or telomerase, by using both telomere and multiplex *in situ* hybridization (FISH). The data revealed an increased number of translocation, deletion and complex rearrangements in ALT-positive cell lines compared to those with telomerase activity.

The work of Montgomery et al. (2004) also proposed that there is a correlation between very large telomeres and pleomorphic sarcomas that typically possess complex karyotypes. Consistent with the present study, pleomorphic liposarcomas showed a high percentage (92%) of very large telomere signals, whereas 54% of these tumors lacked any detectable telomerase activity. In strong contrast, synovial sarcoma and myxoid round cell liposarcoma, both comprising to sarcomas with specific translocations, showed no evidence for heterogeneous telomere length distribution. APBs were found independently

in both soft tissue sarcomas subtypes translocation-associated and with complex karyotype. It is known that the specific spatial arrangements in normal cells are important for the generation of chromosomal translocation. Consequently the organization of the human genome seems to be crucial in the generation of translocation-associated malignancies (Zink et al. 2004). It is possible, that the spatial rearrangement of the human genome is organized differently in cells that show telomeres, which are equal in size and those tumors which have exceptionally long telomeres. Nevertheless, it is not yet known, which mechanism is responsible for translocation-associated sarcomas being more likely to exhibit telomerase activity, than sarcomas with complex karyotypes, which tend to lack high telomerase expression levels. It is also not known why, on the contrary, tumors with complex karyotypes show an increased number of very large telomeres, whereas sarcomas of simple karyotypes do not possess telomeres, which are exceptionally long. Further studies with a higher number of translocation-associated tumors and tumors with komplex karyotypes will need to be done to address this issue and clarify this observation.

The detection of frequently over- or underrepresented chromosomal regions and the comparison to markers of telomere maintenance mechanisms by comparative genomic hybridization (CGH) suggests the presence of genomic regions being involved in the regulation of telomere maintenance mechanisms. We investigated very different subgroups of soft tissue sarcoma with respect to genetic alterations, CGH analyses revealed that tumors with high telomerase activity share some common imbalances. The same observations were found for markers of ALT, which suggests that these markers are linked to one another. Furthermore, several loci with respect to the different TMMs turned out to be inversely altered. Investigations of these regions might encode genes, which are linked to both or either telomere maintenance mechanism. The observation that tumors with moderate telomerase activity share some of the same alterations with the ALT markers, which are inversely altered compared to those tumors with high telomerase activity, suggests that genes in these region are involved in the up-regulation of high telomerase expression level. Furthermore, these data suggest that tumors with high telomerase expression level and tumors with moderate telomerase activity are genetically different.

The chromosomal region 17p11-p12 was frequently gained in tumors possessing ALT, detected by the markers Col 2, Col 3 and VLT. These chromosome bands are of great interest, as they contain three homologous sequences which are known to be involved in recombination processes, resulting in duplications and deletions (Chen et al. 1997).

Tumors exhibiting abundant amounts of Col 2, Col 3 and VLT are frequently gained (40%, 50%, 43% respectively) on chromosome 17p13, where the tumor suppressor gene *TP53* is located. These findings are in contrast with other studies that proposed that the interference of *TP53* might create a more amenable environment for ALT (Johnson et al. 2007) as the loss of p53 increases homologous recombination (Henson et al. 2002). Further studies in ALT positive tumors that address the expression of p53 may explain the association of the p53 protein expression level with the ALT mechanism.

Deletion in tumors with markers for ALT (Col 2, Col 3, VLT) have been frequently

found on chromosome region 16q22. This may be of interest, as TRF2, one of the shelterin-proteins, is localized and is known to play an important role in preventing telomeres from being recognized as sites of DNA damage in order to avoid checkpoint activation and inappropriate DNA-repair (Denchi 2009).

In summary, our data indicate that telomerase expression levels is associated with the subtype of soft tissue sarcomas. Investigating the different telomerase expression level showed that tumors with high telomerase expression levels and those with moderate expression level are on some chromosome bands inversely altered. The genomic regions of this inverse alteration might be involved in the up-regulation of either high or moderate to no telomerase activity. This could have an implication in the response to therapies with telomerase inhibition as the aim. In addition, investigations of non-tumor samples showed that very large telomeres are more tightly associated with the ALT- mechanism than APBs. Further investigation of APBs in non-tumor samples could clarify if these markers are induced by the ALT mechanism or by some other mechanism besides ALT.

2.2 3D geometry-based quantification of colocalizations in three-channel 3D microscopy images in soft tissue tumors

S. Wörz[1], P. Sander[2], M. Pfannmöller[1], R.J. Rieker[3,4],S. Joos[2] G. Mechtersheimer[3], P. Boukamp[4], P. Lichter[2], and K. Rohr[1]

[1]*Dept. Bioinformatics and Functional Genomics, Biomedical Computer Vision Group, University of Heidelberg, BIOQUANT, IPMB, and DKFZ Heidelberg;* [2]*Dept. Molecular Genetics, German Cancer Research Center (DKFZ), Heidelberg;* [3]*Dept. of Pathology, University Hospital, Heidelberg;* [4]*Institute of Pathology, Medical University of Innsbruck;* [5]*Dept. Genetics of Skin Carcinogenesis, German Cancer Research Center (DKFZ), Heidelberg;*

2.2.1 Abstract

We introduce a new model-based approach for automatic quantification of colocalizations in multi-channel 3D microscopy images. The approach is based on different 3D parametric intensity models in conjunction with a model fitting scheme to localize and quantify subcellular structures with high accuracy. The central idea is to determine colocalizations between different channels based on the estimated geometry (position and shape) of subcellular structures as well as to differentiate between different types of colocalizations. Furthermore, we perform a statistical analysis to assess the significance of the determined colocalizations. We have successfully applied our approach to about 400 three-channel 3D microscopy images of human soft-tissue tumors

2.2.2 Introduction

Human *telomeres* are the physical ends of linear chromosomes that protect them from improper DNA metabolism. Telomere shortening, due to the incomplete synthesis of linear DNA during replication, plays an important role aging and cancer. The activation of a *telomere length maintenance mechanism* (TMM) is thus essential for cellular immortalization and long-term tumor growth. Telomerase activity is the most common TMM, particularly in tumors of epithelial origin. However, some tumors, among them specific subtypes of soft tissue sarcomas, have been shown to maintain telomere length by a recombination-based mechanisms that have been termed *alternative lengthening of telomeres* (ALT) (Montgomery et al. 2004). Since the telomere length maintenance mechanisms (TMM) can vary significantly in soft tissue sarcomas, its characterization is crucial for developing new strategies for therapies.

Promyelocytic leukemia (PML) bodies are subnuclear entities colocalizing with various proteins in the cell nucleus. A preferential colocalization of PML bodies with telomeres is indicative for the ALT mechanism (Fasching et al. 2007). A further indication of ALT is their highly heterogeneous telomere lengths with some exceptionally long telomeres (Fasching et al. 2007).

The aim of this study is to assess ALT in human soft tissue sarcomas by combined telomere fluorescence *in situ* hybridization and PML immunofluorescence. Using a confocal laser scanning microscope, we acquired about 400 three-channel 3D fluorescent microscopy images of soft-tissue sarcomas, which visualize telomere spots in the first channel, PML bodies in the second channel, and DAPI-stained nuclei in the third channel (e.g., see Figure 2.13 for maxima intensity projections of a typical example). The central task of image analysis is to automatically detect and classify colocalizations of telomeres and PML bodies within the cell nucleus as well as to automatically detect and quantify very large telomere signals.

In previous work on quantifying the ALT mechanism, colocalizations were often estimated manually or semi-automatically, which is subjective, error prone, and time consuming (e.g., Fasching et al. (2007)). Automatic approaches for colocalization analysis can be classified into intensity-correlation-based and object-based schemes (see Bolte and Cordelières (2006) for a review). With *intensity-correlation-based* schemes, *global* colocalization measures are computed, which directly correlate the intensity information of two channels (e.g., Manders et al. (1993); Comeau et al. (2006)). Main disadvantages are the sensitivity w.r.t. image contrast and noise as well as the global nature of the schemes, i.e., the *number* of colocalizations cannot be quantified. In contrast, with *object-based* schemes a segmentation of the relevant image structures is obtained, which is used to determine colocalizations between two channels (e.g., Fay et al. (1997); Lachmanovich et al. (2003); Zhang et al. (2008)). However, so far typically spot-like structures have been considered using, for example, a threshold-based scheme (Fay et al. 1997), a watershed transform (Lachmanovich et al. 2003), or a wavelet transform (Zhang et al. 2008). Moreover, these approaches only consider distances between spots to deter-

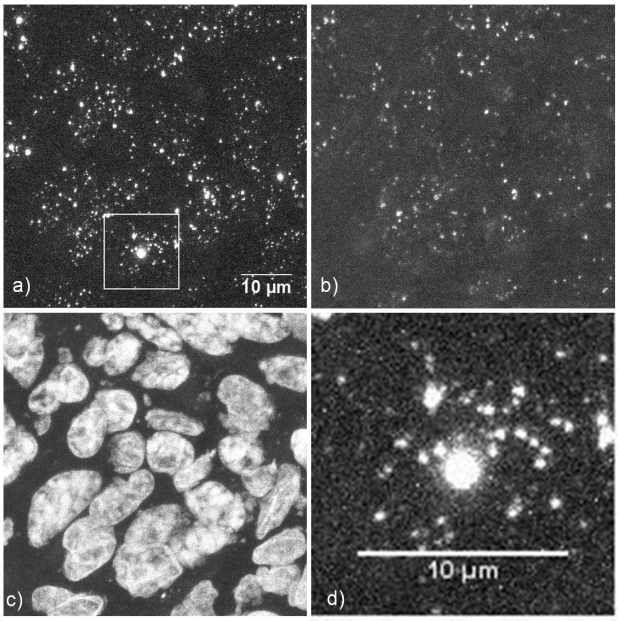

Figure 2.13: Maxima intensity projections of a three-channel 3D microscopy image of a soft tissue tumor and enlarged section a) telomere channel, b) PML channel, c) DAPI- channel, d) enlarged section of telomere spots (framed in picture a).

mine colocalizations (Fay et al. 1997; Zhang et al. 2008) or have only been applied to 2D images (Lachmanovich et al. 2003).

In this contribution, we introduce a new model-based approach for automatic quantification of colocalizations and very large telomere signals in multi-channel 3D microscopy images. Our approach is based on *3D parametric intensity models* in conjunction with a model fitting scheme to localize and quantify telomeres and PML bodies with high accuracy. 3D intensity models have been previously used to segment subcellular structures (e.g., Thomann et al. (2002); Heinzer et al. (2008)). However, so far these approaches only used 3D Gaussian models and they have not been used for the detection of colocalizations. The central idea of our approach is to determine colocalizations of subcellular structures between different channels based on the estimated geometry (position and shape), which is estimated with subvoxel resolution using a combination of different 3D intensity models. In contrast to previous colocalization approaches (e.g., Fay et al. (1997); Lachmanovich et al. (2003); Zhang et al. (2008)), our approach not only allows to accurately detect colocalizations but also to differentiate between *different types* of colocalizations. Furthermore, we perform a *statistical analysis* to assess the significance of the determined colocalizations. In contrast to previous approaches, which analyze manually chosen regions in different areas of both channels (Lachmanovich et al. 2003) or which test the distribution of individual spot distances based on a manual segmentation of the cell area Zhang et al. (2008), we introduce a fully automatic 3D scheme for assessing the significance of the determined colocalizations.

2.2.3 Quantification of colocalizations

In the following, we describe our new model-based approach for the analysis of 3D microscopy images. The approach comprises i) the detection and quantification of subcellular structures and cell nuclei in three different channels, ii) the detection and classification of colocalizations between the segmented subcellular structures, as well as iii) an analysis of the statistical significance of the detected colocalizations.

2.2.3.1 3D Model-Based Segmentation

Telomeres and PML bodies appear as a larger number of bright spots on a diffuse background where both the size and contrast of the spots varies (see Figure 2.13). To segment these structures, we propose a *two-step* approach. In the first step, we apply different image analysis operations to the 3D images to obtain coarse center positions of the different spots. These operations include Gaussian smoothing for noise reduction, image clipping with automatically estimated threshold value for background suppression, and local maxima search for spot detection (see Heinzer et al. (2008) for details).

In the second step, we quantify each detected spot candidate from the first step based on least-squares model fitting. For PML bodies as well as for small and medium sized telomeres, which account for most of the telomeres, the 3D intensity profile can be well represented by a 3D Gaussian function

$$g_{Gaussian3D}(\boldsymbol{x}) = \exp\left(-\frac{x^2}{2\sigma_x^2} - \frac{y^2}{2\sigma_y^2} - \frac{z^2}{2\sigma_z^2}\right) \tag{2.1}$$

where $\boldsymbol{x} = (x, y, z)$ and $(\sigma_x, \sigma_y, \sigma_z)$ are the standard deviations of the Gaussian. By including intensity levels a_0 (background) and a_1 (spot) as well as a 3D rigid transform $\mathcal{R}$ with rotation parameters $\boldsymbol{\alpha} = (\alpha, \beta, \gamma)$ and translation parameters $\boldsymbol{x}_0 = (x_0, y_0, z_0)$, we obtain the 3D parametric intensity model

$$g_M(\boldsymbol{x}, \boldsymbol{p}) = a_0 + (a_1 - a_0)\, g_{Gaussian3D}(\mathcal{R}(\boldsymbol{x})) \tag{2.2}$$

where $\boldsymbol{p}$ represents the overall parameter vector of the model. To fit the model to the image data, we use the non-linear least-squares optimization scheme of Levenberg/Marquardt. As a result, we obtain for each spot estimates of all model parameters. Note that the estimated parameter values are real numbers, i.e., our approach determines, for example, subvoxel positions of the spots as well as subvoxel estimates of the standard deviations which determine the spot size.

However, for very large telomere signals (cf. the center spot in Figure 2.13, d)) the 3D intensity profile significantly deviates from a Gaussian shape. We propose to model these telomeres using a 3D *superellipsoidal* model, which previously has been used to segment bacteria (Wörz et al.) but not to segment subcellular structures. Using the

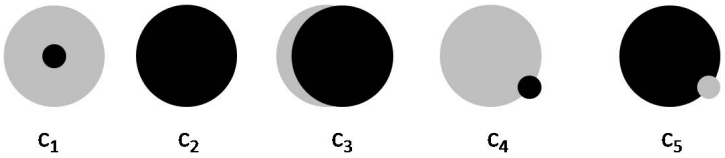

Figure 2.14: Colocalization types c1 to c5

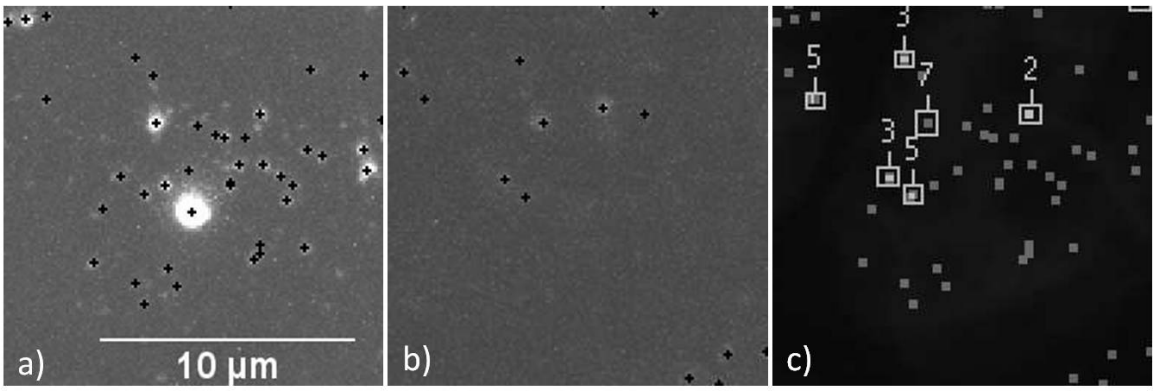

Figure 2.15: Colocalization types c1 to c5 as well as segmentation results Segmentation results for the framed region shown in Figure 2.13 a) telomeres, b) PML NBs, c) identified colocalizations.

Gaussian error function $\Phi(x) = \int_{-\infty}^{x} (2\pi)^{-1/2}\, e^{-\xi^2/2}\, d\xi$, this intensity model is given by

$$g_{SE}(\boldsymbol{x}) = \Phi\left(\frac{\sqrt[3]{r_x r_y r_z}}{\sigma}\left(1 - \sqrt[\epsilon]{\left|\frac{x}{r_x}\right|^{\epsilon} + \left|\frac{y}{r_y}\right|^{\epsilon} + \left|\frac{z}{r_z}\right|^{\epsilon}}\right)\right)$$

where σ is the standard deviation of Gaussian image blur, (r_x, r_y, r_z) are the semi-axes of the superellipsoid, and ϵ describes its roundness (e.g., $\epsilon = 2$ is an ellipsoid and $\epsilon \to \infty$ yields a cuboid). By including intensity parameters and a 3D rigid transform, the 3D parametric intensity model is obtained analogously to (2.2). To segment the telomere channel, we propose a *two-pass* approach. In the first pass, the above described two-step approach with an adaptation to large spots is applied, e.g., using the superellipsoidal model, which is initialized based on the fitting results of the Gaussian model. In the second pass, the smaller spots are segmented using the two-step approach where the regions of the large spots are masked to prevent false spot candidates at the boundary of large spots. To segment the DAPI-stained cell nuclei in the third channel, we apply 3D median and Gaussian filters for noise reduction with subsequent Otsu thresholding. As a result, we obtain a binary segmentation of the cell nuclei.

2.2.3.2 3D Colocalization Quantification

To determine colocalizations between subcellular structures of different channels, we propose the following scheme. The central idea is to utilize the quantified geometry of the structures based on the fitting results of the parametric intensity models, i.e., the 3D position, 3D orientation, and 3D shape (specified by the standard deviations and semi-axes of the Gaussian and superellipsoidal model, respectively). We define a colocalization as an (partial) overlap of two (or more) structures from different channels. Since, in contrast to previous approaches (e.g., Fay et al. (1997); Lachmanovich et al. (2003); Zhang et al. (2008)), we obtain a geometric representation of the structures with *subvoxel* resolution, we are able to differentiate between *different types of colocalizations*.

In this application, we use in total six different types. The types c_1 to c_5 (see Figure 2.14) represent colocalizations between PML bodies (grey) and small/medium sized telomeres (black): c_1 (c_2) is a colocalization where a telomere (PML body) is fully within a PML body (telomere), in a c_3 colocalization both spots overlap and the center of each spot is within the other spot, and c_4 (c_5) is a colocalization where a smaller telomere (PML body) partly overlaps with a larger PML body (telomere). In addition, c_6 denotes a colocalization of a PML body with a very large telomere signal, which is quantified using the superellipsoidal model. Furthermore, in our application also *multiple* colocalizations occur, for example, a colocalization of one PML body with two telomeres. Here we add these cases to the respective types c_1 to c_6 and do not consider them as different types. Overall, we count the number n_{c_i} of colocalizations of each type c_i, the total number n_c summed over all types, as well as the number of colocalized telomeres ($n_{c_{tel}}$) and PML bodies ($n_{c_{pml}}$), which can deviate from n_c due to multiple colocalizations.

2.2.3.3 Analysis of the Significance of Colocalizations

To assess the significance of the estimated number of colocalizations, we perform an *automatic statistical analysis* given the null hypothesis that the observed colocalizations are a result of a random distribution of the spots. This analysis is based on repeated random distributions of the segmented telomeres and PML bodies within the segmented volume of the DAPI channel. For each random distribution, the number of colocalizations $(n_{c_1}, \ldots, n_{c_6}, n_c, n_{c_{tel}}, n_{c_{pml}})_j$ is determined as described above. For all r random distributions, Σ is the number of distributions that yield a number of colocalizations greater than or equal to the experimental result. The empirical p-value is given by $p = \Sigma/r$, which can be compared to a certain level of significance α. Since we finally apply our approach to a large number of $n \approx 500$ images, we use a Bonferroni correction: given the experiment-wide false positive value π, the applied level of significance is $\alpha = \pi/n$. Here, we chose $r = 100,000$ random distributions and a value of $\pi = 0.05$, which yields $\alpha = 0.0001$. Thus, we can state for each type of colocalization in each image if the number of detected colocalizations is significant (i.e., reject the null hypothesis) or not.

	n_{tel}	n_{pml}	n_c	n_{c_1}	n_{c_2}	n_{c_3}	n_{c_4}	n_{c_5}	n_{c_6}
Image 1	458+8	231	89	3	(1)	34	29	16	6
Image 2	479+5	181	22	(0)	(0)	(3)	(11)	(1)	7
Image 3	742+1	331	(16)	(0)	(0)	(0)	(16)	(0)	(0)

Table 2.2: Number n_{tel} of segmented telomeres (normal + very large), number n_{pml} of PML bodies, total number n_c of colocalizations, as well as the numbers $n_{c_1}, \ldots, n_{c_6}$ of different types of colocalizations for three images. Colocalization results which are *not* significant are put in parenthesis.

2.2.4 Experimental results

We have applied our approach to about 400 three-channel 3D fluorescent microscopy images of human soft-tissue tumors. The images have a size of about $512 \times 512 \times 25$ voxels. For all images, we used the same parameter settings. Overall, we achieved quite good segmentation results. For example, Figure 2.15 shows a maxima intensity projection of the segmentation results for the region marked in Figure 2.13. Shown are the center positions of the segmented telomeres and PML bodies as well as the detected colocalizations together with their type.

For the image shown in Figure 2.13 (image 1) as well as for two additional images, Table 2.2 exemplarily shows the number n_{tel} of segmented telomeres (normal + very large), the number n_{pml} of PML bodies, the total number n_c of colocalizations, as well as the numbers $n_{c_1}, \ldots, n_{c_6}$ of different types of colocalizations. Colocalization results which are *not* significant are put in parenthesis. It can be seen that the number of colocalizations as well as the significance of these colocalizations is very different in all three images. Interestingly, whereas the number of segmented telomeres and PML bodies in the first two images is similar, the total number of colocalizations n_c differs by a factor of 4. Still, the total number of colocalizations $n_c = 22$ of image 2 is significant. Considering individual types of colocalizations, it can be seen that the level of significance varies between different types. For example, in image 2 a number of $n_{c_4} = 11$ colocalizations is *not* significant, whereas a number of $n_{c_6} = 7$ colocalizations is significant. As a consequence, the statistical analysis of the significance of the number of colocalizations is important to allow an accurate analysis of the colocalization results. Interestingly, the total number $n_c = 22$ of colocalizations of image 2 is significant even though the types c_1 to c_5 are not significant. The reason is that the type c_6 is significant: there are $n_{c_6} = 7$ (multiple) colocalizations with the 5 very large telomere signals (only two random distributions yielded $n_{c_6} = 7$, the mean is 0.563).

The computation time for a single three-channel 3D image mainly depends on the number of telomeres and PML bodies, and is about 1-2 min for 3D segmentation and colocalization detection (on an AMD Opteron PC with 2.6 GHz).

2.2.5 Discussion

We introduced a new model-based approach for automatic quantification of colocalizations and very large telomere signals in multi-channel 3D microscopy images. The approach is based on 3D parametric intensity models in conjunction with a model fitting scheme to localize and quantify telomeres and PML bodies with high accuracy. The central idea of our approach is to determine colocalizations based on the estimated geometry (position and shape) of subcellular structures as well as to differentiate between different types of colocalizations. Furthermore, we performed a statistical analysis to assess the significance of the determined colocalizations. We have successfully applied our approach to about 400 three-channel 3D fluorescent microscopy images of human soft-tissue tumors. Current and future work are the detailed analysis of the colocalization results w.r.t. biological meaning.

2.2.6 Verification of the automated spot detection by a manual analysis *(unpublished data)*

In order to verify the results of the automated spot detection, we performed a manual analysis of a set of five 3D images with respect to different investigators. The images were segmented twice with an intermission of 4 weeks by investigator 1, once by investigator 2 (Petra Sander), and once by investigator 3. The manual analysis was performed in two steps. First, telomere spots and PML spots were selected with the programm *PointEdit3D* shown in Figure 2.16, provided by Dr. Peter Matula (German Cancer Research Center, Dept. Bioinformatics and Functional Genomics). In a second step, selected spots were imported into ImageJ with a plug-in created by Martin Pfannmöller (CellNetworks - Cluster of Excellence, Heidelberg University). With the assistance of this plug-in, previously picked spots were depicted and used to highlight the spots in the original programm ImageJ. This was further used to determine manual colocalization between the two channels of telomeres and PML. In additional original z-stacks were then consulted to determine the type of colocalization according to the criteria shown in chapter 2.2.

2.2.6.1 Results

The manual spot detection was performed using the *PointEdit3D* application to mark the spots in 3D confocal images. The analysis was done by different experimenters (1-3) in order to assess whether outside factors and personal preferences influence the analysis results. Interestingly enough, investigator 1 (Tabea) counted 3-20% less telomeres (except for test image 4) and 10-75% less PML bodies 4 weeks after her first analysis of the same images. In additional investigator 2 (Petra Sander) counted consistently lower numbers for telomeres and PML bodies than investigator 1 (Tabea). In summary, the results show no consistency between the three sets of results. Furthermore, a high

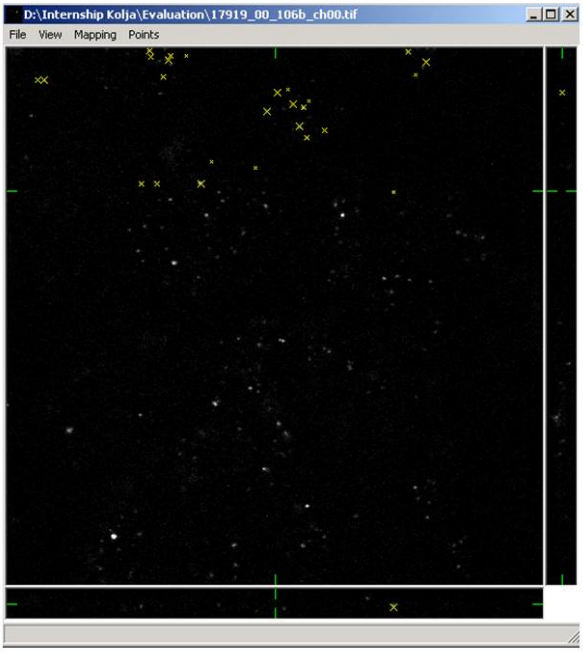

Figure 2.16: Manual analysis of 3D images by the program *PointEdit3D* To verify the automated spot detection a manual analysis was performed assisted by the program *PointEdit3D*. For the spot detection (by 4 different investigator) a x-z-plane (bottom frame) was used. The other two views were used to verify the selected spots

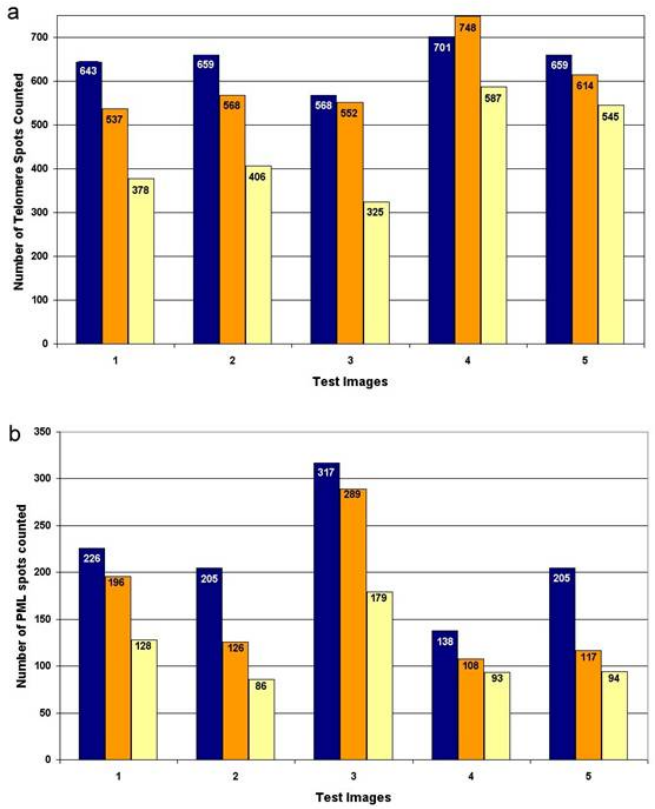

Figure 2.17: Results of manual spot detection by different investigators a) Manual detection of telomeres (a) and manual detection of PML (b) bodies of 5 different test images (using 3D confocal microscopy) First results from investigator 1 (Tabea) are shown in blue and her second results after 5 weeks are shown in orange, results form investigator 2 (Petra Sander) are shown in yellow. Exact number of counted spots are shown within the bar graphs. (Data provided by Stefan Wörz)

instability in the number of spots occurs for almost all images between the different investigators. Results are illustrated in Figure 2.17 and 2.19. Same results are observed for the manual detection of colocalization by the different experimenters. Data shown in Figure 2.18

For the automatic analysis, different parameters for the program *CellSegmentation* were chosen in order to find a standard set to analyze the images optimally, regardless of their quality. Using the chosen parameters the five test images that had been analyzed manually were evaluated by the program. The results, shown in Figure 2.20, indicate that the automated detected signals fall into the range of the manual results for almost all images. Some images were re-evaluated using a different set of parameters for the program *CellSegmentation*. These results are more similar to the results obtained manually. Finally the parameters chosen to evaluate more than 400 3D images by confocal microscopy have been done by Petra Sander. Therefore automated detected spots in

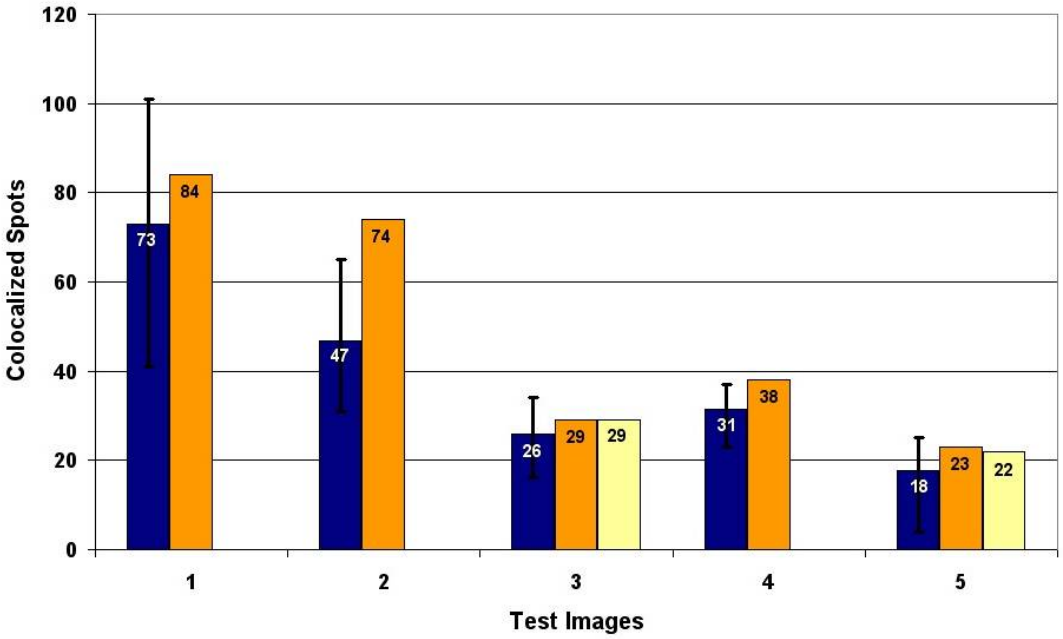

Figure 2.18: Results of manual colocalization detection by different investigators a) Manual detection colocalization of 5 different test images (using 3D confocal microscopy) Manual analysis are shown in blue with error bars. Error bars showing highest and lowest values of the different manual analysis. Results from automated analysis with *standard* parameters are illustrated in orange. In yellow are re-analyzed automated colocalization with changed parameters. Exact numbers of detected colocalizations are shown within the bar graphs.(Data provided by Stefan Wörz)

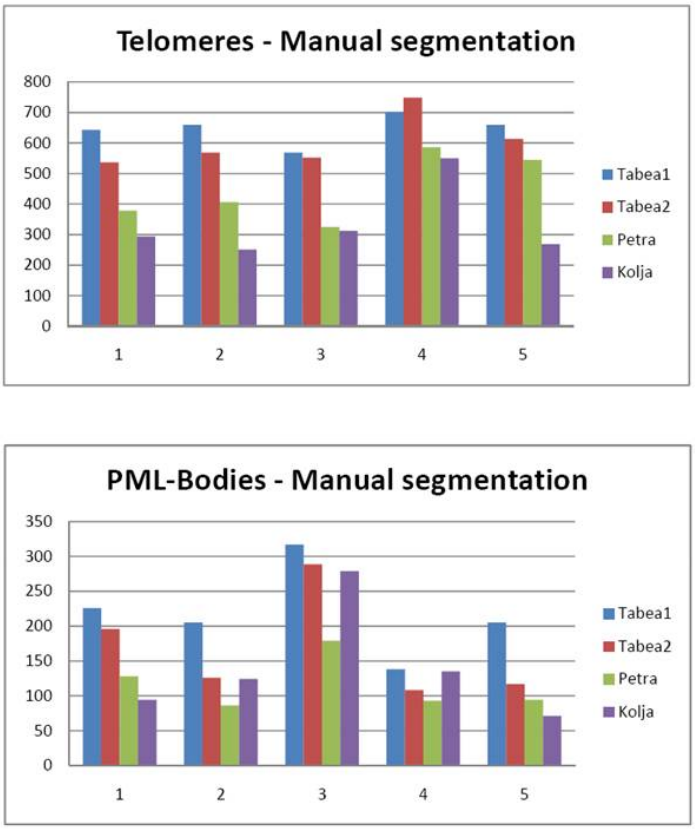

Figure 2.19: Manual spot detection of 3 different investigators The manual analysis of telomeres and PML bodies by three different experimenters (Tabea, Petra Sander and Kolja) shows obviously a strong variety of the counted spots in both channels. (Data provided by Stefan Wörz)

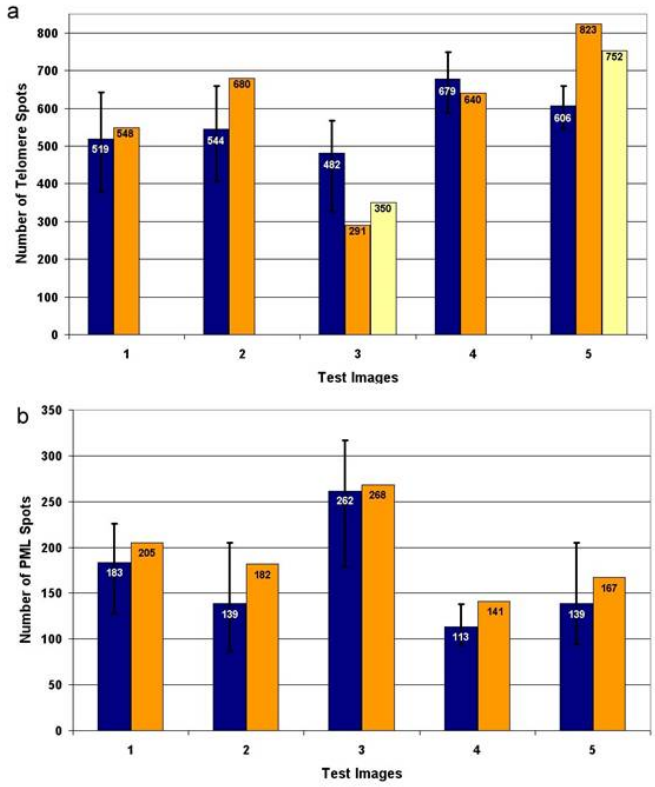

Figure 2.20: Comparison of manual and automated spot detection of 3D confocal microscopy images a) detected telomere spots b) detected PML spots. Manual analysis illustrate in blue, error bars showing the highest and lowest counted spots of the different experimenters. Results of the automated spot detection are shown in orange. Re-analyzed automated spot detection with changed parameters are shown in yellow. Raw data of counted spots are shown within the bar graphs. (Data provided by Stefan Wörz)

about 100 3D images of soft tissue sarcoma were proven and for the parameters of the *CellSegmentation* program adapted (Data not shown). These sets of parameters were finally used for the screening of tumor samples and non-tumor samples to investigate the ALT-mechanism.

Most work on quantifying the ALT mechanism, and colocalization was measured manually or semi-automatically. The results of these small experiments show that the manual spot detection and colocalization analysis strongly varies among different experiments. Consequently, manually estimations are not only time consuming but also subjective and error prone.

3 Unpublished additional experiments

3.1 ALT-associated PML bodies: Does any PML-isoform colocalize preferential with telomeres?

3.1.1 Abstract

Cancer cells are able to prevent telomere shortening by activating a telomere maintenance mechanism. Most immortalized cells and cancer cells apply a telomerase-dependent mechanism for telomere maintenance. Some tumors maintain telomere length by a recombination based mechanism that has been termed *alternative lengthening of telomeres* (ALT). Promyelocytic leukemia (*PML*) has been implicated in a variety of functions, including a preferential colocalization of PML bodies with telomeres, also referred as ALT-associated PML bodies (APBs) and are indicative for the ALT mechanism. The aim of this study was to investigate the PML protein isoforms in cell lines with different mechanisms of telomere maintenance. For our analyses the cell lines HeLa and MCF7 (Telomerase positive), U2OS (ALT positive) and VH7 (without telomere maintenance mechanism) were used. The protein level of the individual PML isoforms were investigated by Western-blot analysis of whole-cell extracts and nuclear fraction from whole cell extracts and found different bands representing different spliced PML isoforms. With respect to the cell lines exhibiting different telomere maintenance mechanisms, the results showed no significant differences in the protein-level of the specific PML isoforms. In order to show to which extent any PML protein isoform colocalizes preferentially to telomeres, the different PML isoforms were investigated. Six GFP-tagged PML isoforms (located in the nucleus) were transiently transfected into U2OS (ALT positive) cell lines, MCF7 and Hela cell lines, both telomerase positive. From our results, we cannot conclude that any PML splice variants preferentially colocalize with telomeres. These findings suggest that a knock down of PML protein isoforms might be a better approach to investigate the role of individual PML isoforms and their role in APBs assembling and therefore in the alternative pathway of telomere maintenance.

3.1.2 Introduction

Most immortalized human cells, as well as most cancer cells, maintain their telomeres by activating a telomere maintenance mechanism, either by telomerase (Greider and

Blackburn 1985), or by alternative lengthening of telomeres (ALT) (Bryan et al. 1995). One indication of ALT is their highly heterogenous telomere lengths with some exceptionally long telomeres (Fasching et al. 2007). Another hallmark is the colocalization promyelocytic leukemia (PML) bodies with specific proteins such as TRF1 and TRF2, and telomeres.

PML is expressed in all mammalian tissue and cell lines (Gambacorta et al. 1996). The typical number of PML nuclear bodies (PML NB) in mammalian cells is 1 to 30 per nucleus, depending on cell cycle phase, differentiation stage and cell type. PML nuclear foci are between 0.2 and 1.0 µm wide. Many proteins localize permanently or transiently to PML nuclear bodies. As a consequence, PML bodies have been implicated in the regulation of different cellular function such as the induction of apoptosis, inhibition of proliferation, induction of cellular senescence, maintenance of genomic stability and antiviral responses. Further, cellular processes, in which PML NB might be involved, are modulation of chromatin structures, transcriptional regulation of specific genes, protein sequestration and posttranslational modification of target proteins (Bernardi and Pandolfi 2007).

The characteristic protein of PML NBs is the promyelocytic leukemia gene product PML. The human gene *PML* was identified as the fusion partner of the gene *RARA* (retinoic acid receptor alpha) in the chromosomal translocation t(15:17) in acute promyelocytic leukemia (APL) (de Thé et al. 1991). *PML* is composed of nine exons of which exon 5-9 can be alternatively spiced, resulting in specific isoforms (Jensen et al. 2001). Exon 1 to 3 encodes the TRIM motif (RBBC, Ring finger, B-box, coiled-coil) and is present in all PML isoforms. PML harbors three SUMOylation sites, and SUMOylation of PML is essential for PML nuclear body assembly (Zhong et al. 2000a). Further motifs have been identified in the C-terminus of PML and all PML isoforms, such as the nuclear localization signal (NLS) and a SUMO-interacting motif (Henderson and Eleftheriou 2000).

In this study, we first analyzed the composition and functions of the PML protein isoforms in cell lines, showing different telomere maintenance mechanisms. Isoform protein expression patterns were detected by Western blot analysis. Further we established a combination of GFP-tagged PML isoforms transfection with fluorescence *in situ* hybridization followed by immunofluorescence in order to analyze the colocalization between specific PML isoforms, endogenous PML and telomeres.

3.1.3 Material and Methods

3.1.3.1 Plasmids

GFP-expression constructs (GFP-tagged PML isoforms 1 to 6) were provided by Prof. Dr. Peter Hemmerich (Fritz-Lipmann-Institut Jena)

3.1.3.2 Cell culture and transfection

U2OS and HeLa cells were obtained from the American Tissue Cultured Collection (ATCC) and the fibroblast cell lines VH7, were provided by Prof. Dr. P. Boukamp (DKFZ, Heidelberg, Germany). All cell lines were cultured in Dulbecco's modified Eagle's medium (DMEM) supplemented with 10% fetal calf serum in a 5% CO_2 atmosphere at 37°C. 1-2 day before transfection, cells were seeded on glass slides and transfected with plasmid DNA by using FuGENE HD Transfection reagent (Roche, Basel, Switzerland) according to the manufacturer's protocol. Cells were fixed at different time points. Alternatively, cells were also transfected with Amaxa's Nucleofector Reagent according to the manufacturer's protocol. Cells, transfected with AMAXA, were seeded and cultured on glass slides after transfection and were fixed at different time points.

3.1.3.3 Western blots

Cellular fractionation was achieved by following the manufactures protocol with slight modifications (Calbiochem / Merck Protein Fractionation Kit subcellular). Whole-cell extracts, produced from the cultured cell lines and nuclear proteins were separated by SDS-PAGE and transferred to the Immobilon(TM) -P-PVDF membrane (Millipore, Schwalbach). The membrane was first incubated with primary antibodies (PBS + 1% serum) and then with a secondary HRP-conjugated anti-mouse IgG (Amersham Bioscience, Freiburg, dilution 1:10000). Signals were detected using ECL Western Blot detection Kit (Amersham Bioscience, Freiburg). Anti PML monoclonal mouse antibody was from Linaris (PG-M3) and beta-actin antibody from Biozol.

3.1.3.4 Combined FISH with immunofluorescence and microscopy

The PML nuclear bodies (for all isoforms) were detected by immunolocalization of PML (PG-M3, mouse monoclonal, Linaris; dilution 1:200). The secondary antibody used as reporter were tagged with FITC (Linaris, Germany; dilution 1:200) or Cy5 (Dianova, dilution 1:200). The telomeres were revealed by a Cy3-labeled $(CCCTAA)_3$ peptide nucleic acid (PNA) probe (Dako, Dennmark). For combined telomere-FISH and PML immunofluorescence, cells were fixed on glass slides with 3.7% formaldehyde (freshly prepared, from 37% formaldehyde, J.T.Baker) in PBS (phosphate-buffered saline). After fixation the specimens were washed in PBS. Samples were then dehydrated by series of ethanol (70%, 90%, 100%) each for 2 min incubation time and briefly air dried. Thereafter, 8 µm of Cy3-labeled PNA probe were added and then denatured for 3 min at 80°C. After hybridization for 2h at room temperature, the slides were washed several times at room temperature with 70% formamide/10 mM Tris-HCL, pH 7.2 (25min), PBS (30 sec), 0.1xSSC for 5min at 65°C, and PBS containing 0.05% Tween-20 (2 x 5 min at room temperature). After telomere-FISH the specimens were permeablized by incubation with 0.02% Triton X-100 (Sigma) in PBS for three minutes at room temperature. Then a protein block was applied by incubation with 4% goat serum in PBS for 10 minutes.

Antibodies, diluted in PBS containing 1% goat serum, were incubated for 30 minutes at 37°C for the primary antibody and at room temperature for the secondary antibody. Each antibody incubation was followed by three washes with PBS. Finally slides were covered by 1 drop of anitfade solution (VectaSield, Linaris) containing 4,6-Diamidino-2phenylindole (DAPI). 3D fluorescence signals were detected in Z-stacks of about 10 to 30 frames with 0.28 µm spacing by confocal laser scanning microscopy (TCS SP5/SP2 Leica Microsystems, Germany) Images were processed using MacBiophotonics ImageJ and subsequently exported and saved as JPEG files.

3.1.3.5 Quantification of colocalization in three/four-channel 3D microscopy images

For automated image analysis a program called *CellSegmentation* was used, which was especially designed for this approach. (see chapter 2.2). In brief: To segment the DAPI-stained cell nuclei in the third channel, we applied 3D median and Gaussian filters for noise reduction with subsequent Otsu thresholding for segmentation of nuclei and non-nuclei compartments. To detect structures such as telomere- and PML-spots, coarse center positions of spot were determined by detection of intensity maxima. In the next step, each detected spot candidate is quantified by the 3D intensity profile with an underlying Gaussian function. To determine colocalizations between telomeres and endogenous PML, we utilized the geometry of the structures based on the fitting results, i.e. 3D position, 3D orientation and 3D shape. A colocalization was defined as an (partial) overlap of two or more structures from the different channels using the geometry of these structures. Due to the geometric representation of those structures with sub-voxel resolution we were able to differentiate between different types of colocalization (see chapter 2.2).

3.1.3.6 Immunofluorescence with endogenous PML-isoforms

The endogenous PML-isoforms are kindly provided by Hugues de Thé (Centre National de la Recherche Scientifique UMR7151, Equipe Labellisée par La Ligne Contre le Cancer, Paris Cedex, France). For more details see Condemine et al. (2006).

The PML nuclear bodies of the different isoforms (1, 2, 4 and 5) were detected by immunolocalization of the endogenous PML isoforms (Condemine et al. 2006) (dilution 1:200). The secondary antibody used as a reporter were tagged with FITC (Linaris, Germany; dilution 1:200). U2OS cell lines were fixed on glass slides with 3.7% formaldehyde (freshly prepared, J.T.Baker) in PBS (phosphate-buffered saline). After fixation the specimens were washed in PBS. Then specimens were permeabilized by incubation with 0.02% Triton X-100 (Sigma) in PBS for three minutes at room temperature. Then a protein block was applied by incubation with 4% goat serum in PBS for 10 minutes. Antibodies, diluted in PBS containing 1% goat serum, were incubated for 30 minutes at 37°C for the primary antibody and at room temperature for the secondary antibody.

Each antibody incubation was followed by three washes with PBS. Finally slides were covered by 1 drop of anitfade solution (VectaSield, Linaris) containing 4,6-Diamidino-2phenylindole (DAPI). 3D fluorescence signals were detected in Z-stacks of about 10 to 30 frames with 0.28 µm spacing by confocal laser scanning microscopy (TCS SP2 Leica Microsystems, Germany)

3.1.4 Results

3.1.4.1 Western-blot analysis

To study the abundance distribution of the various PML isoforms in different cell lines (HeLa, U2OS and VH7), in relation to telomere maintenance mechanisms, we performed Western blot analysis. The PG-M3 PML antibody (recognized all PML isoforms) reveals different PML isoforms proteins in the range from 45 kDa to 100 kDa. To avoid false interpretation of the abundance of individual endogenous PML splicing variants, a better approach would be theoretically to achieve western blots for each individual PML isoform. The results of western blot by nuclear extraction, instead of whole cell extracts, shows similar expression patterns of the PML isoforms in the different cell lines.

3.1.4.2 GFP-tagged PML isoforms

The six nuclear isoforms of the PML protein result from alternative splicing of exon 7 to exon 9. All six isoforms were transfected as GFP-tagged fusionproteins to study if any PML-Isoform colocalizes preferentially to the telomeres. GFP-tagged PML isoforms were first transiently transfected to U2OS using two different transfection methods in order to investigate which one is more efficient. We investigated the cell lines 24h, 48h and 72h hours after transfection. At time point 72h after transfection by AMAXA, we were able to observe an expression pattern of all PML isoforms (except for isoform 2, which was not working in any experiment). Suboptimal expression patterns (72h after transfection) were detected in cells transfected by FuGENE HD (data not shown). Therefore, in all further experiments, cells were transfected by AMAXA and investigated at time point 72h. Investigations at the late time point (72h), are based on the fact, that PML number and size increases in response to cellular stress, which is given at the time of transfection.

We studied U2OS transfected cells by the given GFP-construct, followed by telomere FISH with subsequent immunofluorescence (PG-M3 PML antibody). The goal was to investigate the colocalization events between the different PML isoforms, telomere signals and endogenous PML antibody (recognizing all PML isoforms). Our results showed the possibility to combine the transfection protocol for the GFP-constructs with subsequent telomere-FISH, as shown in Figure 3.1, followed by immunofluorescence as shown in Figure 3.2.

To study whether any PML isoform colocalizes preferentially to the telomeres, we also

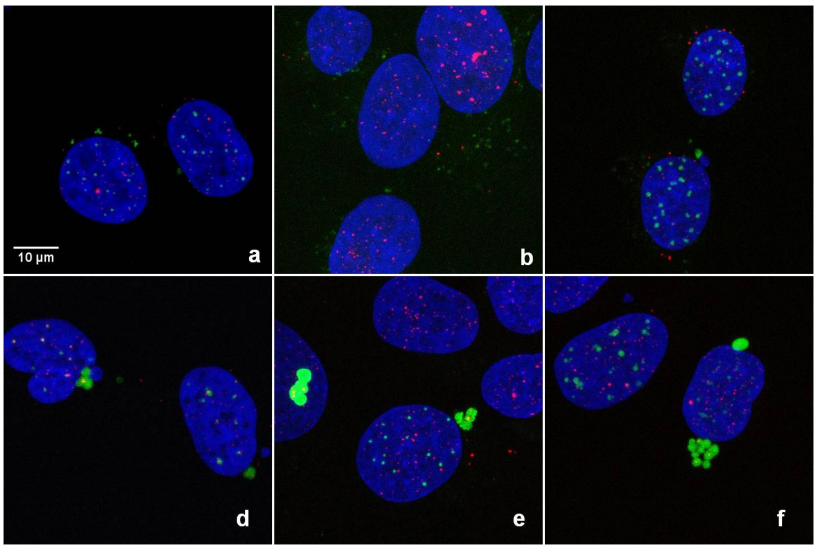

Figure 3.1: U2OS cell lines were transfected with GFP-tagged PML isoforms 1-6 (green) and subsequent telomere-FISH (red), nuclei stained with 4'6-diamidino-2-phenylindole (DAPI, in blue). **a)** PML isoform 1, 72h after transfection **b)** PML isoform 2, 72h after transfection (not working in any experiment, for not known reasons); **c)** PML isoform 3, 72h after transfection;**d)** PML isoform 4, 72h after transfection; **e)** PML isoform 5, 72h after transfection; **f)** PML isoform 6, 72h after transfection. Images have been done by three-channel 3D microscopy (Maximum intensity projection).

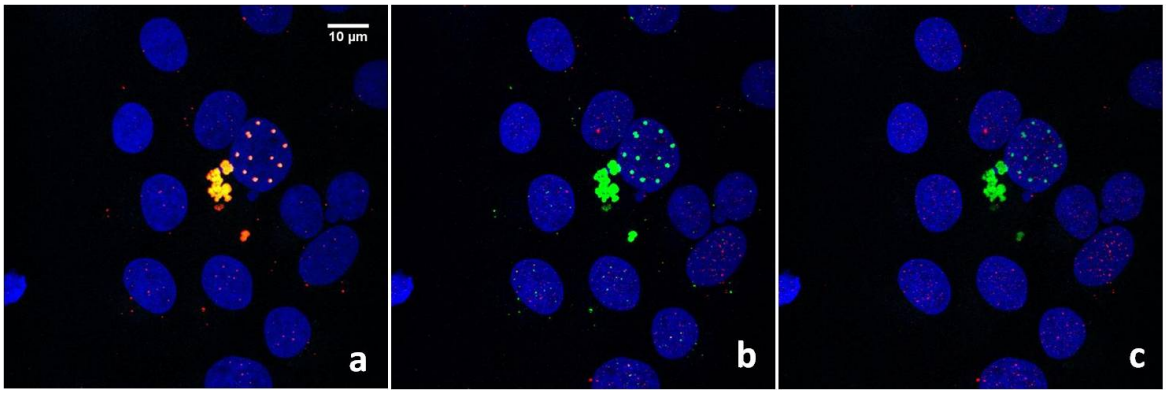

Figure 3.2: Four-channel 3D microscopy images of GFP-tagged PML isoform 4, combined with telomere-FISH and immunofluorescence of endogenous PML U2OS cells were transfected with the GFP-tagged PML isoform 5 by AMAXA and fixed after 72h. **a)** PML isoform 4 (green) and PML Antibody Cy5 (red); **b)** PML antibody (green) and telomere (red); **c)** PML isoform 4 (green) and telomere (red). Images have been done by four-channel 3D microscopy (DNA content stained by DAPI in blue)

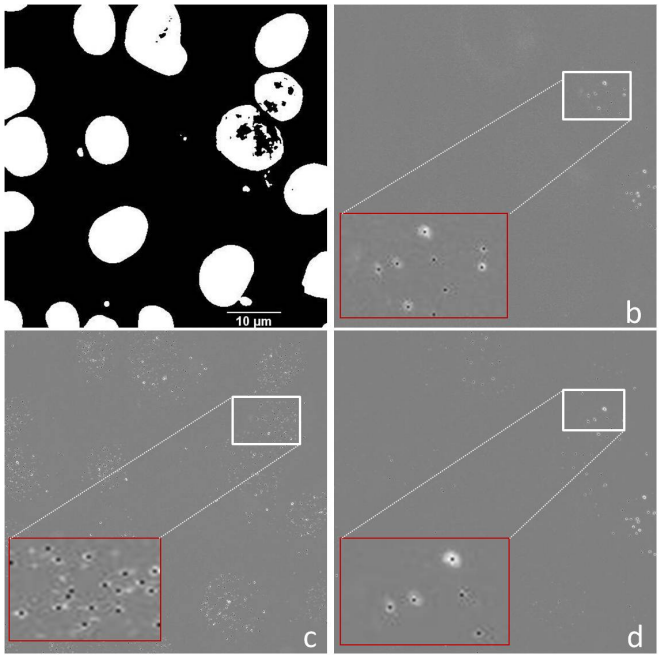

Figure 3.3: Automatic quantification of a four-channel 3D microscopy image with enlarged section framed in red. U2OS cells were transfected with the GFP-tagged PML isoform 1, combined by telomere-FISH and immunofluorescence of endogenous PML. In the enlarged figures (framed in red), quantified spots are marked by the black dots **a)** DAPI channel with nuclear segmentation; **b)** GFP-tagged isoform 5; **c)** telomere-signals. **d)** endogenous PML spots (nucleus stained with DAPI shown in white)

Table 3.1: Analyzed colocalization in a four-channel 3D fluorescence microscopy image

colocalization classes*	between telomeres and endogenous PML	between telomeres and GFP-tagged isoform	between endogenous PML and GFP-tagged isoform
colocalization class1*	0	0	0
colocalization class2*	0	0	0
colocalization class3*	25	15	6
colocalization class4*	0	2	4
colocalization class5*	0	9	0
colocalization class6*	0	0	0

*for more details see chapter 2.2

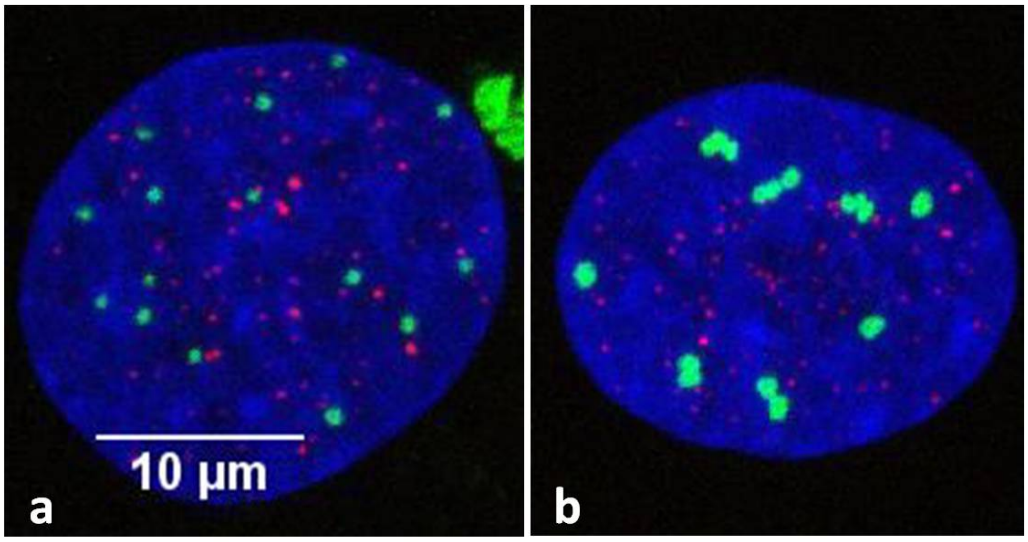

Figure 3.4: Expression of GFP-tagged isoform 5 (green) varies between individual nuclei, Transfection of the ALT positive cell lines U2OS with GFP-tagged isoform 5 (green) as example for different expression patterns. **a)** Moderate GFP expression of PML isoform 5 ; **b)** high GFP expression of PML isoform 5 with aggregate-like structures (Counter staining with DAPI shown in blue)

expanded our program *CellSegmention* from a three-channel into a multi (four)- channel quantification of 3D microscopy images (three directions: x, y, z, and four channels: ch1 for , ch2, ch3, ch4 for PML antibody, telomeres, GFP-tagged isoform and DAPI, respectively). Thus, we were able to automatically quantify the different colocalizations in four-channel 3D microscopy images between PML isoforms, telomeres and endogenous PML in the segmented DAPI (nucleus) channel. Results are shown in Figure 3.3 and Table 3.1. The fact, that the expression patterns varied among individual nuclei, as shown for the GFP-tagged isoform 5 (Figure 3.4), could lead to a misinterpretation of the colocalization results and their relevance.

3.1.4.3 Immunofluorescence of endogenous PML-isoforms

In order to validate carefully our studies which are performed under conditions of GFP-tagged PML isoforms overexpression, we used the endogenous PML isoforms 1,2,4 and 5. Results by immunofluorescence with the different PML isoforms are shown in Figure 3.5. Isoform 1 and 2 were showing a good expression pattern in the nuclei with nearly no background. PML isoform 4 and 5 show unspecific foci with a strong background, which made it impractical to use these antibodies for further experiments. Nevertheless, we were able to acquire images (stacks) for both protocols (Figure 3.6) to study possible differences between endogenous PML isoforms (size and number) in non-transfected cells, and GFP-tagged PML isoforms, which are more and less overexpressed in the nucleus. First results showed that low expression levels only refer to endogenous PML bodies

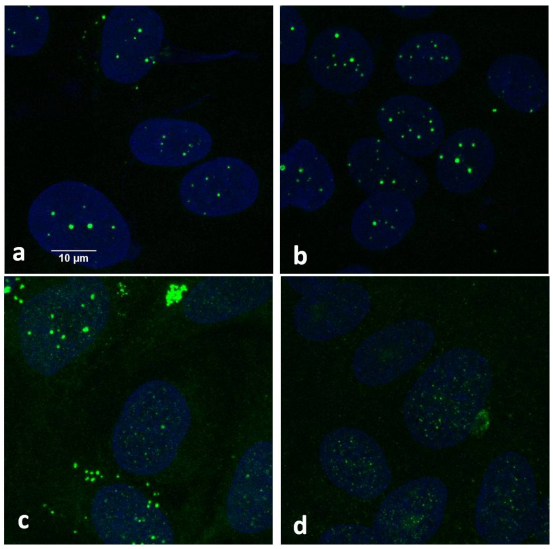

Figure 3.5: Immunofluorescence in U2OS cell lines of endogenous PML-isoforms, Immunofluorescence of the endogenous PML isoforms 1,2,4 and 5 in the ALT positive cell lines U2OS . **a)** endogenous PML isoform 1 with specific protein expression pattern; **b)** endogenous PML isoform 2 with specific protein expression pattern; **c)** endogenous PML isoform 4; protein expression pattern with a strong background **d)** endogenous PML isoform 5 with strong background and non-specific expression pattern (nucleus is revealed by 4'6-diamidino-2-phenylindole shown in blue)

and those of endogenous PML isoforms in non-transfected cells. An example of a low expression pattern of GFP-tagged PML isoforms is shown in Figure 3.6 and for the different expression levels in Figure 3.4.

3.1.5 Concluding remarks and further perspectives

To understand the cellular function of PML NBs, studies have focused primarily on the identification of proteins that localized to these structures. Less is known about the relationship between the PML splice variants and their potential differential regulation. Furthermore, it has been shown, that different PML isoforms did not localize to PML NBs to the same extent. Kinetic studies showed that many PML isoforms are exchanged fast between a individual nuclear body and the nucleoplasm (Bernardi and Pandolfi 2007).

Our hypothesis was, that specific PML isoforms are functionally relevant for the ALT mechanism and therefore for the formation of ALT-associated PML bodies. As such, we first measured the PML protein expression pattern by Western blot analysis of extracts from telomerase positive and ALT-positive cell lines. Our data showed no significant differences in the PML expression levels of the different cell lines. This was due to the difficulties in the precise characterization of the different PML isoforms, which ranged from about 100 kDa to 40 kDa. Therefore antibodies of all specific endogenous PML

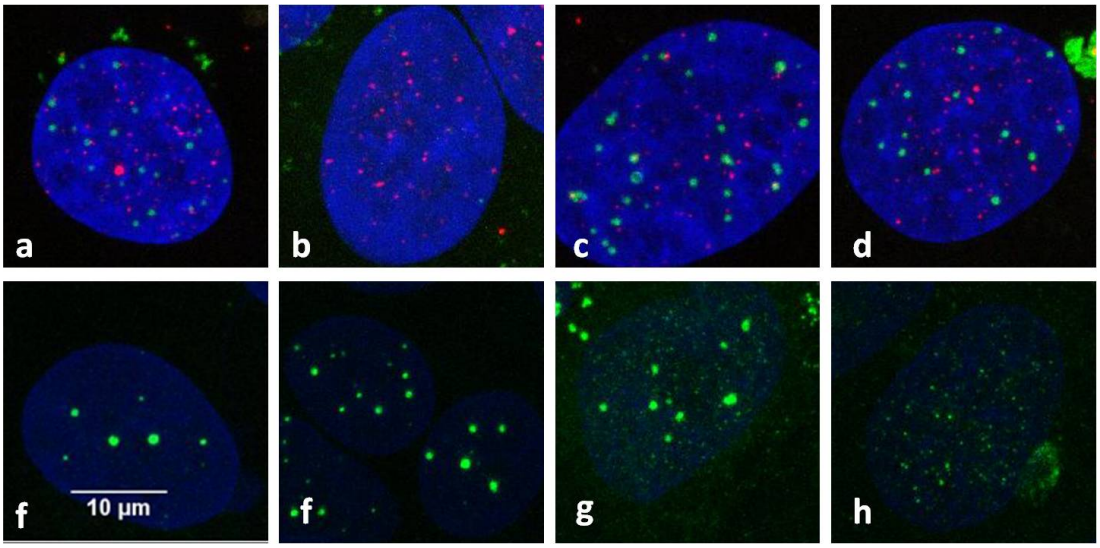

Figure 3.6: Comparison of GFP-tagged PML isoforms 1,2,4 and 5 (all with low GFP-expression level) and immunofluorescence of endogenous PML isoforms in ALT positive cell lines (U2OS), a-d) GFP-tagged PML isoforms (green); a) GFP-tagged PML isoform 1, b) GFP-tagged PML isoform 2; c) GFP-tagged PML isoform 4; d) GFP-tagged PML isoform 5 **e-h)** Immunofluorescence of the endogenous PML isoforms 1,2,4 and 5; e) endogenous PML isoform 1; f) endogenous PML isoform 2; g) endogenous PML isoform 4; h) endogenous PML isoform 5 (nucleus is stained by 4'6-diamidino-2-phenylindole shown in blue)

isoforms would be of great benefit for further work in this field.

Experiments by GFP-tagged PML isoform overexpression in the ALT positive cell line U2OS showed indeed the possibility of combining the protocol of transfection, telomere-FISH and immunofluorescence, which were used to investigate whether any PML isoform preferentially localizes to the telomeres. From our data we cannot conclude that specific PML isforms colocalizes preferentially to telomeres. Nevertheless, some important questions remain to be answered: We do not know, how the cellular stress due to the transfection protocol influences the size and amount of the PML NBs. Further it is not known whether the overexpression of one PML isoform suppresses the expression of all other PML isoforms or even the PML NBs itself. A better approach could be to knock down one isoform to see if ALT positive cell lines still assemble ALT-associated PML bodies.

In the literature, the evidence that not all PML nuclear bodies are composed equally is described. For example, Muratani et al. (2002) has shown that PML NBs have different motilities. Further, often just a few PML NBs per cell are found to localize with proteins, other nuclear organelles or chromatin regions. Nevertheless, for future investigations of the PML isoforms and their function, it would be of great benefit to generate isoform specific PML antibodies, which would not only allow a look into the function of specific PML isoforms but would also allow the study of the structure of PML nuclear bodies.

4 General conclusion

In the last two decades much has been done in understanding the process of tumorigenesis. The role of genomic instability has gained cumulative attention in the last decade due to its evident role in malignant transformation. The most common genetic alterations occurring in tumorigeneses are seen in regulatory genes involved in cell cycle progression and arrest. Although cancers are quite diverse, with a large range of heterogeneity amongst tumors in different tissues, there are some characteristics which all tumors have in common. These properties include unlimited replicative potential and prevalent instability, both of which are described as telomeric dysfunction in Figure 4.1. Unlimited replicative potential is a necessary step in long-term tumor growth and therefore, for the pathogenesis of cancer. Consequently, telomere lengthening by the activation of telomere maintenance mechanisms is discussed as a contributor to tumor progression as they characterize most malignancies. Recent studies have aimed at investigating the roles of ALT and telomerase in tumorigenesis to develop strategies that will improve the treatment of malignancies such as sarcomas. Regarding the response to chemotherapy, sarcomas range from histological subtypes that are very responsive to chemotherapy, to subtypes that are quite resistant (Patel et al. 1997). Telomere maintenance mechanisms as a target treatment to individual sarcomas are discussed as an alternative approach.

One first step in this study was to determine the frequency distribution of different subgroups of the telomere maintenance mechanism in soft tissue sarcoma, such as leiomyosarcoma, malignant fibrous histiocytoma, malignant peripheral nerve sheath tumors, synovial sarcoma and liposarcomas (pleomorphic, dedifferentiated, myxoid round cell). Telomerase-activity was detected by TRAP-assay. For the detection of markers for ALT, we first investigated different telomere length distributions in different subgroups of soft tissue sarcoma by Southern blot analysis. Initial results showed that some of the investigated tumors exhibited exceptionally long telomeres. Although Southern blotting turned out to be a robust method to determine the telomere length, we were not able to analyze the frequency distribution of the different telomere sizes. Therefore, we established a combined telomere-FISH and PML immunofluorescent technique in order to get a direct impression about telomere size within the nuclei. Additionally, with this method it is possible to detect a second marker of ALT which is referred to as ALT-associated PML nuclear bodies. We applied this method and TRAP analysis to more than 120 samples of frozen tumor sections, 18 non-tumor sections and several cell lines exhibiting different telomere maintenance mechanism. A confocal laser scanning microscope was used to obtain images from three independent fields. To analyze these 3D images (stacks) with respect to markers of ALT, we designed in cooperation with Stefan Wörz

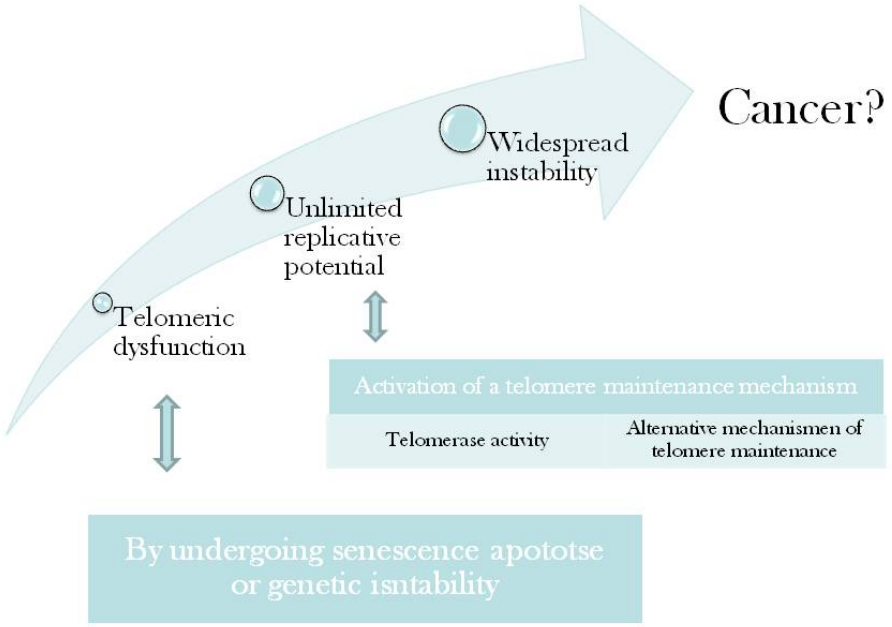

Figure 4.1: Telomeric dysfunction and its possible impact Both, unlimited replicative potential and widespread instability might be partly explained by telomeric dysfunction and is discussed in tumorigenesis.

(Dep. Bioinformatics and Functional Genomics, Biomedical Computer Version Group, University of Heidelberg), a program for fully automated detection of PML NBs, and measured telomere signals (resembling spots) of normal size and those exhibiting exceptionally large spots. To prevent signal detection outside the nucleus, we performed a nuclear segmentation of the DAPI channel using the same analysis program. Therefore, we were able to successfully capture more than 500 images (stacks) (see chapter 2.2). Our data, analyzed with this program, revealed that even non-tumor samples and normal human fibroblasts showed APBs, whereas heterogeneous telomere spot distribution seem to exclusively arise in tumor samples (see chapter 2.1). Further studies of the protein level of the individual PML isoforms, might help to understand more about the function of APBs. It may be that different specific PML isoforms are functional relevant for the assembling of APBs in case this structures are induced by different cellular processes besides ALT.

For a better understanding of the ALT-mechanism and its markers, it was very important to develop this fully automated program. The detailed evaluation of markers for ALT was possible due to the program.This program has impressively shown, that some spots especially colocalization signals, are often difficult to detect, as they are hardly visible due to differing intensities. Furthermore, analysis in 3D is very important, as overlays of maximum intensity projections may lead to artifacts. For the future, such programs will allow to investigate greater amounts of samples, not only for ALT, but for other markers that appear as foci in the cell or even more in the cell nucleus.

To better understand telomere maintenance mechanism in more detail, we studied all corresponding markers. Therefore, we discriminated not only between no and positive telomerase activity but between different expression levels. Even for the markers of ALT we discriminated between different amounts of APBs and very large telomeres. Having distinguished between the occurrences of these different levels of markers for TMM, we were able to show that there are important differences. Analysis by CGH revealed that some of the altered loci are conversely changed. For example, whereas on chromosome 1p13 losses are more frequent for tumors expressing high telomerase activity, tumors with low or no expression levels more commonly have in the same loci gains. Such differences might have important implication in the regulation of the expression level of telomerase. Moreover, markers for ALT are on the same loci (1p13) also gained. We conclude that this might be a strong indication for tumors exhibiting both telomere maintenance mechanisms (see chapter 2.1). Such findings were only possible because we discriminated in more detail among different levels of the markers for ALT and telomerase activity.

This study raises a number of issues that should be addressed in the future. For further evaluation of the frequency distribution of TMM in tumors, it is important that there is discrimination between different levels of telomerase activity und markers for ALT. The finding of APBs also in non-tumor-samples might be an indication that APBs could be induced by different cellular processes besides ALT. This has to be confirmed by further studies. Nevertheless, alternative markers for ALT are needed, as we do not know how

tight APBs are linked to the ALT-mechanism. Even very large telomeres are discussed in some publications as telomeric aggregates. Both seem to be totally different events, whereas large telomeres are a strong indication of ALT, the role of telomeric aggregates is not fully understood. The data analyzed by CGH are also of major interest, as they revealed a number of loci that might be involved in the regulation of both telomerase expression and ALT. In summary, our results may have important implications for the development of new strategies for anti-cancer therapies.

Bibliography

Al-Agha and Igbokwe 2008 Al-Agha, O. M. ; Igbokwe, A. A.: Malignant fibrous histiocytoma: between the past and the present. In: *Arch. Pathol. Lab. Med.* 132 (2008), Jun, pp. 1030–1035

Antonescu et al. 2000a Antonescu, C. R. ; Elahi, A. ; Humphrey, M. ; Lui, M. Y. ; Healey, J. H. ; Brennan, M. F. ; Woodruff, J. M. ; Jhanwar, S. C. ; Ladanyi, M.: Specificity of TLS-CHOP rearrangement for classic myxoid/round cell liposarcoma: absence in predominantly myxoid well-differentiated liposarcomas. In: *J Mol Diagn* 2 (2000), Aug, pp. 132–138

Antonescu et al. 2000b Antonescu, C. R. ; Kawai, A. ; Leung, D. H. ; Lonardo, F. ; Woodruff, J. M. ; Healey, J. H. ; Ladanyi, M.: Strong association of SYT-SSX fusion type and morphologic epithelial differentiation in synovial sarcoma. In: *Diagn. Mol. Pathol.* 9 (2000), Mar, pp. 1–8

Antonescu et al. 2001 Antonescu, C. R. ; Tschernyavsky, S. J. ; Decuseara, R. ; Leung, D. H. ; Woodruff, J. M. ; Brennan, M. F. ; Bridge, J. A. ; Neff, J. R. ; Goldblum, J. R. ; Ladanyi, M.: Prognostic impact of P53 status, TLS-CHOP fusion transcript structure, and histological grade in myxoid liposarcoma: a molecular and clinicopathologic study of 82 cases. In: *Clin. Cancer Res.* 7 (2001), Dec, pp. 3977–3987

Argani et al. 2000 Argani, P. ; Faria, P. A. ; Epstein, J. I. ; Reuter, V. E. ; Perlman, E. J. ; Beckwith, J. B. ; Ladanyi, M.: Primary renal synovial sarcoma: molecular and morphologic delineation of an entity previously included among embryonal sarcomas of the kidney. In: *Am. J. Surg. Pathol.* 24 (2000), Aug, pp. 1087–1096

Argenyi et al. 1988 Argenyi, Z. B. ; Van Rybroek, J. J. ; Kemp, J. D. ; Soper, R. T.: Congenital angiomatoid malignant fibrous histiocytoma. A light-microscopic, immunopathologic, and electron-microscopic study. In: *Am J Dermatopathol* 10 (1988), Feb, pp. 59–67

Atkinson et al. 2005 Atkinson, S. P. ; Hoare, S. F. ; Glasspool, R. M. ; Keith, W. N.: Lack of telomerase gene expression in alternative lengthening of telomere cells is associated with chromatin remodeling of the hTR and hTERT gene promoters. In: *Cancer Res.* 65 (2005), Sep, pp. 7585–7590

Azumi et al. 1987 Azumi, N. ; Curtis, J. ; Kempson, R. L. ; Hendrickson, M. R.: Atypical and malignant neoplasms showing lipomatous differentiation. A study of 111 cases. In: *Am. J. Surg. Pathol.* 11 (1987), Mar, pp. 161–183

Bachor et al. 1999 Bachor, C. ; Bachor, O. A. ; Boukamp, P.: Telomerase is active in normal gastrointestinal mucosa and not up-regulated in precancerous lesions. In: *J. Cancer Res. Clin. Oncol.* 125 (1999), pp. 453–460

Batista and Artandi 2009 Batista, L. F. ; Artandi, S. E.: Telomere uncapping, chromosomes, and carcinomas. In: *Cancer Cell* 15 (2009), Jun, pp. 455–457

Berlin et al. 1984 Berlin, O. ; Stener, B. ; Kindblom, L. G. ; Angervall, L.: Leiomyosarcomas of venous origin in the extremities. A correlated clinical, roentgenologic, and morphologic study with diagnostic and surgical implications. In: *Cancer* 54 (1984), Nov, pp. 2147–2159

Bernardi and Pandolfi 2007 Bernardi, R. ; Pandolfi, P. P.: Structure, dynamics and functions of promyelocytic leukaemia nuclear bodies. In: *Nat. Rev. Mol. Cell Biol.* 8 (2007), Dec, pp. 1006–1016

Berner et al. 1997 Berner, J. M. ; Meza-Zepeda, L. A. ; Kools, P. F. ; Forus, A. ; Schoenmakers, E. F. ; Ven, W. J. Van de ; Fodstad, O. ; Myklebost, O.: HMGIC, the gene for an architectural transcription factor, is amplified and rearranged in a subset of human sarcomas. In: *Oncogene* 14 (1997), Jun, pp. 2935–2941

Best 1987 Best, P. V.: Malignant triton tumour in the cerebellopontine angle. Report of a case. In: *Acta Neuropathol.* 74 (1987), pp. 92–96

Blackburn 1992 Blackburn, E. H.: Telomerases. In: *Annu. Rev. Biochem.* 61 (1992), pp. 113–129

Blackburn 2005 Blackburn, E. H.: Telomeres and telomerase: their mechanisms of action and the effects of altering their functions. In: *FEBS Lett.* 579 (2005), Feb, pp. 859–862

Blackburn and Gall 1978 Blackburn, E. H. ; Gall, J. G.: A tandemly repeated sequence at the termini of the extrachromosomal ribosomal RNA genes in Tetrahymena. In: *J. Mol. Biol.* 120 (1978), Mar, pp. 33–53

Blasco 2005 Blasco, M. A.: Telomeres and human disease: ageing, cancer and beyond. In: *Nat. Rev. Genet.* 6 (2005), Aug, pp. 611–622

Bolte and Cordelières 2006 Bolte, S. ; Cordelières, F. P.: A guided tour into subcellular colocalization analysis in light microscopy. In: *J Microsc* 224 (2006), Dec, pp. 213–232

Borden 2002 Borden, K. L.: Pondering the promyelocytic leukemia protein (PML) puzzle: possible functions for PML nuclear bodies. In: *Mol. Cell. Biol.* 22 (2002), Aug, pp. 5259–5269

Boukamp and Mirancea 2007 Boukamp, P. ; Mirancea, N.: Telomeres rather than telomerase a key target for anti-cancer therapy? In: *Exp. Dermatol.* 16 (2007), Jan, pp. 71–79

Boukamp et al. 2005 Boukamp, P. ; Popp, S. ; Krunic, D.: Telomere-dependent chromosomal instability. In: *J. Investig. Dermatol. Symp. Proc.* 10 (2005), Nov, pp. 89–94

Brady et al. 1992 Brady, M. S. ; Gaynor, J. J. ; Brennan, M. F.: Radiation-associated sarcoma of bone and soft tissue. In: *Arch Surg* 127 (1992), Dec, pp. 1379–1385

Bryan et al. 1995 Bryan, T. M. ; Englezou, A. ; Gupta, J. ; Bacchetti, S. ; Reddel, R. R.: Telomere elongation in immortal human cells without detectable telomerase activity. In: *EMBO J.* 14 (1995), Sep, pp. 4240–4248

Cai et al. 2001 Cai, Y. C. ; McMenamin, M. E. ; Rose, G. ; Sandy, C. J. ; Cree, I. A. ; Fletcher, C. D.: Primary liposarcoma of the orbit: a clinicopathologic study of seven cases. In: *Ann Diagn Pathol* 5 (2001), Oct, pp. 255–266

Calcagnile and Gisselsson 2007 Calcagnile, O. ; Gisselsson, D.: Telomere dysfunction and telomerase activation in cancer–a pathological paradox? In: *Cytogenet. Genome Res.* 118 (2007), pp. 270–276

Cesare and Griffith 2004 Cesare, A. J. ; Griffith, J. D.: Telomeric DNA in ALT cells is characterized by free telomeric circles and heterogeneous t-loops. In: *Mol. Cell. Biol.* 24 (2004), Nov, pp. 9948–9957

Cesare and Reddel 2008 Cesare, A. J. ; Reddel, R. R.: Telomere uncapping and alternative lengthening of telomeres. In: *Mech. Ageing Dev.* 129 (2008), pp. 99–108

Chen et al. 1997 Chen, K. S. ; Manian, P. ; Koeuth, T. ; Potocki, L. ; Zhao, Q. ; Chinault, A. C. ; Lee, C. C. ; Lupski, J. R.: Homologous recombination of a flanking repeat gene cluster is a mechanism for a common contiguous gene deletion syndrome. In: *Nat. Genet.* 17 (1997), Oct, pp. 154–163

Clark et al. 1994 Clark, J. ; Rocques, P. J. ; Crew, A. J. ; Gill, S. ; Shipley, J. ; Chan, A. M. ; Gusterson, B. A. ; Cooper, C. S.: Identification of novel genes, SYT and SSX, involved in the t(X;18)(p11.2;q11.2) translocation found in human synovial sarcoma. In: *Nat. Genet.* 7 (1994), Aug, pp. 502–508

Coindre et al. 1986 Coindre, J. M. ; Trojani, M. ; Contesso, G. ; David, M. ; Rouesse, J. ; Bui, N. B. ; Bodaert, A. ; De Mascarel, I. ; De Mascarel, A. ; Goussot, J. F.: Reproducibility of a histopathologic grading system for adult soft tissue sarcoma. In: *Cancer* 58 (1986), Jul, pp. 306–309

Coindre et al. 2001 Coindre, J. M. ; Terrier, P. ; Guillou, L. ; Le Doussal, V. ; Collin, F. ; Ranchère, D. ; Sastre, X. ; Vilain, M. O. ; Bonichon, F. ; N'Guyen Bui, B.: Predictive value of grade for metastasis development in the main histologic types of adult soft tissue sarcomas: a study of 1240 patients from the French Federation of Cancer Centers Sarcoma Group. In: *Cancer* 91 (2001), May, pp. 1914–1926

Comeau et al. 2006 Comeau, J. W. ; Costantino, S. ; Wiseman, P. W.: A guide to accurate fluorescence microscopy colocalization measurements. In: *Biophys. J.* 91 (2006), Dec, pp. 4611–4622

Condemine et al. 2006 Condemine, W. ; Takahashi, Y. ; Zhu, J. ; Puvion-Dutilleul, F. ; Guegan, S. ; Janin, A. ; Thé, H. de: Characterization of endogenous human promyelocytic leukemia isoforms. In: *Cancer Res.* 66 (2006), Jun, pp. 6192–6198

Cordon-Cardo et al. 1994 Cordon-Cardo, C. ; Latres, E. ; Drobnjak, M. ; Oliva, M. R. ; Pollack, D. ; Woodruff, J. M. ; Marechal, V. ; Chen, J. ; Brennan, M. F. ; Levine, A. J.: Molecular abnormalities of mdm2 and p53 genes in adult soft tissue sarcomas. In: *Cancer Res.* 54 (1994), Feb, pp. 794–799

Costa and Weiss 1990 Costa, M. J. ; Weiss, S. W.: Angiomatoid malignant fibrous histiocytoma. A follow-up study of 108 cases with evaluation of possible histologic predictors of outcome. In: *Am. J. Surg. Pathol.* 14 (1990), Dec, pp. 1126–1132

Costa et al. 2006 Costa, A. ; Daidone, M. G. ; Daprai, L. ; Villa, R. ; Cantù, S. ; Pilotti, S. ; Mariani, L. ; Gronchi, A. ; Henson, J. D. ; Reddel, R. R. ; Zaffaroni, N.: Telomere maintenance mechanisms in liposarcomas: association with histologic subtypes and disease progression. In: *Cancer Res.* 66 (2006), Sep, pp. 8918–8924

Counter et al. 1998 Counter, C. M. ; Hahn, W. C. ; Wei, W. ; Caddle, S. D. ; Beijersbergen, R. L. ; Lansdorp, P. M. ; Sedivy, J. M. ; Weinberg, R. A.: Dissociation among in vitro telomerase activity, telomere maintenance, and cellular immortalization. In: *Proc. Natl. Acad. Sci. U.S.A.* 95 (1998), Dec, pp. 14723–14728

Dahl and Angervall 1974 Dahl, I. ; Angervall, L.: Cutaneous and subcutaneous leiomyosarcoma. A clinicopathologic study of 47 patients. In: *Pathol Eur* 9 (1974), pp. 307–315

DeVita et al. 2001 DeVita, V.T. J. ; Hellmans, S. ; Rosenberg, S.A.: *Cancer: Principles and Practice of Oncology.* Philadelphia : Lippinocott Williams and Wilkins, 2001

Dei Tos et al. 1996 Dei Tos, A. P. ; Maestro, R. ; Doglioni, C. ; Piccinin, S. ; Libera, D. D. ; Boiocchi, M. ; Fletcher, C. D.: Tumor suppressor genes and related molecules in leiomyosarcoma. In: *Am. J. Pathol.* 148 (1996), Apr, pp. 1037–1045

Dei Tos et al. 1997 Dei Tos, A. P. ; Doglioni, C. ; Piccinin, S. ; Maestro, R. ; Mentzel, T. ; Barbareschi, M. ; Boiocchi, M. ; Fletcher, C. D.: Molecular abnormalities of the p53 pathway in dedifferentiated liposarcoma. In: *J. Pathol.* 181 (1997), Jan, pp. 8–13

Dei Tos et al. 1998 Dei Tos, A. P. ; Mentzel, T. ; Fletcher, C. D.: Primary liposarcoma of the skin: a rare neoplasm with unusual high grade features. In: *Am J Dermatopathol* 20 (1998), Aug, pp. 332–338

Dellaire and Bazett-Jones 2004 Dellaire, G. ; Bazett-Jones, D. P.: PML nuclear bodies: dynamic sensors of DNA damage and cellular stress. In: *Bioessays* 26 (2004), Sep, pp. 963–977

Denchi 2009 Denchi, E. L.: Give me a break: how telomeres suppress the DNA damage response. In: *DNA Repair (Amst.)* 8 (2009), Sep, pp. 1118–1126

Deng et al. 2008 Deng, Y. ; Chan, S. S. ; Chang, S.: Telomere dysfunction and tumour suppression: the senescence connection. In: *Nat. Rev. Cancer* 8 (2008), Jun, pp. 450–458

Downes et al. 2001 Downes, K. A. ; Goldblum, J. R. ; Montgomery, E. A. ; Fisher, C.: Pleomorphic liposarcoma: a clinicopathologic analysis of 19 cases. In: *Mod. Pathol.* 14 (2001), Mar, pp. 179–184

Ducatman et al. 1986 Ducatman, B. S. ; Scheithauer, B. W. ; Piepgras, D. G. ; Reiman, H. M. ; Ilstrup, D. M.: Malignant peripheral nerve sheath tumors. A clinicopathologic study of 120 cases. In: *Cancer* 57 (1986), May, pp. 2006–2021

El-Rifai et al. 1998 El-Rifai, W. ; Sarlomo-Rikala, M. ; Knuutila, S. ; Miettinen, M.: DNA copy number changes in development and progression in leiomyosarcomas of soft tissues. In: *Am. J. Pathol.* 153 (1998), Sep, pp. 985–990

Enzinger 1979 Enzinger, F. M.: Angiomatoid malignant fibrous histiocytoma: a distinct fibrohistiocytic tumor of children and young adults simulating a vascular neoplasm. In: *Cancer* 44 (1979), Dec, pp. 2147–2157

Fagioli et al. 1998 Fagioli, M. ; Alcalay, M. ; Tomassoni, L. ; Ferrucci, P. F. ; Mencarelli, A. ; Riganelli, D. ; Grignani, F. ; Pozzan, T. ; Nicoletti, I. ; Grignani, F. ; Pelicci, P. G.: Cooperation between the RING + B1-B2 and coiled-coil domains of PML is necessary for its effects on cell survival. In: *Oncogene* 16 (1998), Jun, pp. 2905–2913

Fanburg-Smith and Miettinen 1999 Fanburg-Smith, J. C. ; Miettinen, M.: Angiomatoid "malignant" fibrous histiocytoma: a clinicopathologic study of 158 cases and further exploration of the myoid phenotype. In: *Hum. Pathol.* 30 (1999), Nov, pp. 1336–1343

Farshid et al. 2002 Farshid, G. ; Pradhan, M. ; Goldblum, J. ; Weiss, S. W.: Leiomyosarcoma of somatic soft tissues: a tumor of vascular origin with multivariate analysis of outcome in 42 cases. In: *Am. J. Surg. Pathol.* 26 (2002), Jan, pp. 14–24

Fasching et al. 2007 Fasching, C. L. ; Neumann, A. A. ; Muntoni, A. ; Yeager, T. R. ; Reddel, R. R.: DNA damage induces alternative lengthening of telomeres (ALT) associated promyelocytic leukemia bodies that preferentially associate with linear telomeric DNA. In: *Cancer Res.* 67 (2007), Aug, pp. 7072–7077

Fay et al. 1997 Fay, F. S. ; Taneja, K. L. ; Shenoy, S. ; Lifshitz, L. ; Singer, R. H.: Quantitative digital analysis of diffuse and concentrated nuclear distributions of nascent transcripts, SC35 and poly(A). In: *Exp. Cell Res.* 231 (1997), Feb, pp. 27–37

Fisher 1998 Fisher, C.: Synovial sarcoma. In: *Ann Diagn Pathol* 2 (1998), Dec, pp. 401–421

Fletcher 1992 Fletcher, C. D.: Pleomorphic malignant fibrous histiocytoma: fact or fiction? A critical reappraisal based on 159 tumors diagnosed as pleomorphic sarcoma. In: *Am. J. Surg. Pathol.* 16 (1992), Mar, pp. 213–228

Fletcher et al. 1996 Fletcher, C. D. ; Akerman, M. ; Dal Cin, P. ; Wever, I. de ; Mandahl, N. ; Mertens, F. ; Mitelman, F. ; Rosai, J. ; Rydholm, A. ; Sciot, R. ; Tallini, G. ; Berghe, H. van den ; Ven, W. van de ; Vanni, R. ; Willen, H.: Correlation between clinicopathological features and karyotype in lipomatous tumors. A report of 178 cases from the Chromosomes and Morphology (CHAMP) Collaborative Study Group. In: *Am. J. Pathol.* 148 (1996), Feb, pp. 623–630

Fletcher et al. 2002 Fletcher, Christopher D. ; Krishnan, Unni. ; Mertesn, Frederik.: *Pathology and Genetics of Tumours of Soft Tissue and Bone.* Lyon : International Agency for Research on Cancer Press, 2002. – World Health Organization Classification of Tumours

Flieder and Moran 1998 Flieder, D. B. ; Moran, C. A.: Primary cutaneous synovial sarcoma: a case report. In: *Am J Dermatopathol* 20 (1998), Oct, pp. 509–512

Fong et al. 1993 Fong, Y. ; Coit, D. G. ; Woodruff, J. M. ; Brennan, M. F.: Lymph node metastasis from soft tissue sarcoma in adults. Analysis of data from a prospective database of 1772 sarcoma patients. In: *Ann. Surg.* 217 (1993), Jan, pp. 72–77

Friedberg et al. 1999 Friedberg, J. W. ; Abbeele, A. D. Van den ; Kehoe, K. ; Singer, S. ; Fletcher, C. D. ; Demetri, G. D.: Uptake of radiolabeled somatostatin analog is detectable in patients with metastatic foci of sarcoma. In: *Cancer* 86 (1999), Oct, pp. 1621–1627

Fritz et al. 2002 Fritz, B. ; Schubert, F. ; Wrobel, G. ; Schwaenen, C. ; Wessendorf, S. ; Nessling, M. ; Korz, C. ; Rieker, R. J. ; Montgomery, K. ; Kucherlapati, R. ; Mechtersheimer, G. ; Eils, R. ; Joos, S. ; Lichter, P.: Microarray-based copy number and expression profiling in dedifferentiated and pleomorphic liposarcoma. In: *Cancer Res.* 62 (2002), Jun, pp. 2993–2998

Gambacorta et al. 1996 Gambacorta, M. ; Flenghi, L. ; Fagioli, M. ; Pileri, S. ; Leoncini, L. ; Bigerna, B. ; Pacini, R. ; Tanci, L. N. ; Pasqualucci, L. ; Ascani, S. ; Mencarelli, A. ; Liso, A. ; Pelicci, P. G. ; Falini, B.: Heterogeneous nuclear expression of the promyelocytic leukemia (PML) protein in normal and neoplastic human tissues. In: *Am. J. Pathol.* 149 (1996), Dec, pp. 2023–2035

Grande et al. 1996 Grande, M. A. ; Kraan, I. van der ; Steensel, B. van ; Schul, W. ; Thé, H. de ; Voort, H. T. van der ; Jong, L. de ; Driel, R. van: PML-containing nuclear bodies: their spatial distribution in relation to other nuclear components. In: *J. Cell. Biochem.* 63 (1996), Dec, pp. 280–291

Greider and Blackburn 1985 Greider, C. W. ; Blackburn, E. H.: Identification of a specific telomere terminal transferase activity in Tetrahymena extracts. In: *Cell* 43 (1985), Dec, pp. 405–413

Görisch et al. 2004 Görisch, S. M. ; Wachsmuth, M. ; Ittrich, C. ; Bacher, C. P. ; Rippe, K. ; Lichter, P.: Nuclear body movement is determined by chromatin accessibility and dynamics. In: *Proc. Natl. Acad. Sci. U.S.A.* 101 (2004), Sep, pp. 13221–13226

HAYFLICK and MOORHEAD 1961 HAYFLICK, L. ; MOORHEAD, P. S.: The serial cultivation of human diploid cell strains. In: *Exp. Cell Res.* 25 (1961), Dec, pp. 585–621

Hakin-Smith et al. 2003 Hakin-Smith, V. ; Jellinek, D. A. ; Levy, D. ; Carroll, T. ; Teo, M. ; Timperley, W. R. ; McKay, M. J. ; Reddel, R. R. ; Royds, J. A.: Alternative lengthening of telomeres and survival in patients with glioblastoma multiforme. In: *Lancet* 361 (2003), Mar, pp. 836–838

Hanahan and Weinberg 2000 Hanahan, D. ; Weinberg, R. A.: The hallmarks of cancer. In: *Cell* 100 (2000), Jan, pp. 57–70

Hardell and Sandström 1979 Hardell, L. ; Sandström, A.: Case-control study: soft-tissue sarcomas and exposure to phenoxyacetic acids or chlorophenols. In: *Br. J. Cancer* 39 (1979), Jun, pp. 711–717

Harley et al. 1990 Harley, C. B. ; Futcher, A. B. ; Greider, C. W.: Telomeres shorten during ageing of human fibroblasts. In: *Nature* 345 (1990), May, pp. 458–460

Hashimoto et al. 1986 Hashimoto, H. ; Daimaru, Y. ; Tsuneyoshi, M. ; Enjoji, M.: Leiomyosarcoma of the external soft tissues. A clinicopathologic, immunohistochemical, and electron microscopic study. In: *Cancer* 57 (1986), May, pp. 2077–2088

Hayflick 2000 Hayflick, L.: The illusion of cell immortality. In: *Br. J. Cancer* 83 (2000), Oct, pp. 841–846

Heinzer et al. 2008 Heinzer, S. ; Wörz, S. ; Kalla, C. ; Rohr, K. ; Weiss, M.: A model for the self-organization of exit sites in the endoplasmic reticulum. In: *J. Cell. Sci.* 121 (2008), Jan, pp. 55–64

Helman and Meltzer 2003 Helman, L. J. ; Meltzer, P.: Mechanisms of sarcoma development. In: *Nat. Rev. Cancer* 3 (2003), Sep, pp. 685–694

Henderson and Eleftheriou 2000 Henderson, B. R. ; Eleftheriou, A.: A comparison of the activity, sequence specificity, and CRM1-dependence of different nuclear export signals. In: *Exp. Cell Res.* 256 (2000), Apr, pp. 213–224

Henricks et al. 1997 Henricks, W. H. ; Chu, Y. C. ; Goldblum, J. R. ; Weiss, S. W.: Dedifferentiated liposarcoma: a clinicopathological analysis of 155 cases with a proposal for an expanded definition of dedifferentiation. In: *Am. J. Surg. Pathol.* 21 (1997), Mar, pp. 271–281

Henson et al. 2002 Henson, J. D. ; Neumann, A. A. ; Yeager, T. R. ; Reddel, R. R.: Alternative lengthening of telomeres in mammalian cells. In: *Oncogene* 21 (2002), Jan, pp. 598–610

Henson et al. 2005 Henson, J. D. ; Hannay, J. A. ; McCarthy, S. W. ; Royds, J. A. ; Yeager, T. R. ; Robinson, R. A. ; Wharton, S. B. ; Jellinek, D. A. ; Arbuckle, S. M. ; Yoo, J. ; Robinson, B. G. ; Learoyd, D. L. ; Stalley, P. D. ; Bonar, S. F. ; Yu, D. ; Pollock, R. E. ; Reddel, R. R.: A robust assay for alternative lengthening of telomeres in tumors shows the significance of alternative lengthening of telomeres in sarcomas and astrocytomas. In: *Clin. Cancer Res.* 11 (2005), Jan, pp. 217–225

Hieken and Das Gupta 1996 Hieken, T. J. ; Das Gupta, T. K.: Mutant p53 expression: a marker of diminished survival in well-differentiated soft tissue sarcoma. In: *Clin. Cancer Res.* 2 (1996), Aug, pp. 1391–1395

Hisaoka et al. 2008 Hisaoka, M. ; Ishida, T. ; Kuo, T. T. ; Matsuyama, A. ; Imamura, T. ; Nishida, K. ; Kuroda, H. ; Inayama, Y. ; Oshiro, H. ; Kobayashi, H. ; Nakajima, T. ; Fukuda, T. ; Ae, K. ; Hashimoto, H.: Clear cell sarcoma of soft tissue: a clinicopathologic, immunohistochemical, and molecular analysis of 33 cases. In: *Am. J. Surg. Pathol.* 32 (2008), Mar, pp. 452–460

Hothorn et al. 2008 Hothorn, T. ; Hornik, K. ; Wiel, M.A. van de ; Zeileis, A.: Implementing a class of permutation tests: The coin package. In: *Journal of Statistical Software* 28 (2008)

Jemal et al. 2004 Jemal, A. ; Tiwari, R. C. ; Murray, T. ; Ghafoor, A. ; Samuels, A. ; Ward, E. ; Feuer, E. J. ; Thun, M. J.: Cancer statistics, 2004. In: *CA Cancer J Clin* 54 (2004), pp. 8–29

Jemal et al. 2005 Jemal, A. ; Murray, T. ; Ward, E. ; Samuels, A. ; Tiwari, R. C. ; Ghafoor, A. ; Feuer, E. J. ; Thun, M. J.: Cancer statistics, 2005. In: *CA Cancer J Clin* 55 (2005), pp. 10–30

Jemal et al. 2008 Jemal, A. ; Siegel, R. ; Ward, E. ; Hao, Y. ; Xu, J. ; Murray, T. ; Thun, M. J.: Cancer statistics, 2008. In: *CA Cancer J Clin* 58 (2008), pp. 71–96

Jensen et al. 2001 Jensen, K. ; Shiels, C. ; Freemont, P. S.: PML protein isoforms and the RBCC/TRIM motif. In: *Oncogene* 20 (2001), Oct, pp. 7223–7233

Jhanwar et al. 1994 Jhanwar, S. C. ; Chen, Q. ; Li, F. P. ; Brennan, M. F. ; Woodruff, J. M.: Cytogenetic analysis of soft tissue sarcomas. Recurrent chromosome abnormalities in malignant peripheral nerve sheath tumors (MPNST). In: *Cancer Genet. Cytogenet.* 78 (1994), Dec, pp. 138–144

Jiang et al. 2005 Jiang, W. Q. ; Zhong, Z. H. ; Henson, J. D. ; Neumann, A. A. ; Chang, A. C. ; Reddel, R. R.: Suppression of alternative lengthening of telomeres by Sp100-mediated sequestration of the MRE11/RAD50/NBS1 complex. In: *Mol. Cell. Biol.* 25 (2005), Apr, pp. 2708–2721

Jiang et al. 2007 Jiang, W. Q. ; Zhong, Z. H. ; Henson, J. D. ; Reddel, R. R.: Identification of candidate alternative lengthening of telomeres genes by methionine restriction and RNA interference. In: *Oncogene* 26 (2007), Jul, pp. 4635–4647

Jiang et al. 2009 Jiang, W. Q. ; Zhong, Z. H. ; Nguyen, A. ; Henson, J. D. ; Toouli, C. D. ; Braithwaite, A. W. ; Reddel, R. R.: Induction of alternative lengthening of telomeres-associated PML bodies by p53/p21 requires HP1 proteins. In: *J. Cell Biol.* 185 (2009), Jun, pp. 797–810

Johnson and Broccoli 2007 Johnson, J. E. ; Broccoli, D.: Telomere maintenance in sarcomas. In: *Curr Opin Oncol* 19 (2007), Jul, pp. 377–382

Johnson et al. 2001 Johnson, F. B. ; Marciniak, R. A. ; McVey, M. ; Stewart, S. A. ; Hahn, W. C. ; Guarente, L.: The Saccharomyces cerevisiae WRN homolog Sgs1p participates in telomere maintenance in cells lacking telomerase. In: *EMBO J.* 20 (2001), Feb, pp. 905–913

Johnson et al. 2005 Johnson, J. E. ; Varkonyi, R. J. ; Schwalm, J. ; Cragle, R. ; Klein-Szanto, A. ; Patchefsky, A. ; Cukierman, E. ; Mehren, M. von ; Broccoli, D.: Multiple mechanisms of telomere maintenance exist in liposarcomas. In: *Clin. Cancer Res.* 11 (2005), Aug, pp. 5347–5355

Johnson et al. 2007 Johnson, J. E. ; Gettings, E. J. ; Schwalm, J. ; Pei, J. ; Testa, J. R. ; Litwin, S. ; Mehren, M. von ; Broccoli, D.: Whole-genome profiling in liposarcomas reveals genetic alterations common to specific telomere maintenance mechanisms. In: *Cancer Res.* 67 (2007), Oct, pp. 9221–9228

Jonckheere 1954 Jonckheere, A. R.: A distribution-free k-sample test against ordered alterntives. In: *Biometrica* 41 (1954), pp. 133–145

Joos et al. 1995 Joos, S. ; Bergerheim, U. S. ; Pan, Y. ; Matsuyama, H. ; Bentz, M. ; Manoir, S. du ; Lichter, P.: Mapping of chromosomal gains and losses in prostate cancer by comparative genomic hybridization. In: *Genes Chromosomes Cancer* 14 (1995), Dec, pp. 267–276

Joos et al. 1996 Joos, S. ; Otaño-Joos, M. I. ; Ziegler, S. ; Brüderlein, S. ; Manoir, S. du ; Bentz, M. ; Möller, P. ; Lichter, P.: Primary mediastinal (thymic) B-cell lymphoma is characterized by gains of chromosomal material including 9p and amplification of the REL gene. In: *Blood* 87 (1996), Feb, pp. 1571–1578

Kevorkian and Cento 1973 Kevorkian, J. ; Cento, D. P.: Leiomyosarcoma of large arteries and veins. In: *Surgery* 73 (1973), Mar, pp. 390–400

Klein et al. 2007 Klein, G. ; Imreh, S. ; Zabarovsky, E. R.: Why do we not all die of cancer at an early age? In: *Adv. Cancer Res.* 98 (2007), pp. 1–16

Klimstra et al. 1995 Klimstra, D. S. ; Moran, C. A. ; Perino, G. ; Koss, M. N. ; Rosai, J.: Liposarcoma of the anterior mediastinum and thymus. A clinicopathologic study of 28 cases. In: *Am. J. Surg. Pathol.* 19 (1995), Jul, pp. 782–791

Klobutcher et al. 1981 Klobutcher, L. A. ; Swanton, M. T. ; Donini, P. ; Prescott, D. M.: All gene-sized DNA molecules in four species of hypotrichs have the same terminal sequence and an unusual 3' terminus. In: *Proc. Natl. Acad. Sci. U.S.A.* 78 (1981), May, pp. 3015–3019

Kobayashi et al. 2006 Kobayashi, C. ; Oda, Y. ; Takahira, T. ; Izumi, T. ; Kawaguchi, K. ; Yamamoto, H. ; Tamiya, S. ; Yamada, T. ; Oda, S. ; Tanaka, K. ; Matsuda, S. ; Iwamoto, Y. ; Tsuneyoshi, M.: Chromosomal aberrations and microsatellite instability of malignant peripheral nerve sheath tumors: a study of 10 tumors from nine patients. In: *Cancer Genet. Cytogenet.* 165 (2006), Mar, pp. 98–105

Kourea et al. 1998 Kourea, H. P. ; Bilsky, M. H. ; Leung, D. H. ; Lewis, J. J. ; Woodruff, J. M.: Subdiaphragmatic and intrathoracic paraspinal malignant peripheral nerve sheath tumors: a clinicopathologic study of 25 patients and 26 tumors. In: *Cancer* 82 (1998), Jun, pp. 2191–2203

Kransdorf 1995 Kransdorf, M. J.: Malignant soft-tissue tumors in a large referral population: distribution of diagnoses by age, sex, and location. In: *AJR Am J Roentgenol* 164 (1995), Jan, pp. 129–134

Kumar et al. 2007 Kumar, P. P. ; Bischof, O. ; Purbey, P. K. ; Notani, D. ; Urlaub, H. ; Dejean, A. ; Galande, S.: Functional interaction between PML and SATB1 regulates chromatin-loop architecture and transcription of the MHC class I locus. In: *Nat. Cell Biol.* 9 (2007), Jan, pp. 45–56

Lachmanovich et al. 2003 Lachmanovich, E. ; Shvartsman, D. E. ; Malka, Y. ; Botvin, C. ; Henis, Y. I. ; Weiss, A. M.: Co-localization analysis of complex formation among membrane proteins by computerized fluorescence microscopy: application to immunofluorescence co-patching studies. In: *J Microsc* 212 (2003), Nov, pp. 122–131

Lahat et al. 2009 Lahat, G. ; Tuvin, D. ; Wei, C. ; Wang, W. L. ; Pollock, R. E. ; Anaya, D. A. ; Bekele, B. N. ; Corely, L. ; Lazar, A. J. ; Pisters, P. W. ; Lev, D.: Molecular prognosticators of complex karyotype soft tissue sarcoma outcome: a tissue microarray-based study. In: *Ann. Oncol.* (2009), Oct

Larramendy et al. 1997 Larramendy, M. L. ; Tarkkanen, M. ; Blomqvist, C. ; Virolainen, M. ; Wiklund, T. ; Asko-Seljavaara, S. ; Elomaa, I. ; Knuutila, S.: Comparative genomic hybridization of malignant fibrous histiocytoma reveals a novel prognostic marker. In: *Am. J. Pathol.* 151 (1997), Oct, pp. 1153–1161

Latres et al. 1994 Latres, E. ; Drobnjak, M. ; Pollack, D. ; Oliva, M. R. ; Ramos, M. ; Karpeh, M. ; Woodruff, J. M. ; Cordon-Cardo, C.: Chromosome 17 abnormalities and TP53 mutations in adult soft tissue sarcomas. In: *Am. J. Pathol.* 145 (1994), Aug, pp. 345–355

Legius et al. 1993 Legius, E. ; Marchuk, D. A. ; Collins, F. S. ; Glover, T. W.: Somatic deletion of the neurofibromatosis type 1 gene in a neurofibrosarcoma supports a tumour suppressor gene hypothesis. In: *Nat. Genet.* 3 (1993), Feb, pp. 122–126

Legius et al. 1994 Legius, E. ; Dierick, H. ; Wu, R. ; Hall, B. K. ; Marynen, P. ; Cassiman, J. J. ; Glover, T. W.: TP53 mutations are frequent in malignant NF1 tumors. In: *Genes Chromosomes Cancer* 10 (1994), Aug, pp. 250–255

Levine 1999 Levine, E. A.: Prognostic factors in soft tissue sarcoma. In: *Semin Surg Oncol* 17 (1999), pp. 23–32

Lewis and Brennan 1996 Lewis, J. J. ; Brennan, M. F.: Soft tissue sarcomas. In: *Curr Probl Surg* 33 (1996), Oct, pp. 817–872

Lewis et al. 2000 Lewis, J. J. ; Antonescu, C. R. ; Leung, D. H. ; Blumberg, D. ; Healey, J. H. ; Woodruff, J. M. ; Brennan, M. F.: Synovial sarcoma: a multivariate analysis of prognostic factors in 112 patients with primary localized tumors of the extremity. In: *J. Clin. Oncol.* 18 (2000), May, pp. 2087–2094

Mairal et al. 1999 Mairal, A. ; Terrier, P. ; Chibon, F. ; Sastre, X. ; Lecesne, A. ; Aurias, A.: Loss of chromosome 13 is the most frequent genomic imbalance in malignant fibrous histiocytomas. A comparative genomic hybridization analysis of a series of 30 cases. In: *Cancer Genet. Cytogenet.* 111 (1999), Jun, pp. 134–138

Mandahl et al. 1985 Mandahl, N. ; Heim, S. ; Kristoffersson, U. ; Mitelman, F. ; Rööser, B. ; Rydholm, A. ; Willén, H.: Telomeric association in a malignant fibrous histiocytoma. In: *Hum. Genet.* 71 (1985), pp. 321–324

Mandahl et al. 2000 Mandahl, N. ; Fletcher, C. D. ; Dal Cin, P. ; De Wever, I. ; Mertens, F. ; Mitelman, F. ; Rosai, J. ; Rydholm, A. ; Sciot, R. ; Tallini, G. ; Van Den Berghe, H. ; Vanni, R. ; Willén, H.: Comparative cytogenetic study of spindle cell and pleomorphic leiomyosarcomas of soft tissues: a report from the CHAMP Study Group. In: *Cancer Genet. Cytogenet.* 116 (2000), Jan, pp. 66–73

Manders et al. 1993 Manders, E. ; Verbeek, F. ; J., Aten: Measurement of co-localization of objects in dual color conocal images. In: *J Microsc* 169 (1993), pp. 375–382

Matsuo et al. 2008 Matsuo, T. ; Sugita, T. ; Shimose, S. ; Kubo, T. ; Ishikawa, M. ; Yasunaga, Y. ; Ochi, M.: Immunohistochemical expression of promyelocytic leukemia body in soft tissue sarcomas. In: *J. Exp. Clin. Cancer Res.* 27 (2008), pp. 73

McClintock 1941 McClintock, B.: The Stability of Broken Ends of Chromosomes in Zea Mays. In: *Genetics* 26 (1941), Mar, pp. 234–282

McCormick et al. 1994 McCormick, D. ; Mentzel, T. ; Beham, A. ; Fletcher, C. D.: Dedifferentiated liposarcoma. Clinicopathologic analysis of 32 cases suggesting a better prognostic subgroup among pleomorphic sarcomas. In: *Am. J. Surg. Pathol.* 18 (1994), Dec, pp. 1213–1223

McEachern et al. 2000 McEachern, M. J. ; Krauskopf, A. ; Blackburn, E. H.: Telomeres and their control. In: *Annu. Rev. Genet.* 34 (2000), pp. 331–358

Meis-Kindblom et al. 2001 Meis-Kindblom, J. M. ; Sjögren, H. ; Kindblom, L. G. ; Peydró-Mellquist, A. ; Röijer, E. ; Aman, P. ; Stenman, G.: Cytogenetic and molecular genetic analyses of liposarcoma and its soft tissue simulators: recognition of new variants and differential diagnosis. In: *Virchows Arch.* 439 (2001), Aug, pp. 141–151

Meloni-Ehrig et al. 1999 Meloni-Ehrig, A. M. ; Chen, Z. ; Guan, X. Y. ; Notohamiprodjo, M. ; Shepard, R. R. ; Spanier, S. S. ; Trent, J. M. ; Sandberg, A. A.: Identification of a ring chromosome in a myxoid malignant fibrous histiocytoma with chromosome microdissection and fluorescence in situ hybridization. In: *Cancer Genet. Cytogenet.* 109 (1999), Feb, pp. 81–85

Mentzel et al. 1996 Mentzel, T. ; Calonje, E. ; Wadden, C. ; Camplejohn, R. S. ; Beham, A. ; Smith, M. A. ; Fletcher, C. D.: Myxofibrosarcoma. Clinicopathologic analysis of 75 cases with emphasis on the low-grade variant. In: *Am. J. Surg. Pathol.* 20 (1996), Apr, pp. 391–405

Mentzel et al. 2001 Mentzel, T. ; Brown, L. F. ; Dvorak, H. F. ; Kuhnen, C. ; Stiller, K. J. ; Katenkamp, D. ; Fletcher, C. D.: The association between tumour progression and vascularity in myxofibrosarcoma and myxoid/round cell liposarcoma. In: *Virchows Arch.* 438 (2001), Jan, pp. 13–22

Merck et al. 1983 Merck, C. ; Angervall, L. ; Kindblom, L. G. ; Odén, A.: Myxofibrosarcoma. A malignant soft tissue tumor of fibroblastic-histiocytic origin. A clinicopathologic and prognostic study of 110 cases using multivariate analysis. In: *Acta Pathol Microbiol Immunol Scand Suppl* 282 (1983), pp. 1–40

Mertens et al. 1998 Mertens, F. ; Fletcher, C. D. ; Dal Cin, P. ; De Wever, I. ; Mandahl, N. ; Mitelman, F. ; Rosai, J. ; Rydholm, A. ; Sciot, R. ; Tallini, G. ; Berghe, H. Van den ; Vanni, R. ; Willén, H.: Cytogenetic analysis of 46 pleomorphic soft tissue sarcomas and correlation with morphologic and clinical features: a report of the CHAMP Study Group. Chromosomes and MorPhology. In: *Genes Chromosomes Cancer* 22 (1998), May, pp. 16–25

Miettinen and Enzinger 1999 Miettinen, M. ; Enzinger, F. M.: Epithelioid variant of pleomorphic liposarcoma: a study of 12 cases of a distinctive variant of high-grade liposarcoma. In: *Mod. Pathol.* 12 (1999), Jul, pp. 722–728

Mitelman and Mertens 2009 Mitelman, Johansson B. ; Mertens, F.: *Mitelman Database of Chromosome Aberrations in Cancer*. Website. 2009. – Available online at `http://cgap.nci.nih.gov/Chromosomes/Mitelman`; visited on May 8th 2009.

Molenaar et al. 1989 Molenaar, W. M. ; DeJong, B. ; Buist, J. ; Idenburg, V. J. ; Seruca, R. ; Vos, A. M. ; Hoekstra, H. J.: Chromosomal analysis and the classification of soft tissue sarcomas. In: *Lab. Invest.* 60 (1989), Feb, pp. 266–274

Montgomery et al. 2004 Montgomery, E. ; Argani, P. ; Hicks, J. L. ; DeMarzo, A. M. ; Meeker, A. K.: Telomere lengths of translocation-associated and nontranslocation-associated sarcomas differ dramatically. In: *Am. J. Pathol.* 164 (2004), May, pp. 1523–1529

Moon and Jarstfer 2007 Moon, I. K. ; Jarstfer, M. B.: The human telomere and its relationship to human disease, therapy, and tissue engineering. In: *Front. Biosci.* 12 (2007), pp. 4595–4620

Muller et al. 1987 Muller, R. ; Hajdu, S. I. ; Brennan, M. F.: Lymphangiosarcoma associated with chronic filarial lymphedema. In: *Cancer* 59 (1987), Jan, pp. 179–183

Muratani et al. 2002 Muratani, M. ; Gerlich, D. ; Janicki, S. M. ; Gebhard, M. ; Eils, R. ; Spector, D. L.: Metabolic-energy-dependent movement of PML bodies within the mammalian cell nucleus. In: *Nat. Cell Biol.* 4 (2002), Feb, pp. 106–110

Murnane et al. 1994 Murnane, J. P. ; Sabatier, L. ; Marder, B. A. ; Morgan, W. F.: Telomere dynamics in an immortal human cell line. In: *EMBO J.* 13 (1994), Oct, pp. 4953–4962

Müller 1938 Müller, H.J.: The remaking of the chromosomes. In: *The Collecting Net* 13 (1938), pp. 181–195

Nielsen et al. 1999 Nielsen, G. P. ; Stemmer-Rachamimov, A. O. ; Ino, Y. ; Moller, M. B. ; Rosenberg, A. E. ; Louis, D. N.: Malignant transformation of neurofibromas in neurofibromatosis 1 is associated with CDKN2A/p16 inactivation. In: *Am. J. Pathol.* 155 (1999), Dec, pp. 1879–1884

Nilbert et al. 1994 Nilbert, M. ; Rydholm, A. ; Willén, H. ; Mitelman, F. ; Mandahl, N.: MDM2 gene amplification correlates with ring chromosome in soft tissue tumors. In: *Genes Chromosomes Cancer* 9 (1994), Apr, pp. 261–265

Nilsson et al. 1999 Nilsson, G. ; Skytting, B. ; Xie, Y. ; Brodin, B. ; Perfekt, R. ; Mandahl, N. ; Lundeberg, J. ; Uhlén, M. ; Larsson, O.: The SYT-SSX1 variant of synovial sarcoma is associated with a high rate of tumor cell proliferation and poor clinical outcome. In: *Cancer Res.* 59 (1999), Jul, pp. 3180–3184

Nittis et al. 2008 Nittis, T. ; Guittat, L. ; Stewart, S. A.: Alternative lengthening of telomeres (ALT) and chromatin: is there a connection? In: *Biochimie* 90 (2008), Jan, pp. 5–12

Ogino et al. 1998 Ogino, H. ; Nakabayashi, K. ; Suzuki, M. ; Takahashi, E. ; Fujii, M. ; Suzuki, T. ; Ayusawa, D.: Release of telomeric DNA from chromosomes in immortal human cells lacking telomerase activity. In: *Biochem. Biophys. Res. Commun.* 248 (1998), Jul, pp. 223–227

Olovnikov 1971 Olovnikov, A. M.: [Principle of marginotomy in template synthesis of polynucleotides]. In: *Dokl. Akad. Nauk SSSR* 201 (1971), pp. 1496–1499

Olovnikov 1973 Olovnikov, A. M.: A theory of marginotomy. The incomplete copying of template margin in enzymic synthesis of polynucleotides and biological significance of the phenomenon. In: *J. Theor. Biol.* 41 (1973), Sep, pp. 181–190

Orndal et al. 1994 Orndal, C. ; Rydholm, A. ; Willén, H. ; Mitelman, F. ; Mandahl, N.: Cytogenetic intratumor heterogeneity in soft tissue tumors. In: *Cancer Genet. Cytogenet.* 78 (1994), Dec, pp. 127–137

Parente et al. 1999 Parente, F. ; Grosgeorge, J. ; Coindre, J. M. ; Terrier, P. ; Vilain, O. ; Turc-Carel, C.: Comparative genomic hybridization reveals novel chromosome deletions in 90 primary soft tissue tumors. In: *Cancer Genet. Cytogenet.* 115 (1999), Dec, pp. 89–95

Parkinson et al. 2002 Parkinson, G. N. ; Lee, M. P. ; Neidle, S.: Crystal structure of parallel quadruplexes from human telomeric DNA. In: *Nature* 417 (2002), Jun, pp. 876–880

Patel et al. 1997 Patel, S. R. ; Vadhan-Raj, S. ; Papadopolous, N. ; Plager, C. ; Burgess, M. A. ; Hays, C. ; Benjamin, R. S.: High-dose ifosfamide in bone and soft tissue sarcomas: results of phase II and pilot studies–dose-response and schedule dependence. In: *J. Clin. Oncol.* 15 (1997), Jun, pp. 2378–2384

Perrem et al. 1999 Perrem, K. ; Bryan, T. M. ; Englezou, A. ; Hackl, T. ; Moy, E. L. ; Reddel, R. R.: Repression of an alternative mechanism for lengthening of telomeres in somatic cell hybrids. In: *Oncogene* 18 (1999), Jun, pp. 3383–3390

Perrone et al. 2003 Perrone, F. ; Tabano, S. ; Colombo, F. ; Dagrada, G. ; Birindelli, S. ; Gronchi, A. ; Colecchia, M. ; Pierotti, M. A. ; Pilotti, S.: p15INK4b, p14ARF, and p16INK4a inactivation in sporadic and neurofibromatosis type 1-related malignant peripheral nerve sheath tumors. In: *Clin. Cancer Res.* 9 (2003), Sep, pp. 4132–4138

Pilotti et al. 1997 Pilotti, S. ; Della Torre, G. ; Lavarino, C. ; Di Palma, S. ; Sozzi, G. ; Minoletti, F. ; Rao, S. ; Pasquini, G. ; Azzarelli, A. ; Rilke, F. ; Pierotti, M. A.: Distinct mdm2/p53 expression patterns in liposarcoma subgroups: implications for different pathogenetic mechanisms. In: *J. Pathol.* 181 (1997), Jan, pp. 14–24

Raymond et al. 2000 Raymond, E. ; Soria, J. C. ; Izbicka, E. ; Boussin, F. ; Hurley, L. ; Von Hoff, D. D.: DNA G-quadruplexes, telomere-specific proteins and telomere-associated enzymes as potential targets for new anticancer drugs. In: *Invest New Drugs* 18 (2000), May, pp. 123–137

Reid et al. 1996 Reid, A. H. ; Tsai, M. M. ; Venzon, D. J. ; Wright, C. F. ; Lack, E. E. ; O'Leary, T. J.: MDM2 amplification, P53 mutation, and accumulation of the P53 gene product in malignant fibrous histiocytoma. In: *Diagn. Mol. Pathol.* 5 (1996), Mar, pp. 65–73

Ricci et al. 1984 Ricci, A. ; Parham, D. M. ; Woodruff, J. M. ; Callihan, T. ; Green, A. ; Erlandson, R. A.: Malignant peripheral nerve sheath tumors arising from ganglioneuromas. In: *Am. J. Surg. Pathol.* 8 (1984), Jan, pp. 19–29

R Development Core Team 2008 R Development Core Team, R.: A language and enviroment for statistical computing. (2008)

Sakabe et al. 1999 Sakabe, T. ; Shinomiya, T. ; Mori, T. ; Ariyama, Y. ; Fukuda, Y. ; Fujiwara, T. ; Nakamura, Y. ; Inazawa, J.: Identification of a novel gene, MASL1, within an amplicon at 8p23.1 detected in malignant fibrous histiocytomas by comparative genomic hybridization. In: *Cancer Res.* 59 (1999), Feb, pp. 511–515

Sakaguchi et al. 1996 Sakaguchi, N. ; Sano, K. ; Ito, M. ; Baba, T. ; Fukuzawa, M. ; Hotchi, M.: A case of von Recklinghausen's disease with bilateral pheochromocytoma-malignant peripheral nerve sheath tumors of the adrenal and gastrointestinal autonomic nerve tumors. In: *Am. J. Surg. Pathol.* 20 (1996), Jul, pp. 889–897

Sandberg and Bridge 2002 Sandberg, A. A. ; Bridge, J. A.: Updates on the cytogenetics and molecular genetics of bone and soft tissue tumors. Synovial sarcoma. In: *Cancer Genet. Cytogenet.* 133 (2002), Feb, pp. 1–23

Scheel et al. 2001 Scheel, C. ; Schaefer, K. L. ; Jauch, A. ; Keller, M. ; Wai, D. ; Brinkschmidt, C. ; Valen, F. van ; Boecker, W. ; Dockhorn-Dworniczak, B. ; Poremba, C.: Alternative lengthening of telomeres is associated with chromosomal instability in osteosarcomas. In: *Oncogene* 20 (2001), Jun, pp. 3835–3844

Scheithauer and Woodruff J.M. 1999 Scheithauer, B.W. ; Woodruff J.M., Erlandson R.: *Tumors of the Peripheral Nervous System.* Washington, DC : Armed Forces Institute of Pathology, 1999

Schneider-Stock et al. 1998 Schneider-Stock, R. ; Walter, H. ; Radig, K. ; Rys, J. ; Bosse, A. ; Kuhnen, C. ; Hoang-Vu, C. ; Roessner, A.: MDM2 amplification and loss of heterozygosity at Rb and p53 genes: no simultaneous alterations in the oncogenesis of liposarcomas. In: *J. Cancer Res. Clin. Oncol.* 124 (1998), pp. 532–540

Seeler and Dejean 2003 Seeler, J. S. ; Dejean, A.: Nuclear and unclear functions of SUMO. In: *Nat. Rev. Mol. Cell Biol.* 4 (2003), Sep, pp. 690–699

Shampay et al. 1984 Shampay, J. ; Szostak, J. W. ; Blackburn, E. H.: DNA sequences of telomeres maintained in yeast. In: *Nature* 310 (1984), pp. 154–157

Sharma et al. 1998 Sharma, S. ; Abbott, R. I. ; Zagzag, D.: Malignant intracerebral nerve sheath tumor: a case report and review of the literature. In: *Cancer* 82 (1998), Feb, pp. 545–552

Shay and Roninson 2004 Shay, J. W. ; Roninson, I. B.: Hallmarks of senescence in carcinogenesis and cancer therapy. In: *Oncogene* 23 (2004), Apr, pp. 2919–2933

Shin et al. 2006 Shin, J. S. ; Hong, A. ; Solomon, M. J. ; Lee, C. S.: The role of telomeres and telomerase in the pathology of human cancer and aging. In: *Pathology* 38 (2006), Apr, pp. 103–113

Simons et al. 2000 Simons, A. ; Schepens, M. ; Jeuken, J. ; Sprenger, S. ; Zande, G. van de ; Bjerkehagen, B. ; Forus, A. ; Weibolt, V. ; Molenaar, I. ; Berg, E. van den ; Myklebost, O. ; Bridge, J. ; Kessel, A. G. van ; Suijkerbuijk, R.: Frequent loss of 9p21 (p16(INK4A)) and other genomic imbalances in human malignant fibrous histiocytoma. In: *Cancer Genet. Cytogenet.* 118 (2000), Apr, pp. 89–98

Smith and Feigon 1992 Smith, F. W. ; Feigon, J.: Quadruplex structure of Oxytricha telomeric DNA oligonucleotides. In: *Nature* 356 (1992), Mar, pp. 164–168

Smith et al. 1984 Smith, A. H. ; Pearce, N. E. ; Fisher, D. O. ; Giles, H. J. ; Teague, C. A. ; Howard, J. K.: Soft tissue sarcoma and exposure to phenoxyherbicides and chlorophenols in New Zealand. In: *J. Natl. Cancer Inst.* 73 (1984), Nov, pp. 1111–1117

Smith et al. 1996 Smith, T. A. ; Easley, K. A. ; Goldblum, J. R.: Myxoid/round cell liposarcoma of the extremities. A clinicopathologic study of 29 cases with particular attention to extent of round cell liposarcoma. In: *Am. J. Surg. Pathol.* 20 (1996), Feb, pp. 171–180

Spillane et al. 2000 Spillane, A. J. ; A'Hern, R. ; Judson, I. R. ; Fisher, C. ; Thomas, J. M.: Synovial sarcoma: a clinicopathologic, staging, and prognostic assessment. In: *J. Clin. Oncol.* 18 (2000), Nov, pp. 3794–3803

Sreekantaiah et al. 1992 Sreekantaiah, C. ; Karakousis, C. P. ; Leong, S. P. ; Sandberg, A. A.: Cytogenetic findings in liposarcoma correlate with histopathologic subtypes. In: *Cancer* 69 (1992), May, pp. 2484–2495

Stratton et al. 1990 Stratton, M. R. ; Moss, S. ; Warren, W. ; Patterson, H. ; Clark, J. ; Fisher, C. ; Fletcher, C. D. ; Ball, A. ; Thomas, M. ; Gusterson, B. A.: Mutation of the p53 gene in human soft tissue sarcomas: association with abnormalities of the RB1 gene. In: *Oncogene* 5 (1990), Sep, pp. 1297–1301

Swanson et al. 1991 Swanson, P. E. ; Wick, M. R. ; Dehner, L. P.: Leiomyosarcoma of somatic soft tissues in childhood: an immunohistochemical analysis of six cases with ultrastructural correlation. In: *Hum. Pathol.* 22 (1991), Jun, pp. 569–577

Szymanska et al. 1996 Szymanska, J. ; Tarkkanen, M. ; Wiklund, T. ; Virolainen, M. ; Blomqvist, C. ; Asko-Seljavaara, S. ; Tukiainen, E. ; Elomaa, I. ; Knuutila, S.: Gains and losses of DNA sequences in liposarcomas evaluated by comparative genomic hybridization. In: *Genes Chromosomes Cancer* 15 (1996), Feb, pp. 89–94

Taylor et al. 1996 Taylor, R. S. ; Ramirez, R. D. ; Ogoshi, M. ; Chaffins, M. ; Piatyszek, M. A. ; Shay, J. W.: Detection of telomerase activity in malignant and nonmalignant skin conditions. In: *J. Invest. Dermatol.* 106 (1996), Apr, pp. 759–765

Telo Website. – Available online at `http://www.mun.ca/biochem/courses/3107/images/telomerase_model.gif`; visited on March 8th 2009.

Thomann et al. 2002 Thomann, D. ; Rines, D. R. ; Sorger, P. K. ; Danuser, G.: Automatic fluorescent tag detection in 3D with super-resolution: application to the analysis of chromosome movement. In: *J Microsc* 208 (2002), Oct, pp. 49–64

Tokutake et al. 1998 Tokutake, Y. ; Matsumoto, T. ; Watanabe, T. ; Maeda, S. ; Tahara, H. ; Sakamoto, S. ; Niida, H. ; Sugimoto, M. ; Ide, T. ; Furuichi, Y.: Extra-chromosomal telomere repeat DNA in telomerase-negative immortalized cell lines. In: *Biochem. Biophys. Res. Commun.* 247 (1998), Jun, pp. 765–772

Tran et al. 2008 Tran, P. T. ; Hara, W. ; Su, Z. ; Lin, H. J. ; Bendapudi, P. K. ; Norton, J. ; Teng, N. ; King, C. R. ; Kapp, D. S.: Intraoperative radiation therapy for locally advanced and recurrent soft-tissue sarcomas in adults. In: *Int. J. Radiat. Oncol. Biol. Phys.* 72 (2008), Nov, pp. 1146–1153

Turc-Carel et al. 1986 Turc-Carel, C. ; Limon, J. ; Dal Cin, P. ; Rao, U. ; Karakousis, C. ; Sandberg, A. A.: Cytogenetic studies of adipose tissue tumors. II. Recurrent reciprocal translocation t(12;16)(q13;p11) in myxoid liposarcomas. In: *Cancer Genet. Cytogenet.* 23 (1986), Dec, pp. 291–299

Ulaner et al. 2003 Ulaner, G. A. ; Huang, H. Y. ; Otero, J. ; Zhao, Z. ; Ben-Porat, L. ; Satagopan, J. M. ; Gorlick, R. ; Meyers, P. ; Healey, J. H. ; Huvos, A. G. ; Hoffman, A. R. ; Ladanyi, M.: Absence of a telomere maintenance mechanism as a favorable prognostic factor in patients with osteosarcoma. In: *Cancer Res.* 63 (2003), Apr, pp. 1759–1763

Ulaner et al. 2004 Ulaner, G. A. ; Hoffman, A. R. ; Otero, J. ; Huang, H. Y. ; Zhao, Z. ; Mazumdar, M. ; Gorlick, R. ; Meyers, P. ; Healey, J. H. ; Ladanyi, M.: Divergent patterns of telomere maintenance mechanisms among human sarcomas: sharply contrasting prevalence of the alternative lengthening of telomeres mechanism in Ewing's sarcomas and osteosarcomas. In: *Genes Chromosomes Cancer* 41 (2004), Oct, pp. 155–162

Vorburger and Hunt 2002 Vorburger, S.A. ; Hunt, K.K.: *Soft tissue sarcomas.* Lyon : BC Decker, Inc, 2002. – Experimental Approaches, in Pollock RE

Wang and Harris 1996 Wang, X. W. ; Harris, C. C.: TP53 tumour suppressor gene: clues to molecular carcinogenesis and cancer therapy. In: *Cancer Surv.* 28 (1996), pp. 169–196

Wang et al. 2001 Wang, R. ; Lu, Y. J. ; Fisher, C. ; Bridge, J. A. ; Shipley, J.: Characterization of chromosome aberrations associated with soft-tissue leiomyosarcomas by twenty-four-color karyotyping and comparative genomic hybridization analysis. In: *Genes Chromosomes Cancer* 31 (2001), May, pp. 54–64

Waters et al. 2000 Waters, B. L. ; Panagopoulos, I. ; Allen, E. F.: Genetic characterization of angiomatoid fibrous histiocytoma identifies fusion of the FUS and ATF-1 genes induced by a chromosomal translocation involving bands 12q13 and 16p11. In: *Cancer Genet. Cytogenet.* 121 (2000), Sep, pp. 109–116

Watson 1972 Watson, J. D.: Origin of concatemeric T7 DNA. In: *Nature New Biol.* 239 (1972), Oct, pp. 197–201

Wei and Sedivy 1999 Wei, W. ; Sedivy, J. M.: Differentiation between senescence (M1) and crisis (M2) in human fibroblast cultures. In: *Exp. Cell Res.* 253 (1999), Dec, pp. 519–522

Weinberg 2007 Weinberg, A. R.: *the biology of CANCER.* New York : by Graland Science, Tayler and Francis Group, LLC, 2007

Weiss 2001 Weiss, Goldblum J.: *Enzinger and Weiss's Soft Tissue Tumors.* St. Louis : Mosby, St. Louis, 2001

Weiss and Enzinger 1977 Weiss, S. W. ; Enzinger, F. M.: Myxoid variant of malignant fibrous histiocytoma. In: *Cancer* 39 (1977), Apr, pp. 1672–1685

Weiss and Rao 1992 Weiss, S. W. ; Rao, V. K.: Well-differentiated liposarcoma (atypical lipoma) of deep soft tissue of the extremities, retroperitoneum, and miscellaneous sites. A follow-up study of 92 cases with analysis of the incidence of "dedifferentiation". In: *Am. J. Surg. Pathol.* 16 (1992), Nov, pp. 1051–1058

Woodruff et al. 1994 Woodruff, J. M. ; Selig, A. M. ; Crowley, K. ; Allen, P. W.: Schwannoma (neurilemoma) with malignant transformation. A rare, distinctive peripheral nerve tumor. In: *Am. J. Surg. Pathol.* 18 (1994), Sep, pp. 882–895

Wörz et al. Wörz, S. ; Kappel, C. ; Eils, R. ; Rohr, K.: Mmodel-based segmentation and quantification of fluorescent bacteria in 3D microscopy live cell images. In: *[Proc. SPIE Medical Imaging 2007: Image Processing], Pluim, J. and Reinhardt, J., eds.,Proc. SPIE, SPEI Bellingham, WA/USA, San Diego, CA/USA Year=*

Yanez et al. 2005 Yanez, G. H. ; Khan, S. J. ; Locovei, A. M. ; Pedroso, I. M. ; Fletcher, T. M.: DNA structure-dependent recruitment of telomeric proteins to single-stranded/double-stranded DNA junctions. In: *Biochem. Biophys. Res. Commun.* 328 (2005), Mar, pp. 49–56

Yeager et al. 1999 Yeager, T. R. ; Neumann, A. A. ; Englezou, A. ; Huschtscha, L. I. ; Noble, J. R. ; Reddel, R. R.: Telomerase-negative immortalized human cells contain a novel type of promyelocytic leukemia (PML) body. In: *Cancer Res.* 59 (1999), Sep, pp. 4175–4179

Zahm and Fraumeni 1997 Zahm, S. H. ; Fraumeni, J. F.: The epidemiology of soft tissue sarcoma. In: *Semin. Oncol.* 24 (1997), Oct, pp. 504–514

Zhang et al. 2008 Zhang, B. ; Chenourard, N. ; Olivo-Marin, J.-C. ; Meas-Yedid, V.: Satistical Colocalization In Biological Imaging With False Discovery Control. In: *[Proc. ISBI'08], Olivo-Marin., ed.,* (2008), May, pp. 1327–1330

Zhong et al. 2000a Zhong, S. ; Müller, S. ; Ronchetti, S. ; Freemont, P. S. ; Dejean, A. ; Pandolfi, P. P.: Role of SUMO-1-modified PML in nuclear body formation. In: *Blood* 95 (2000), May, pp. 2748–2752

Zhong et al. 2000b Zhong, S. ; Salomoni, P. ; Pandolfi, P. P.: The transcriptional role of PML and the nuclear body. In: *Nat. Cell Biol.* 2 (2000), May, pp. 85–90

Zink et al. 2004 Zink, D. ; Fischer, A. H. ; Nickerson, J. A.: Nuclear structure in cancer cells. In: *Nat. Rev. Cancer* 4 (2004), Sep, pp. 677–687

de Lange 2002 Lange, T. de: Protection of mammalian telomeres. In: *Oncogene* 21 (2002), Jan, pp. 532–540

de Lange 2004 Lange, T. de: T-loops and the origin of telomeres. In: *Nat. Rev. Mol. Cell Biol.* 5 (2004), Apr, pp. 323–329

de Lange 2005 Lange, T. de: Shelterin: the protein complex that shapes and safeguards human telomeres. In: *Genes Dev.* 19 (2005), Sep, pp. 2100–2110

de Leeuw et al. 1995 Leeuw, B. de ; Balemans, M. ; Olde Weghuis, D. ; Kessel, A. Geurts van: Identification of two alternative fusion genes, SYT-SSX1 and SYT-SSX2, in t(X;18)(p11.2;q11.2)-positive synovial sarcomas. In: *Hum. Mol. Genet.* 4 (1995), Jun, pp. 1097–1099

de Saint Aubain Somerhausen and Fletcher 1999 Saint Aubain Somerhausen, N. de ; Fletcher, C. D.: Leiomyosarcoma of soft tissue in children: clinicopathologic analysis of 20 cases. In: *Am. J. Surg. Pathol.* 23 (1999), Jul, pp. 755–763

de Thé et al. 1990 Thé, H. de ; Chomienne, C. ; Lanotte, M. ; Degos, L. ; Dejean, A.: The t(15;17) translocation of acute promyelocytic leukaemia fuses the retinoic acid receptor alpha gene to a novel transcribed locus. In: *Nature* 347 (1990), Oct, pp. 558–561

de Thé et al. 1991 Thé, L. de ; Lavau, C. ; Marchio, A. ; Chomienne, C. ; Degos, L. ; Dejean, A.: The PML-RAR alpha fusion mRNA generated by the t(15;17) translocation in acute promyelocytic leukemia encodes a functionally altered RAR. In: *Cell* 66 (1991), Aug, pp. 675–684

dos Santos et al. 1997 Santos, N. R. dos ; Bruijn, D. R. de ; Balemans, M. ; Janssen, B. ; Gärtner, F. ; Lopes, J. M. ; Leeuw, B. de ; Kessel, A. Geurts van: Nuclear localization of SYT, SSX and the synovial sarcoma-associated SYT-SSX fusion proteins. In: *Hum. Mol. Genet.* 6 (1997), Sep, pp. 1549–1558

dos Santos et al. 2001 Santos, N. R. dos ; Bruijn, D. R. de ; Kessel, A. G. van: Molecular mechanisms underlying human synovial sarcoma development. In: *Genes Chromosomes Cancer* 30 (2001), Jan, pp. 1–14

Curriculum Vitae

Persönliche Daten

Petra Sander
Breubergstraße 9
64546 Mörfelden-Walldorf

geboren am 21. Mai 1973 in Darmstadt

ledig, ein Kind

Schulbildung

1979–1983	Grundschule in Darmstadt
1983–1985	Förderstufe in Darmstadt
1983–1989	Realschule in Darmstadt
1989–1992	Gymnasium in Darmstadt; Abschluss: Abitur

Hochschulstudium

10/1992–9/1993	Lehramt für Sonderschule an der Wolfgang-Goethe-Universität in Frankfurt
10/1993–12/2004	Lehramt für das Gymnasium an der Technischen Universität Darmstadt; Fächer: Biologie und Politikwissenschaften; Titel der Examensarbeit: "Untersuchung von biologischen Faktoren, die den Zellzyklus-Verlauf und die Apoptoserate nach Bestrahlung beeinflussen" (Professor Kraft); Abschluss: 1.Staatsexamen

Berufstätigkeit

seit 03/2005	Anfertigung einer Dissertation am Deutschen Krebsforschungzentrum, Heidelberg; Titel der Dissertation: "Frequency distribution of telomere maintenance mechanisms in soft tissue sarcoma" (Professor Peter Lichter)

Darmstadt, 10. Dezember 2009

Erklärung gemäß § 9 der Promotionsordnung

Hiermit erkläre ich gemäß § 9 der Allgemeinen Bestimmungen der Promotionsordnung der Technischen Universität Darmstadt vom 12. Januar 1990 in der Fassung der IV. Änderung vom 16. August 2001, dass ich die vorliegende Arbeit mit dem Titel

Frequency distribution of telomere maintenance mechanisms in soft tissue sarcoma

selbständig verfasst und bei ihrer Anfertigung keine außer den ausdrücklich genannten Hilfsmitteln benutzt habe.

Darmstadt, 10. Dezember 2009

Danksagung

Die vorliegende Dissertation wurde in der Abteilung Molekulare Genetik, Deutsches Krebsforschungszentrum, unter der Leitung von Prof. Dr. P. Lichter in der Zeit von März 2005 bis Januar 2010 angefertigt. Den Abschluss dieser Arbeit möchte ich dazu nutzen, all denjenigen Menschen zu danken, die bei der Anfertigung dieser Arbeit involviert waren.

Prof. Dr. Peter Lichter danke ich ganz herzlich für die Aufnahme in seine Abteilung und Überlassung der Fragestellungen, die Ausgangspunkt dieser Arbeit waren. Sein Interesse am Fortgang der Arbeit und sein hohes Engagement in vielen Bereichen der Krebsforschung waren für mich eine große Motivation. Jenseits der fachlichen Aspekte war auch seine stete Unterstützung in vielen Angelegenheiten eine sehr wertvolle Hilfe.

Prof. Dr. Gerhard Thiel aus dem Fachbereich Botanik der TU Darmstadt hat sich freundlicherweise als mein Doktorvater zur Verfügung gestellt, dafür danke ich ihm ganz herzlich. Des weiteren Danke ich ihm ganz besonders für das stetige Interesse und die Mithilfe an der Fertigstellung meiner Doktorarbeit.

Weiterhin danke ich dem **Tumorzentrum Heidelberg/Mannheim** für die Förderung des Projekts, in dessen Rahmen diese Arbeit entstand.

PD Dr. Gunhild Mechtersheimer und Prof. Dr. Petra Boukamp. Gunhild Mechtersheimer möchte ich herzlich danken, da Sie für dieses Projekt unersetzlich war. Petra Boukamp möchte ich für die Interpretation der TRAP-Daten herzlich danken, sowie für die stets konstruktive Kritik.

Prof. Dr. Stefan Joos danke ich herzlich für die Betreuung in der ersten Phase meiner Doktorarbeit.

Dr. Stefan Wörz und Martin Pfannmöller Herzlichen Dank für den Einblick in die Welt der digitalen Bildverarbeitung, es hat mir riesig Spass gemacht. Stefan möchte ich ganz herzliche dafür danken, dass er mit so viel Geduld meine Ideen fürs Programm umgesetzt hat. Martin möchte ich ganz herzlich für die ganze investierte Zeit auch neben den "normalen" Arbeitszeiten danken, er war eine unersetzliche Hilfe.

Dr. Karsten Richter danke ich für die die Einarbeitung am konfokalen Mikroskop und die Geduld für meine doch sehr vielen Fragen. Vielen Dank für die vielen interessanten Diskussionen und stets konstruktive Kritik.

Dr. Damir Krunic möchte ich ganz herzlich für die Einführung rund um die Welt der Telomere danken, und für weitere interessante Diskussionen rund um die Enden humaner

Chromosomen. Mit ihm im Labor zu arbeiten ist einfach TOP, macht riesig Spass und lässt immer Raum für lustige und nette Überraschungen.

Dr. Marcus Winter aus meiner *alten* Arbeitsgruppe (auch beruflich nach Heidelberg umgesiedelt) möchte ich mich ganz herzlich Bedanken für die Unterstützung beim Anfertigen meiner Dissertation in LaTeX. Dank seiner Hilfe ist dieses Format nicht nur ins Leben gerufen worden sondern auch am "Leben" geblieben :-)

PD Dr. Michael Rogers and PD Dr. Ralf Rieker danke ich für das kritische lesen meiner Dissertation.

Weiterhin danke ich dem **Nationalem Zentrum für Tumorerkrankung in Heidelberg** für die Bereitstellung des gesunden Gewebes die für unsere Analyse von hoher Bedeutung sind.

Meiner Freundin Angela: Ihr möchte ich ganz herzlich für viele aufbauende Worte danken, durch sie habe ich ein Lichtschimmer am Ende des Tunnels gesehen, auch wenn dort vielleicht noch gar keiner war ;-)

Zum Schluss möchte ich für die Unterstützung danken, die mir von meiner Familie zuteil wurde, ein Dank, der nur schwer in Worte zu fassen ist. **Meinen Eltern** danke ich ganz herzlich weil sie für mich einfach die besten Eltern sind und, dass sie mich hinsichtlich Berufswahl immer unterstützt haben, ohne mich zu beeinflussen. Sie sind immer für mich da, und haben mich stets in meinen Ideen unterstützt - auch wenn sie noch so verrückt waren. Meinen Geschwistern und besonders meinem Bruder danke ich für die viele Joggingstunden in Heidelberg - auch wenn er mich oft den Philosophenweg hinauf gejagt hat - durch ihn durfte ich jedoch feststellen, dass es neben dem TP3 in Heidelberg noch weitere schöne Ecken gibt ;-)

Nicht zuletzt danke ich meinem lieben **Freund Thorsten**, der auch in den schwierigen Momenten immer zu mir gestanden und so manche meiner chaotischen Phasen, besonders in der Schlussphase, mit viel Humor ertragen hat. Und nun zu meiner lieben **Tochter Emma Maria**: ihr danke ich, weil sie einfach da ist und ich sie für nichts auf der Welt mehr missen will - auch wenn so ein 3-jähriger Starrkopf ab und an die lieben Eltern ganz schön auf die Probe stellen kann ;-)!! Dennoch, Sie hatte absolut recht, wenn sie das ein oder andere mal einfach den Bildschirm von meinem Notebook zugeklappt hat.